

**MODELING AND CHARACTERIZATION OF
ABRASIVE-FREE COPPER CHEMICAL MECHANICAL
PLANARIZATION PROCESS**

TABASSUMUL HAQUE
(B. Sc. Eng., BUET)

**A THESIS SUBMITTED
FOR THE DEGREE OF MASTER OF ENGINEERING
DEPARTMENT OF MECHANICAL ENGINEERING
NATIONAL UNIVERSITY OF SINGAPORE**

2004

Acknowledgments

First of all, I would like to express my deepest and heartiest appreciation and gratitude to my academic supervisors Dr. Subramaniam Balakumar and Assoc. Prof. A. Senthil Kumar for their support, guidance and encouragement throughout the entire research work. I am very happy to express my sincere gratitude to Professor Mustafizur Rahman for his prudent advice and spiritual support that helped me to carry out research work with confidence and spirit.

Thanks to the Department of Mechanical Engineering, National University of Singapore for providing me handsome scholarship, and thanks to the Semiconductor Processing Technology (SPT) Laboratory, Institute of Microelectronics, Singapore for giving me huge research facilities. Special thanks to Dr. Rakesh who provided me opportunity to perform research in his group. I am grateful to the lab officers, Selvaraj and Catherine, who helped me in learning the equipment and doing experiments.

I am very thankful to my friends, Zahid, Majhar, Biddut, Kibria, Sharif, Atiq, Ariful, Nabila, Awrangjeb, Ibrahim, Mithun, Nipun, Rubina and Tanveer for giving me inspiration during my entire study period. I heartily acknowledge the encouraging support of my lab mates, Tauhid, Aziz, Zhigang, Angel, Sreeram and Fatima. My cordial thanks also go for my fellow committee members of Graduate Students' Society, NUS who spent their valuable time for me in organizing several events when I was extremely busy with my research work.

It is beyond my ability to express my feelings towards my parents, Muhammad Abu Zafor and Masuda Begum, who have brought me up to this position through their unconditional love, support and encouragement.

Last but not the least, it is my belief that Allah, to whom everything belongs, helped me to come out from all difficulties of my research and allowed me to complete this thesis in time. My ultimate gratitude and glories are devoted to Him.

Table of Contents

Acknowledgements	i
Table of Contents	iii
Summary	viii
List of Tables	x
List of Figures	xi
List of Symbols	xv
Chapter 1 Introduction	1
1.1 State-of-the-Art of Chemical Mechanical Planarization	1
1.2 Problem Definition and Scope of This Study	3
1.3 Thesis Organization	6
Chapter 2 Literature Review	7
2.1 Introduction	7
2.2 Origins and Evolution of the CMP Process	8
2.3 The New Era of Copper CMP	9
2.4 Fundamental Study of Abrasive and Abrasive-free Copper CMP	10
2.4.1 Material Removal Mechanism in CMP	10
2.4.2 CMP Process Characterization	14
2.4.3 Particle Scale and Pad Scale CMP Modeling	15
Chapter 3 Experimental Investigations	23
3.1 Introduction	23

3.2	Wafer Preparation	23
3.3	Experimental Setup	25
3.3.1	CMP Polishing and Cleaning Unit	25
3.3.2	Polishing Pad and Cleaning Pad	27
3.3.3	Abrasive-free Slurry	28
3.4	Experimental Procedure of Copper CMP	28
3.5	Metrology Tool	30
3.5.1	Four-Point Probe	30
3.5.2	Standard Mechanical Inter-face (SMIF) Profiler	31
3.5.3	Therma Wave Opti-Probe-5250I	32
3.5.4	Scanning Electron Microscopy (SEM) and Energy Dispersive X-ray (EDX)	32
3.5.5	Atomic Force Microscopy	33
3.5.6	Mitutoyo FORMTRACER	33
3.6	Experimental Plan	34
Chapter 4	Material Removal Mechanism in Abrasive-free Copper CMP Process	36
4.1	Introduction	36
4.2	Theory of Material Removal Mechanism	37
4.2.1	Material Removal/ Wear Mechanism in CMP Process	38
4.2.2	Pressure and Velocity Distribution across the Wafer	40
4.2.3	The Possible Wear Mechanisms in Abrasive Free CMP	43
4.2.3.1	Corrosive (Chemical) Wear	43
4.2.3.2	Adhesive Wear	43

4.2.3.3	Surface Fatigue Wear	44
4.3	Experimental Findings	44
4.3.1	Effect of Polishing Conditions in Wear Mechanisms	45
4.3.2	Elemental Analysis of the Polished Surface Using EDX	50
4.3.3	Surface Analysis of Wafers Polished in DI Water CMP Process	51
4.4	Results and Discussions	54
4.4.1	Surface Analysis of Wafers Polished in Abrasive-Free Copper CMP Process	54
4.4.1.1	Incomplete Growth and Faceting	55
4.4.1.2	Mechanical Failure of Cu ₂ O Layers	58
4.4.1.3	Clean and Etched Surface Having Some Residue	60
4.4.2	Effect of Polishing Conditions on Wear Mechanism	61
4.5	Conclusions	63
Chapter 5	Characterization of Abrasive-free Copper CMP Process	66
5.1	Introduction	66
5.2	Theory of Process Characterization	66
5.2.1	Study of the Synergistic Effect of Process Parameters	66
5.2.1.1	Sommerfeld Number	69
5.2.1.2	Modes of Contact (MOC)	70
5.2.2	Relative Velocity and Pressure in MOC Analysis	72
5.2.2.1	Selection of Rotation Rate in Rotary CMP	72
5.2.2.2	Selection of Pressure	74

5.3	Role of Process Parameters in MRR and WIWNU	74
5.3.1	Role of Slurry Flow Rate	75
5.3.2	Role of Applied Pressure	78
5.3.3	Role of Relative Velocity	80
5.4	The synergistic Effect of Pressure and Velocity on MRR and WIWNU	82
5.4.1	Study of Modes of Contact	82
5.4.1.1	Solid Contact Mode (SCM)	85
5.4.1.2	Mixed Contact Mode (MCM)	85
5.4.1.3	Hydroplaning Contact Mode (HCM)	86
5.4.2	Synergistic Effect of Pressure and Velocity on WIWNU	87
5.5	Development of Abrasive-free CMP Process	88
5.5.1	Pre-CMP Issue: Determination of Optimum Polishing Conditions	89
5.5.2	In-situ CMP Issues: Determination of Main Polishing and over Polishing Time of Copper	90
5.5.3	Post-CMP Issues: Dishing of Copper, Erosion of Dielectrics, Oxide Loss and Defect Count	91
5.5.4	Polishing of Copper/Oxide Patterned Wafer with Optimized Polishing Condition	93
5.6	Conclusions	98
Chapter 6	A Material Removal Rate Model for Abrasive-free Copper CMP Process	100
6.1	Introduction	100
6.2	Formulation of MRR model	101
6.2.1	Assumptions	101

6.2.2	Determination of the Area of Direct Etching and Indirect Etching	105
6.2.3	Material Removal by Chemical Etching (corrosive wear)	107
6.2.3.1	Material Removal by Direct Etching	107
6.2.3.2	Material Removal by Indirect Etching	108
6.2.3.3	Total Material Removal Rate	109
6.3	Discussions	111
6.3.1	Model Evaluation	111
6.3.2	Experimental Verification of the Model	115
6.4	Conclusions	119
Chapter 7	Thesis Contributions and Recommendations for Future Work	120
7.1	Introduction	120
7.2	Thesis Contributions	120
7.3	Recommendations for Future Work	121
	Bibliography	123
	Appendix-A	A-i
A-1	Multilayer Metal Interconnects and the Role of CMP	A-i
A-2	International Technology Roadmap for Semiconductors (ITRS)	A-ii
A-3	Ideal Oxide ILD CMP	A-iv
A-4	Dual Damascene Interconnects Fabrication Process	A-iv
A-5	Prestonian and Non-Prestonian Behaviour of MRR	A-vi

Summary

Chemical Mechanical Planarization (CMP) has appeared as a crucial part for multiple integration strategies in semiconductor processing technology. Recently, the semiconductor industries are facing big challenges in the integration of copper and low-k materials, especially in removing the copper of Dual Damascene structure. The fragile low-k materials beneath copper layer, which is porous and have poor mechanical strength, experiences severe mechanical damage in conventional abrasive copper CMP process. This is because the abrasive particle requires high pressure to remove the material from wafer surface by means of mechanical abrasion. A recently developed low pressure abrasive-free copper CMP process, where the chemically active slurry does not contain hard abrasive particle and material is chiefly removed by chemical wear (etching), has shown excellent performance over the conventional copper CMP process. Although the chemical dominance is high in abrasive-free CMP process, still the process is controlled by modulating the key mechanical parameters namely pressure, velocity and slurry flow rate. However, the role of those process parameters on the overall performance of copper CMP process is yet poorly understood.

A little research has been performed to understand the fundamentals of abrasive-free copper CMP process. In order to understand the material removal mechanism (wear mechanism) in abrasive-free copper CMP process, the surface analyses were performed using SEM, AFM and EDX. From the experimental investigation, chemical etching (corrosive wear), fatigue wear, particle adhesion wear and particle abrasion wear have been found as the wear mechanisms in abrasive-free copper CMP. The increase of slurry flow rate and relative velocity and the decrease of pressure give the dominance of

corrosive wear in material removal mechanism, and vice versa. Because of subambient pressure issue, the center of the wafers never experience mechanical wear while the wear phenomena at the middle and edge of the wafers are greatly influenced by process parameters.

In addition, the process has been characterized to understand the effect of pressure, relative velocity and slurry flow rate on Material Removal Rate (MRR) and With-in Wafer Non-Uniformity (WIWNU). The non-prestonian phenomenon of MRR (the critical pressure issue and nonlinear dependence of MRR on pressure) has been identified which shows the consequence of direct etch rate and indirect etch rate on total MRR. Besides, the synergistic effect of relative velocity and pressure on MRR has been investigated from the 'Modes of Contact' (interfacial contact condition between wafer and pad) view point. Such analysis shows that MRR is maximum and WIWNU is within the allowable range in the early stage of Mixed Contact Mode. The polishing recipe of this contact mode has been used to develop the abrasive-free copper CMP process which gives over polishing time, dishing, erosion, oxide loss, defect count and leakage current within the allowable limit.

Finally, a MRR model for abrasive-free copper CMP has been developed based on the assumption of periodic distribution of pad asperities, elastic contact between pad and wafer surface and corrosive wear theory. In addition, this model takes into account the non-prestonian phenomenon of MRR, and the effect of velocity, chemical reactivity of slurry, pad surface geometry and the material property of pad and wafer on MRR can be explained by the MRR model. Moreover, the good agreement of the predicted MRR with experimental results proves the practicability of the model.

List of Tables

Table 4.1	Material removal rate at different polishing conditions in DI water CMP process	52
Table 5.1	Experimental polishing conditions of abrasive-free copper CMP process (blanket wafer polishing)	75
Table 5.2	Barrier (Ta) polishing conditions	94
Table 5.3	Polishing data of copper/oxide wafers polished with abrasive-free slurry	95
Table 6.1	Operating conditions and other parameters used for MRR modeling	116
Table A.1	SIA International technology roadmap for semiconductors (ITRS) for interconnect technology	A-iii

List of Figures

Figure 1.1	Schematic of rotary type CMP polisher	2
Figure 1.2	Schematic of CMP process with input variables, process parameters and output variables	4
Figure 3.1	Preparation of blanket copper wafer	23
Figure 3.2	Preparation of Copper/Oxide pattern wafer	24
Figure 3.3	Mirra Polishing Unit	25
Figure 3.4	Mesa Cleaning Unit	26
Figure 3.5	Polishing Pads: a) A polyurethane copper polishing pad with XY groove b) A Politex cleaning pad	27
Figure 3.6	Schematic diagram of copper CMP system	30
Figure 3.7	Atomic Force Microscope	33
Figure 3.8	Mitutoyo FORMTRACER (CS-5000)	34
Figure 4.1	Schematic of material removal using slurry of low pH and high oxidizer concentration: a) dissolution of abraded CuO/Cu ₂ O wear debris in abrasive CMP Process, b) direct etching of CuO/Cu ₂ O layer in abrasive-free CMP process	37
Figure 4.2	Steps of copper removal in CMP process using acidic slurry	37
Figure 4.3	Mechanism of material removal: a) indirect etching at floating/hydroplaning contact, b) direct etching at sliding contact	39
Figure 4.4	Schematic of pressure distribution across the wafer	41
Figure 4.5	Schematic of velocity distribution across the wafer	42
Figure 4.6	Effect of slurry flow rate on polished surface at 100 ml/min (a, b, c), 150 ml/min (d, e, f) and 200 ml/min (g, h, i) on WIWWV and WTWWV (10 μm × 10 μm)	45

Figure 4.7	Effect of pressure on polished surface at 6.89/9.65 kPa (a, b, c), 10.34/13.1 kPa (d, e, f) and 13.7/16.54 kPa (g, h, i) on WIWWV and WTWWV ($10\ \mu\text{m} \times 10\ \mu\text{m}$)	47
Figure 4.8	Effect of velocity at 30/27 rpm (a, b, c), 78/75 rpm (d, e, f) and 120/117 rpm (g, h, i) on WIWWV and WTWWV ($10\ \mu\text{m} \times 10\ \mu\text{m}$)	48
Figure 4.9	Wear characteristics of abrasive-free CMP at pressure 6.89/9.65 kPa, rotation rate 78/75 rpm and slurry flow rate 200 ml/min ($10\ \mu\text{m} \times 10\ \mu\text{m}$)	49
Figure 4.10	EDX (Energy Dispersive X-Ray) analysis of wafer surface polished in abrasive-free copper CMP process	50
Figure 4.11	EDX analysis of wafer surface polished in DI water CMP process	51
Figure 4.12	Surface analysis of wafer polished in DI water CMP: a) adhesion wear, b) formation of scratches and grooves, c) wedge type ploughing, d) formation of pitted surface	53
Figure 4.13	Incomplete growth of CuO/Cu ₂ O layer	55
Figure 4.14	Sectional analysis of the incompletely grown oxide layers at: a) 6.89/9.85 kPa b) 10.34/13.1 kPa c) 13.7/16.54 kPa	56
Figure 4.15	Effect of applied pressure on the oxide layer thickness	57
Figure 4.16	Mechanical failure of CuO/Cu ₂ O layers	58
Figure 4.17	Clean and etched surface: a) with residue b) without residue	60
Figure 4.18	Sectional analysis of the area having residue	60
Figure 5.1	Generic Stribeck curve based on the Sommerfeld number	67
Figure 5.2	Effect of slurry flow rate on MRR at constant pressure (11.72kPa) and velocity (1.02 m/sec).	68
Figure 5.3	Roughness profile of copper polishing pad ($R_a = 0.23\ \mu\text{m}$)	70
Figure 5.4	Schematic of different contact modes at wafer pad interface:	

	a. solid contact mode, b. mixed contact mode, c. hydroplaning contact mode	71
Figure 5.5	Kinematic parameters of rotary CMP	72
Figure 5.6	Schematic of the application of pressure on wafer	74
Figure 5.7	Effect of flow rate on MRR and WIWNU	76
Figure 5.8	WIWNU of material removal / wear rate across the wafer in abrasive-free CMP	76
Figure 5.9	Effect of pressure on MRR and WIWNU	78
Figure 5.10	Non-prestonian effect of pressure on MRR	79
Figure 5.11	Effect of relative velocity on MRR and WIWNU	81
Figure 5.12	Modes of contact analysis with normalized MRR and Sommerfeld number	82
Figure 5.13	Schematic of the interfacial contact modes between pad and wafer	83
Figure 5.14	Two dimensional (right) and three dimensional (left) AFM picture of the surface of copper blanket wafer polished at: a) SCM (0.49 m/sec) b) MCM-A (1.02 m/sec) c) HCM-B (1.56 m/sec) of MRR at 11.27 kPa	84
Figure 5.15	Relationship between WIWNU and relative velocity at different pressure	88
Figure 5.16	End point detection profile	91
Figure 5.17	Dishing, erosion and oxide loss at different metal lines	91
Figure 5.18	Dishing of copper interconnect at bond pad	93
Figure 5.19	Erosion of dielectrics at pattern density 10% and 30%	93
Figure 5.20	Copper/Oxide pattern wafer polishing process	94
Figure 5.21	Dishing after copper bulk polish and over polish	96
Figure 5.22	Dishing after barrier polish	96
Figure 5.23	Erosion of dielectric material after barrier polish	97

Figure 5.24	Leakage current at copper interconnects of pattern wafers	98
Figure 6.1	SEM picture of copper polishing polyurethane pad	102
Figure 6.2	Schematic diagram of: a) the prestonian and non-prestonian behavior of material removal rate b) the wafer- pad asperity contact at different locations of non-prestonian curve	104
Figure 6.3	Different kinds of areas at wafer-slurry and wafer-pad contact	105
Figure 6.4	Change of MRR with pressure: a) direct etching and b) indirect etching (At relative velocity 0.49 m/sec)	111
Figure 6.5	Comparison between the change of direct etch rate and indirect etch rate with pressure (At relative velocity 0.49 m/sec)	112
Figure 6.6	X-SEM of copper oxide layer formed after dipping 24 hours in the abrasive free slurry	115
Figure 6.7	Experimental MRR versus theoretical (predicted by abrasive-free MRR model) MRR at relative velocity: a) 0.49 m/sec b) 0.76 m/sec and c) 1.02 m/sec	117
Figure A-1	Cross sectional view of a microelectronic chip	A-i
Figure A-2	Multilevel interconnects: a) without CMP, b) with CMP	A-ii
Figure A-3	Ideal oxide ILD CMP	A-iv
Figure A-4	Via-first approach of Dual Damascene interconnect fabrication process	A-v
Figure A-5	Prestonian and non-prestonian behaviour of MRR	A-vi

List of Symbols

α	A dimensionless number which is the ratio of the area of up features to the area of the pad surface exposed to wafer
δ_T	Total thickness of material removed from wafer per unit time
δ_c	Thickness of material removed from wafer per unit time at or below critical pressure
δ_{groove}	Depth of pad groove
δ_f	Effective fluid film thickness
η	Area density of asperities on pad surface
μ	Slurry viscosity
ω_w	Angular velocity of wafer
ω_p	Angular velocity of pad
γ_w	Poisson ratio of wafer material (copper)
γ_p	Poisson ratio of pad material (polyurethane)
ξ	Coefficient taking into accounts the material property
A	Area of the wafer surface
A_p	Area of the pad block / apparent contact area between wafer and pad
A_g	Area of the pad grooves exposed to wafer surface
A_{wa}	Area of wafer-pad contact at the peak of asperity
A_{wv}	Area of wafer- slurry contact at the valley of asperity
A_{de}	Area of direct etching at wafer-pad contact
A_{ie}	Area of indirect etching at wafer-slurry contact
E_w	Young's modulus of wafer material (copper)
E_p	Young's modulus of pad material (polyurethane)
E^*	Equivalent modulus of elasticity

e	Eccentricity between wafer and pad
k	Coefficient taking into accounts the corrosive wear and other CMP parameters
k_{de}	Wear coefficient of direct etching
k_{ie}	Wear coefficient of indirect etching
k_p	Preston's constant
P	Applied pressure
P_c	Critical pressure
R_a	Pad roughness
R	Average radius of asperity curvatures on pad surface
R_s	Sheet resistance of copper layer
S_o	Sommerfeld Number
V	Relative velocity of wafer with respect to pad
MRR_T	Total material removal rate in blanket wafer polishing
MRR_{de}	Material removal rate for direct etching
MRR_{cw}	Material removal rate for chemical wear
MRR_{ie}	Material removal rate for indirect etching
MRR_{ie_c}	Material removal for indirect etching at critical pressure

Chapter 1

Introduction

1.1 State-of-the-Art of Chemical Mechanical Planarization

The semiconductor industries are facing big challenges in meeting the growing demand of high performance, smaller feature size, higher resolution, denser packing, and multi-layer interconnects of microelectronic devices. At present, 10^8 or more devices can be fabricated on semiconductor substrates. The number of components becomes double at each year following Moore's law [Moore, 1965]. The high demand of integration and miniaturization has made the fabrication and design of microchip more complex. The demand of fast shrinkage of feature size and high performance ICs forced the industries to produce ICs with more multilayer interconnects [A-1]. The electrical resistance and parasitic capacitance associated with the metal interconnects which is usually defined by RC time delay [Steigerwald et al., 1997] has become a major factor that limits circuit speed of such high performance ICs. The patterns for vias and trenches are made lithographically on the inter layer dielectrics (ILD). The smaller wavelength light used for lithography requires global planarity on the ILD surface. Chemical Mechanical Planarization (CMP) has been shown as the key technology since last two decades that accomplishes the demand of global planarity and surface smoothness of ILD surfaces. In addition, CMP is used in both front-end (Shallow Trench Isolation CMP) and back-end (Oxide CMP, Tungsten CMP, Copper CMP) IC fabrication processes to selectively remove raised films, to reduce step heights around patterned features, and to meet other planarization criteria. Besides, according to ITRS roadmap [A-2], CMP has been

considered as the leading planarization technology in current and future semiconductor manufacturing. However, different fundamental issues of the CMP processes are still poorly understood, and better understanding of CMP process is essentially important for process optimization, higher process yield and throughput.

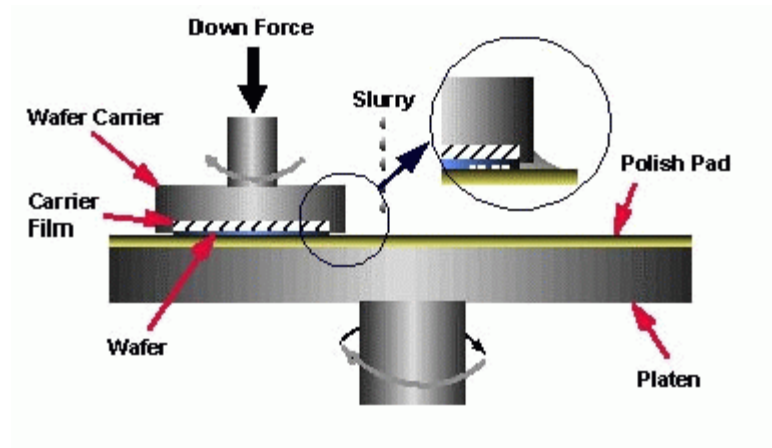


Figure 1.1 Schematic of rotary type CMP polisher [Danyluk, 2004]

CMP is a kind of tribochemical polishing technique where the formation of chemically modified surface is removed without micro fracture. The schematic of a rotary CMP polisher is shown in Figure 1.1. The CMP process involves pressing the face of the wafer to be polished against a compliant polymeric polishing pad and generating relative motion between the two surfaces. A slurry consisting of abrasives and chemicals (Abrasive CMP) or only chemicals (Abrasive-free CMP) is fed in between the interface of wafer and pad. The combined chemical action of the chemicals in the slurry and the mechanical action of the abrasives and/or pad asperities cause material to be removed from the wafer.

1.2 Problem Definition and Scope of This Study

Recently, the semiconductor industries are facing big challenges in the integration of copper and low-k materials, especially in Dual Damascene interconnect fabrication process [A-4]. In this process, the 90 nm node technology requires true low-k materials ($k=2.7$) while porous low-k dielectrics ($k<2.2$) are required for the 65nm node technology. The introduction of porosity reduces dielectric constant, but it also decreases mechanical strength of low-k materials. Therefore, the porous low-k materials are quite susceptible to CMP consumables because the application of pressure, velocity and the use of slurry and pad materials cause mechanical failure of the underneath fragile low-k materials. The mechanism of conventional copper CMP (using abrasive slurry) is mechanical abrasion followed by chemical dissolution of abraded material. But the future technology node (less than 90nm node) demands the decrease of mechanical aspect and the increase of chemical aspects so that the mechanical failure of low-k material (low-k film fracture, peeling, etc) resulting from down pressure can be eliminated. If the hard abrasive particles which require high pressure to be indented on the wafer are removed from the slurries and if the chemical activity or etching capability of those slurries is increased, the problem concerning mechanical failure can be eliminated to a greater extent. Abrasive-free CMP process uses such chemically active abrasive-free slurry and thereby, in this process, the formation of defects on copper surface resulting from particle abrasion and the failure of low-k materials resulting from high down force can be significantly reduced. In addition, the occurrence of dishing at copper interconnects resulting from pad bending (usually takes place in high pressure CMP) can also be eliminated by adopting chemically dominant low pressure abrasive-free CMP process. Thus the chemically active abrasive-

free CMP provides a robust Cu/low-k integration process giving very clean, scratch-free, anticorrosive polished surface resulting in high yield and process throughput [Kondo et al., 2000].

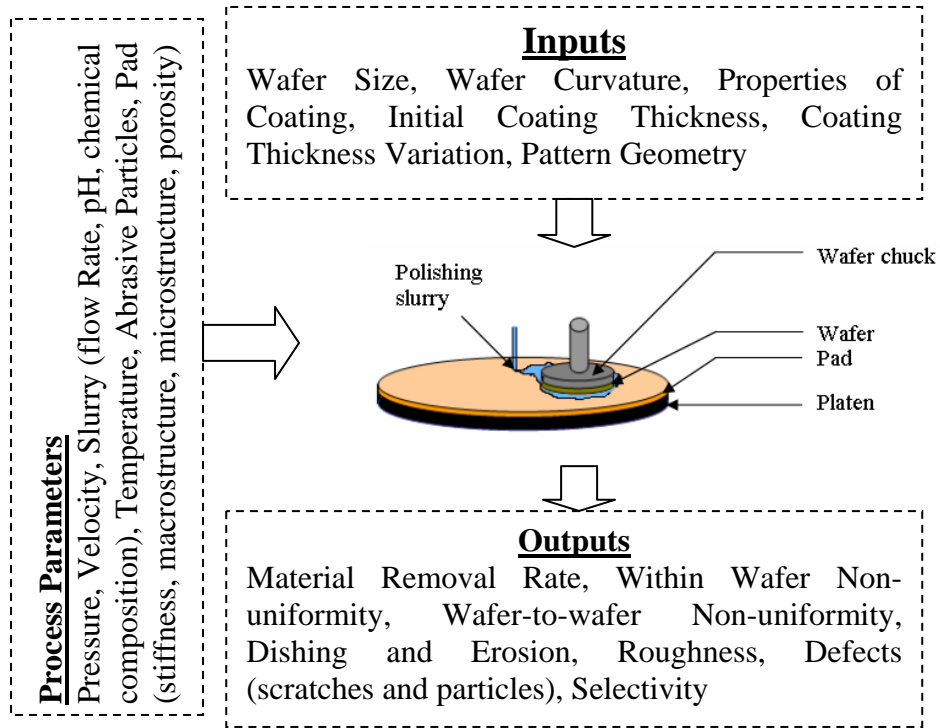


Figure 1.2 Schematic of CMP process with input variables, process parameters and output variables.

The existence of several material removal mechanisms (abrasion, erosion, adhesion, burnishing, etching, etc) in CMP has made this process fairly complex. Besides, the effect of more than twenty input variables and process variables on the process outputs has made the CMP process even more complex (Figure 1.2). Furthermore, mechanism of material removal and other fundamental issues of CMP process, especially for the newly developed abrasive-free CMP are poorly understood, and yet to be explored. In addition, there is no quantitative model that takes into account the interesting non-prestonian nature

of Material Removal Rate (MRR) and material removal mechanism of abrasive-free CMP. These problems have made an excellent platform to do research in area of abrasive-free CMP process. However, the scope of this study is to understand the material removal mechanism, to characterize the abrasive-free CMP process, and finally, to develop a MRR model for the process.

The scope of this study can be briefly summarized as follows:

- The material removal mechanisms are studied by investigating the wear phenomenon in abrasive-free copper CMP. The investigations were carried out by surface analysis using SEM, AFM and by elemental analysis of the polished surface using EDX.
- The abrasive-free CMP process was characterized by investigating the effect of pressure, relative velocity and slurry flow rate on wafer level geometry, i.e. MRR and With-in Wafer Non-Uniformity (WIWNU) of MRR. In addition, the synergistic effect of applied pressure and relative velocity on MRR was investigated analyzing ‘Modes of Contact’ between wafer and pad during polishing. Based on the investigated results, an optimized condition of bulk copper polishing was selected which was further used to develop the abrasive-free CMP copper process for pattern wafers.
- Finally, a MRR model for abrasive-free copper CMP is developed based on taking into account the non-prestonian nature of MRR [A-5] and the investigated material removal mechanism (corrosive wear theory). In addition, this model presents the role of pressure on different kind of etch rates.

However, the MRR model can also explain the effect of the chemical reactivity of slurry, pad surface geometry and the material property of pad and wafer on MRR in abrasive-free copper CMP process.

1.3 Thesis Organization

The overall goal of this thesis is to study the fundamental aspects of wafer-level polishing with abrasive-free slurry and to develop a MRR model that incorporates major parameters affecting the MRR. The experimental and theoretical study of this work will definitely augment our fundamental understanding of the abrasive-free copper CMP process.

A brief summary of relevant literature pertaining to the investigations performed with abrasive and abrasive-free slurry in copper CMP process are discussed in Chapter 2. Chapter 3 describes the experimental setup and procedure. In the subsequent chapters, the experimental results will be analyzed for understanding abrasive-free CMP and to verify a MRR model. Chapter 4 explains the mechanism of material removal in abrasive-free copper CMP process. The effect of process parameters on wafer level geometry and process characterization are discussed in Chapter 5. A MRR model has been developed in Chapter 6. In chapter 7, the conclusions derived from the experimental and theoretical work are summarized in the form of thesis contributions, and the future directions of this work are recommended.

Chapter 2

Literature Review

2.1 Introduction

CMP has appeared as an indispensable part for multiple integration strategies in semiconductor processing technology. The emergence of new materials such as Cu in ULSI fabrication requires extensive use of the CMP process to form inlaid interconnect structures. Besides, the future technology node below 90 nm will require upwards of twenty three planarization steps. The planarization performance of one layers strongly affects the planarization of next layers and, higher the planarization steps poorer the post CMP topology. Therefore, a fundamental understanding of these metal CMP processes is needed to improve process optimization and control, and to increase the process yield and throughput that will continue to escalate as more devices migrate to future technology node where metallization schemes are more complicated. Although lots of efforts have already been made to understand the CMP process over the last few decades, the role of more than twenty inputs and process variables on output variables is still poorly understood. In addition, the use of low-k material for future technology node has put the use of CMP in a big challenge. Several new technologies have been implemented in CMP since last couple of years. Abrasive-free copper CMP is such a technique that enables higher polishing rates under low polishing pressure resulting in scratch free surface with lower dishing, erosion, and less or no mechanical damage of low-k materials. The literature review in this chapter will mainly focus on the following relevant features:

- Origins and evolution of the CMP process

- The new era of copper CMP
- Fundamental study of abrasive and abrasive-free copper CMP:
 - Material Removal Mechanism
 - Process Characterization
 - CMP Modeling

2.2 Origins and Evolution of the CMP Process

The polishing process has been employed for optical lens fabrication for centuries. The first commercial CMP machine, invented by Monsanto, was used in the optical industry. Monsanto's machine was first commercially used in semiconductor industry in early sixties [Walsh et al., 1965; Hippel, 1988]. This process was first used to prepare raw silicon wafers, especially the mechanically damaged surface of sawed single crystal silicon wafer. The purpose of using CMP at that time was to produce flat, scratch free and planarize silicon substrate for VLSI devices. The use of submicron abrasive particle of silicon dioxide in alkaline solution offered the polishing time almost 18 times lower than that of earlier CMP. In late sixties, IBM improved the CMP process [Silvey et al., 1966] where they used cupric salt slurry which provided lesser polishing time and better surface finish than that of silica based CMP [Blake et al., 1970]. In 1988, the first commercial polisher designed specifically for CMP was introduced by Cybeq in Japan. In early nineties, SEMATECH and Westech jointly tried to develop a competitive and advanced CMP polisher [Lai, 2001].

2.3 The New Era of Copper CMP

The smaller feature size and higher performance ICs requires more interconnects on the same substrate. Higher interconnect results in higher buildup of the surface topology resulting in poorer step-coverage of the metal deposition. Intel extensively used oxide CMP [A-3] to manufacture Pentium Chips using Al as the interconnect material in 1993. Because of the shrinkage of device, the dimension of the aluminum interconnect also decreases resulting in the increase of interconnect resistivity. The high resistivity of Al interconnects impairs the digital signal transmission because of the poor electron migration. This phenomenon is widely known as RC time delay [Steigerwald et al., 1997]. Because of low resistivity (about two thirds of aluminum) and low processing cost, copper replaced aluminum in mid nineties. The new era of copper CMP started when the major chipmakers, such as IBM, Motorola and Texas Instruments declared their plans in 1997 to put copper into production in 1998. They implemented damascene process [A-4] where copper CMP became an integral part for multilevel interconnect fabrication.

Although the low resistivity of copper material gives low RC delay, but the demand of continued shrinkage of device dimension and the increase of packing density in ULSI manufacturing requires further reduced value of RC delay. This is satisfied by adopting low-k dielectric technology. Low-k materials can replace the present oxide ILD layer to reduce the capacitance loss and increase the signal transmission rate of the circuits. According to ITRS [A-2], the demand of technology node below 90 nm in the coming years requires porous low-k dielectrics ($k < 2.2$). The requirement of high pressure for abrasive CMP causes the mechanical failure of the underlying low strength porous and fragile low-k dielectrics. Kondo et al. (2000) proposed a new low pressure abrasive-free

CMP that eliminates the occurrence of mechanical failure to a greater extent. The chemically active slurry having no hard particle of silica or alumina is called abrasive-free slurry and, the CMP process using such slurry for copper polishing is called abrasive-free copper CMP process. Since the abrasive particle is removed from slurry and the slurry is highly chemically active, the chemical aspect shows much dominance over mechanical aspects. Thus the formation of scratches on copper surface and the failure of low-k materials are reduced to a greater extent. Furthermore, the dishing at interconnect that results from pad bending in high pressure CMP is much reduced by adopting the low pressure abrasive-free CMP. The fundamental understanding of this newly developed abrasive-free CMP process is essentially important for process optimization and control.

2.4 Fundamental Study of Abrasive and Abrasive-free Copper CMP

The fundamental understanding usually involves the investigation of material removal mechanism, effect of the process parameters on output variables, etc. In this chapter, literature review has been made pertaining to the mentioned areas for both abrasive and abrasive-free CMP techniques. In addition, extensive literature review of CMP modeling has been made in a view to making an excellent platform for developing a MRR model for abrasive-free CMP.

2.4.1 Material Removal Mechanism in CMP

There are a number of material removal mechanisms reported in literature namely surface melting, abrasion wear, adhesion wear, single cycle fatigue, erosion wear, burnishing, etching wear, etc. The material removal in CMP process also involves several

mechanisms which have made the CMP process more complex, and the process is not yet clearly understood [Lai, 2001].

Surface melting is one of the important mechanisms of material removal in polishing [Beilby, 1921; Bowden et al., 1937]. According to the concept of surface melting, it is necessary that the melting point of abrasive particle should be higher than that of the material to be abraded, rather than having higher hardness of abrasive particle at room temperature. Rabinowicz (1968) and Samuels (1971) showed that material removal rate does not depend on the melting temperature rather it depends on the relative hardness at rubbing temperature which is similar to abrasion mechanism. However, because of slurry flow, the temperature at the wafer pad or wafer particle interface cannot be raised up to the melting point of the corresponding temperature [Lai, 2001]. Hence, the mechanism of surface melting is certainly absent in CMP process.

The abrasion of hard particle between the two sliding surfaces is one of the most established material removal mechanisms in polishing. Newton (1695) observed that the size of scratch decreases with the decrease of the size of the abrasive particles, and the scratches on polished surface is rarely visible. Raleigh (1901) observed that the highly reflective surface with discontinuous facets can be achieved by polishing, and further polishing does not improve the quality of the surface. He also noticed that very small force on abrasive particle removes material on a much finer scale. The work of Samuel (1971) shows that the polishing is similar to ordinary abrasion but at reduced scale. Rabinowicz (1968) noticed that the abrasive particle used for polishing process should be such that it is generally below the minimum size needed for the formation of wear particles and hence, the total force on each particle also becomes very small. Analyzing the erosion and abrasion wear model, and taking energy into consideration, Larsen et al. (1999) pointed

that material is removed by the synergistic process of active-passive reaction and removal of weak surface film by the abrasives. However, the chief mechanism of material removal in conventional abrasive CMP was found to be microcutting by Jiun-Yu Lai (2002). He also verified that brittle fracture and surface melting are not the possible mechanism while burnishing, although not dominant in CMP, might be a possible mechanism in CMP

The wear mechanism at lubricated contact can suitably explain the material mechanism in CMP process. In lubricated contact, the abrasive particle or the particles coming from wear debris or from other sources are responsible for two-body and three-body wear [Williams et al., 1992]. The firmly embedded particle in two-body wear causes scratches or grooves while the tumbling or rolling action in three-body abrasion causes the occasional indentation resulting in the formation of pitted surface. According to the definition of erosion wear [Rabinowicz, 1995], the three body abrasion wear at sufficiently high speed CMP can be defined as the erosion wear. The presence of adhesion wear in lubricated surface was noticed by Lisowski et al. (1981). They developed a wear model for lubricated sliding contact taking adhesive wear as the only mechanism of material removal. Zhang et al. (1998) suggested that adhesion exists in between particle and work piece during floating CMP process. On the other hand, Bhushan (2002) defined adhesion as liquid-mediated adhesion in lubricated contact, and noticed insignificant amount of friction and adhesion wear at well lubricated surfaces. However, there is no such work that clearly indicates that adhesion is a dominant material removal mechanism in CMP.

Fischer et al. (1988) defined CMP as a tribochemical process, where they discussed that chemical reaction accelerates mechanical wear which is further accelerated by friction force. Steigerwald et al. (1995) explained the material removal mechanism of

CMP process as the synergistic effect of both mechanical and chemical components. He argued that the thick CuO/Cu₂O layer formed on the top is mechanically removed by particle abrasion followed by the dissolution of the wear debris by etchant. Hernandez et al. (2001) pointed out that the material removal solely depends on the oxidation of copper and removal and solubility of cupric films in slurry. For process optimization and CMP modeling, it is essentially important to identify which component (mechanical or chemical) is dominating the material removal mechanism. However, in abrasive CMP process, plastic deformation of wafer surface resulting from particle rolling or ploughing was found as the dominant material removal mechanism by Liang et al. (1997). On the other hand, because of the absence of abrasive particle and high chemical reactivity of abrasive-free slurry, the chemical dominance was noticed in the material removal mechanism in abrasive-free CMP by Kondo et al. (2000). Matsuda et al. (2003) investigated the characteristics of abrasive-free micelle slurry for copper CMP. They showed that the pressure assisted etching is a dominant mechanism of material removal where Heteropolyacid encircled by surfactant etches copper during polishing. However, detail investigation of material removal mechanism in chemically active abrasive-free CMP is yet to be explored.

2.4.2 CMP Process Characterization

The main process variables that are used to tune the CMP process are pressure, relative velocity and slurry flow rate. Preston (1927) developed the first MRR equation of polishing which demonstrates pressure and relative velocity as the chief process parameters that control the MRR in polishing. Apart from pressure and velocity, the flow rate was found as a very important process parameter because MRR significantly

decreases with the increase of slurry flow rate in abrasive copper CMP process [Li et al., 2004]. Homma et al. (2003) claimed that the MRR is linear with frictional force in abrasive CMP. Therefore, they incorporated the coefficient of friction (COF) in their material removal rate model. Moon et al. (1998) experimentally proved that the slurry film thickness changes with the change of COF and consequently, the interfacial contact between wafer and pad changes which directly affects the MRR. Researchers [Phillipossian et al. , 2004; Mullany et al., 2003, Liang et al., 2002; Denardis et al., 2003; Moon et al., 1998] found that the COF in CMP is strongly influenced by pressure, relative velocity, slurry viscosity, slurry flow rate, etc. In order to select the suitable polishing condition, a suitable COF is usually selected by the study of the 'Modes of Contact' between the wafer and pad during polishing [Phillipossian et al., 2004; Moon et al., 1998; Denardis et al., 2003]. But it was not explicitly noticed how the windows of those contact modes changed with the process parameters. For conventional abrasive slurry, both Phillipossian et al. (2004) and Li et al. (2004) noticed that the COF decreases with the increase of slurry flow rate and hence, MRR also decreases.

Since the mechanism of material removal in abrasive-free CMP is very much different from that of abrasive CMP, the role of the process parameters were found quite different and still poorly understood [Kondo et al., 2000; Matsuda et al., 2003]. The absence of hard particle and the high chemical reactivity of slurry have made the abrasive-free CMP process chemically dominant. Therefore, the significance of mechanical parameters (velocity, pressure, etc) on total material removal is much lower than chemical parameters. However, in order to establish the control over the material removal rate and non-uniformity, better understanding of the role of those mechanical parameters are still the key issue for process optimization. Matshuda noticed a critical pressure beyond which

the MRR was found sufficiently low. Thus the critical pressure issue of abrasive-free CMP process deviate the MRR from prestonian nature [A-5]. Boning et al. (2001) explained that if the removal rate does not vary linearly with pressure, it is called the non-prestonian nature of MRR. They also noticed such phenomenon of MRR in abrasive-free copper CMP process.

2.4.3 Particle Scale and Pad Scale CMP Modeling

Although CMP is a well established material processing process used in semiconductor industries, process engineers still follow the method of finding a satisfactory polishing condition by experimenting with alternatives and eliminating failures. Lots of initiatives have been made since the last few decades in both academia and industries to bring CMP from ‘art’ to ‘science’ by developing particle scale, wafer scale and die scale models. The particle scale models involve the investigation of the interactions of slurry particles, slurry chemicals, polishing pad and wafer materials. The models at the feature and die scales are needed to address the topography evolution of integrated circuit (IC) chips as a function of pattern density, line width, pitch width and polishing time. On the other hand, the wafer-scale model is developed to deal with the issues related to the material removal non-uniformity across the wafer surface. Although the abrasive-free slurry does not contain hard particles, the interaction of pad asperity, slurry chemicals and wafer materials roughly falls in particle scale model. Therefore, literature concerning particle scale model has been reviewed in this chapter.

The first ever MRR model, empirically developed by Preston (1921), shows the proportional relation of MRR with the product of applied pressure and relative velocity which may be expressed as:

$$MRR = k_p PV \quad (2.1)$$

where, MRR is the volume removal rate, P the nominal pressure, V the relative velocity, and k_p is a constant known as the Preston constant.

Since the material removal from solid surface is a kind of mechanical action, and some sort of wear mechanism prevails in CMP, efforts were made to predict MRR by using wear equation developed by Holm (1946) and Archard (1953). The wear equation is expressed as,

$$V = k_w \left(\frac{LS}{H} \right) \quad (2.2)$$

where, V is the volume removed, L the load on the sample, S the relative sliding distance, H the hardness of the worn material concerned, and k_w is the wear coefficient

Since different issues of CMP can not be explained by Preston's equation, revised Preston's equations were therefore proposed by some researchers. For example, considering that the MRR does not extrapolate to zero, Maury et al. (1997) introduces a fitting parameter MRR_o into Preston's equation:

$$MRR = k_p PV + MRR_o \quad (2.3)$$

Afterward, Wrschka et al. (1999) proposed a nonlinear experimental equation,

$$MRR = k_p P^\alpha V^\beta \quad (2.4)$$

where, α and β are two fitting parameters to get a better fit of the experimental data.

The effects of consumables and wafer parameters were not explicitly involved in Preston's equation and its revised versions. Therefore, it is difficult to obtain the process window using those models for different consumable sets. Cook (1990) developed a physical model to address this limitation. Taking into consideration the interactions between the abrasive particles and the wafer surface, a Hertzian elastic penetration of a spherical particle under uniform pressure P into the wafer surface, sliding along the surface with a velocity V and removing glass volume proportional to the penetration, a MRR model was proposed as:

$$MRR = (2E)^{-1} PV \quad (2.5)$$

where, E is the Young's modulus of the wafer materials. Liu et al. (1996) developed a similar model based on the statistical method and Hertzian elastic penetration. This model includes wafer hardness H_w , wafer Young's modulus E_w , pad hardness H_p and abrasive Young's modulus E_s :

$$MRR = C \left(\frac{H_w}{H_w + H_p} \right) \left(\frac{E_s + E_w}{E_s E_w} \right) PV \quad (2.6)$$

where, C is a coefficient to account for the effects of slurry chemicals and other consumable parameters. Similar to Cook's model, this model also suggests that the material removal is proportional to the applied pressure and relative speed. The advantages of Cook and Liu's models over Preston's equation are that they provide insights of the roles and interactions of the consumable parameters.

It is quite apparent that the mechanical removal by abrasive particles is the dominant mechanism in Cook and Liu's models. On the other hand, some researchers believe that the material removal is due to the mechanical-enhanced erosion. Assuming that a fluid film exists between the wafer and pad interface that affects the material removal rate at each single point through the fluid stress, Runnel et al. (1994) developed an erosion-based model for CMP:

$$MRR = C\sigma_t\sigma_n \quad (2.7)$$

where, C is an all purpose coefficient, σ_t is the shear stress due to the slurry flow and σ_n the normal stress. This model has been integrated with the particle scale model by Tseng et al. (1997) and Zhang et al. (1998). Those researchers took the normal stress at the particle-wafer contact to the elastic indentation of the particle into the wafer surface, which is similar to that proposed by Cook (1990), and calculated the normal stress over the wafer-particle interface as:

$$\sigma_n = \frac{F}{\pi r_c^2} \quad (2.8)$$

where, F is the force acting on the spherical particles, which is proportional to the down pressure P and,

$$r_c = \left\{ \frac{3}{4} F \left(\frac{d}{2} \right) \left[\frac{(1-\nu^2)}{E} + \frac{(1-\nu'^2)}{E'} \right] \right\} \quad (2.9)$$

where, r_c is the radius of wafer-particle contact, d the diameter of particle, ν and ν' are the Poisson's ratios of wafer surface and the particle and E and E' the elastic modulus of the wafer and particles, respectively. The shear stress due to the slurry flow can be approximated as:

$$\sigma_t = C \sqrt{\mu V P A} \quad (2.10)$$

where, μ is the dynamic viscosity of the slurry and A the area of wafer surface.

Substitution of Eqn. 2.8 & 2.10 into Eqn. 2.7 yields:

$$MRR = \Psi P^{5/6} V^{1/2} \quad (2.11)$$

where, Ψ is a parameter to account for material properties, slurry abrasive concentration and chemical processes. This model demonstrated a non-linear relationship between the material removal and the pressure times velocity. In comparison to the Cook and Liu's model, Tseng's model is attempting to connect the elastic indentation to the erosion rate instead of the mechanical abrasion. While the down pressure dependency (an exponent of

5/6) is still close to a linear dependency, the velocity dependency (an exponent of 1/2) is quite nonlinear. This is because the contribution of velocity has been attributed to the slurry flow instead of a sliding of abrasives.

Zhang et al. (1998) proposed that a plastic deformation is a more likely deformation mechanism of polishing surfaces. The contact pressure over the particles-wafer interfaces is suggested to be equal to the hardness of the wafer materials. Replacing the expression of normal stress of Eqn. 2.8 in Tseng and Wang's model the following material removal rate formulation can be obtained:

$$MRR = \psi(PV)^{1/2} \quad (2.12)$$

where, ψ is a parameter to account for materials properties, slurry abrasive concentration and chemical processes. Zhang et al. (1998) also proposed that an adhesion force (van der waals force or electrostatic effect) contributes to the indentation. A thermodynamic work parameter of adhesion was used in the MRR to account for its effects on the indentation of abrasive particles by Ahmadi et al. (2001) and Mazaheri et al (2002, 2003).

All the models discussed above imply that the abrasives are embedded into the pad and indented into the wafer surface which is generally defined as 'two-body' models. In 'three body' modeling approach, it is assumed that the abrasive particles float in the slurry and impact the wafer surface from time to time. Su (2000) developed a model assuming a three-body abrasion of materials.

Since the material removal rate increases with the pad surface roughness and softer pad yields larger material removal rate [Moon, 1999], some pad based model by some

researchers [Yu et al., 1993; Steigerwald et al. 1997; Zhao et al., 1999; Luo et al., 2001]. Steigerwald et al. (1997) proposed that the material removal rate is proportional to the number of abrasive particles over the contact area. Based on this concept, Zhao et al. (1999) proposed a pad based model for soft pad CMP. Their model explains the nonlinear dependence of material removal rate on pressure at pad asperity contact. In order to predict the material removal rate, they took the real contact area between wafer and pad given by $A \propto P^{2/3}$ as the basis of their model. They assumed that the higher the contact area, higher number of abrasive will come into polishing and, their model can be given as:

$$MRR = k_p P^{2/3} V \quad (2.13)$$

where, MRR is the volume removal rate, P the nominal pressure, V the relative velocity, and k_p is a constant known as the Preston constant.

In abrasive-free CMP, since there is no hard abrasive particle in the slurry, the pad based model can be applicable to explain the direct pad-wafer interaction. But those models are developed based on the material removal mechanisms which are predominantly mechanical. Conversely, the mechanism of material removal in abrasive-free CMP is chemically dominant. Therefore, the existing pad based models are no longer applicable for abrasive-free CMP. The only empirical MRR model for abrasive-free CMP, developed by Zhang et al. (2001), can be expressed as:

$$f(c_{glycine}) = K_1 + K_2 c_{glycine} + K_3 c_{glycine}^2 \quad (2.14)$$

where, $f(c_{glycine})$ is the removal rate in terms of moles of Cu^{+2} per square meter per second, $c_{glycine}$ is the glycine concentration in moles per liter and K_1, K_2 and K_3 are the coefficients to account for all other issues of abrasive-free CMP. This is a kinetic model where the glycine concentration has been considered as the only input parameter. This model was developed to describe the features of the fluid transport model. But this model neither included the main process parameters nor the special non-prestonian nature of MRR of abrasive-free CMP.

From the literature survey, it is quite apparent that detail investigation of material removal mechanism and the effect of process parameters on MRR and WIWNU in chemically active abrasive-free CMP process are yet to be explored. Furthermore, the existing particle scale models, pad scale models and empirical models (for abrasive-free CMP) are not suitable to explain the issues in abrasive-free CMP process. Therefore, in this study, effort has been made to understand the key aspects of abrasive-free CMP process by doing experiments and developing a MRR model.

Chapter 3

Experimental Investigations

3.1 Introduction

This chapter describes the details of the blanket and pattern wafer preparation, polishing and measuring equipments and the procedures of experiments used for the investigation of material removal mechanism (wear mechanism) and the effect of different polishing conditions on process outputs (MRR and WIWNU) in blanket wafer polishing. This chapter also describes the experiments performed in polishing the pattern wafers in order to verify the understanding developed from the polishing results of blanket wafers.

3.2 Wafer Preparation

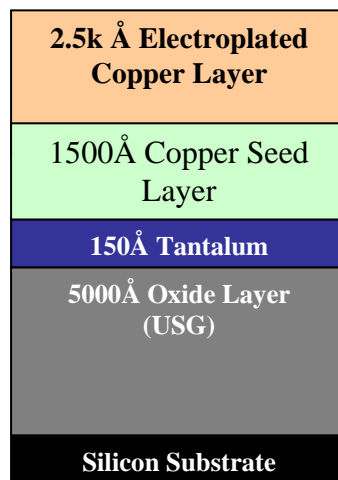


Figure 3.1 Preparation of blanket copper wafer

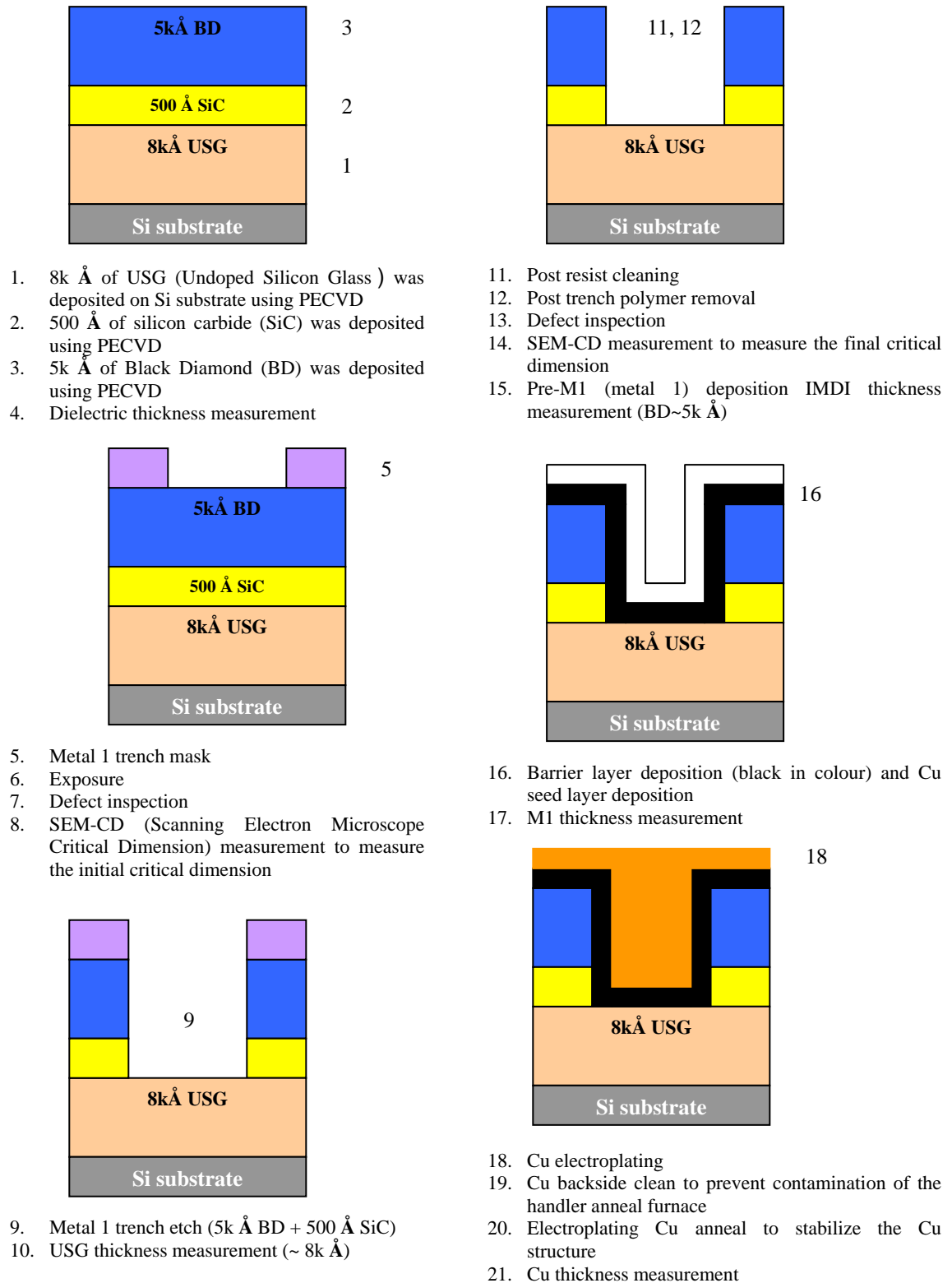


Figure 3.2 Preparation of Copper/Oxide pattern wafer

The blanket copper wafer is prepared by depositing several layers on the top of a silicon substrate as shown in Figure 3.1. An oxide layer of 5000 Å thickness is deposited on the silicon substrate by PECVD (Plasma Enhanced Chemical Vapour Deposition) method followed by deposition of 150Å Ta layer and 1500Å Copper seed layer by PVD (Physical Vapour Deposition). Finally, the copper layer is deposited on the copper seed layer by electroplating method. In order to prepare the pattern wafer, the silicon substrate need to go through a series of process (e.g. film deposition, trench etching and cleaning etc) to obtain the desired test structures. A summary of these steps are given in Figure 3.2.

3.3 Experimental Setup

3.3.1 CMP Polishing and Cleaning Unit

The experiments were carried out using the Mirra Mesa Advanced Integrated CMP machine (Mirra MesaTM - AMAT). The whole CMP machine consists of two main units: Mirra Polisher and Mesa Cleaner.

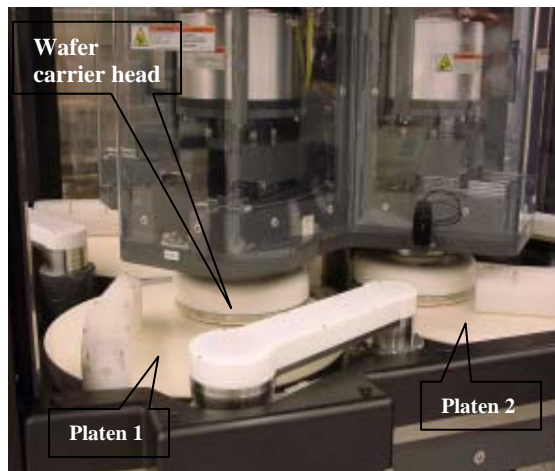


Figure 3.3 Mirra Polishing Unit

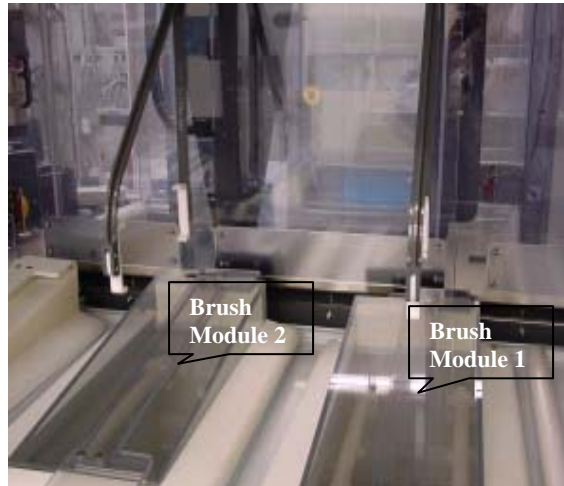


Figure 3.4 Mesa Cleaning Unit

The Mirra polisher as shown in Figure 3.3 is equipped with three platens and four heads, which enables up to three steps polishing on different polishing pads with different slurries. This multi step polishing capability is especially useful for copper CMP where the electrochemical nature of barrier metal differs greatly from copper. One or two-step polishing is also possible according to the materials to be polished. In this study, single step polishing was performed for copper blanket wafer and two-step polishing was carried out for pattern wafer. No matter how many steps are used, Mirra offers excellent process control with its optical end point detection system called ISRMTM (In-situ Rate Monitor). The Mesa post-CMP cleaner as shown in Figure 3.4 is equipped with a megasonic tank, two brush-scrubbing stations and spin-rinse-dry module. Megasonics remove residual polishing debris and slurry particles before entering brush module, which dramatically lowers particle loading to brushes. Brush modules remove particle and metallic ions on the surface by scrubbing with brushes. Different chemicals can be used at modules 1 and 2 for the effective cleaning. After cleaning at brush stations, wafers are passed to spin-rinse-dry

module. At this module, wafers are rinsed with deionized water and completely dried by spinning. Through the integration of Mirra and Mesa, dry-in and dry-out process can be achieved which minimizes particle contamination and corrosion. Total CMP process time is also greatly reduced by such integration. The wafers are transferred from one unit to other units using two robotic systems (Part 2 and 4 in Figure 3.6). The first robot is used to deliver the wafers from the cassette to the Mirra polishing unit and to collect the wafers from Mesa cleaning unit. The other robot is used to transfer the wafers among different parts of Mira Polishing and Mesa Cleaning units.

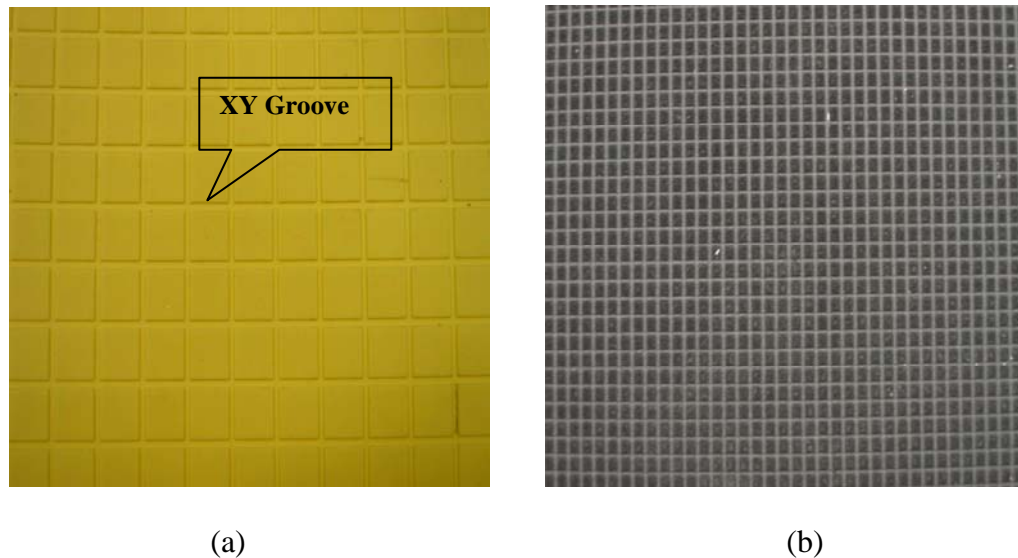


Figure 3.5 Polishing Pads: a) A polyurethane copper polishing pad with XY groove, b) A Politex cleaning pad

3.3.2 Polishing Pad and Cleaning Pad

A Rodel – Nitta IC1000 with XY grooves was used for copper polish and a Politex pad was used to clean (buff) the post –CMP wafers. The Polyurethane and Politex pads was used in this study have been shown in Figure 3.5.

3.3.3 Abrasive-free Slurry

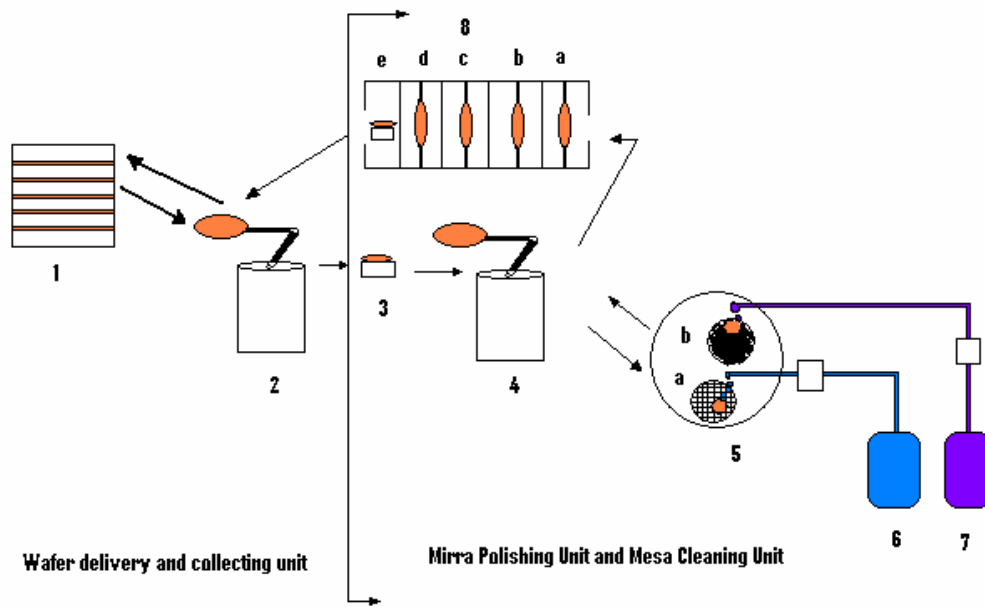
In this study, chemically active slurry (MORESCO™ abrasive free slurry) was used to polish both Cu blanket wafer and the Cu of pattern wafer. It was necessary to prepare the slurry by instant mixing the raw slurry with hydrogen peroxide (oxidizing agent). The ratio of abrasive-free slurry and hydrogen peroxide was 2.23:1 (vol / vol). Besides, the viscosity of the slurry was 1mPa and the slurry used in abrasive-free CMP was usually kept acidic in nature. In this study, the slurry pH was found always between 2.2 to 2.5.

3.4 Experimental Procedure of Copper CMP

The schematic of copper CMP system used in this study has been shown in Figure 3.6. The blanket wafers, kept in the cassette, is delivered to the Mirra Mesa Integrated CMP system by a robotic wafer handler. Another robot of the CMP system carries the wafer to the vacuum cup which holds the wafer and carries it to the pad. The wafer and the pad rotate in the same direction, and the slurry is dispensed on the pad very close to the wafer to ensure the better distribution of slurry at pad wafer interface during polishing. After polishing the blanket wafer, it is again buffed with politex pad to remove fine particles and scratches on the surface. Since DI water is dispensed during buffing operation, it is also called rinsing operation. In this work, since the abrasive-free slurry was chemically active, long rinsing time (50 sec) was selected to remove all reactive chemical agents from the wafer. After polishing and rinsing operation, the blanket wafer is transferred to the Mesa Cleaning Unit where it goes through the megasonic tank, two brush-scrubbing stations and spin-rinse-dry module. Finally, the dry and clean wafer is

collected by the robotic handler and sent it back to the wafer pod or cassette for further experimental investigation.

Single step polishing was performed for copper blanket wafers using platen 1 (Figure 3.3). On the other hand, the pattern wafers were polished in two steps. Firstly, the pattern wafers were polished to remove copper using the abrasive-free slurry in platen. Then the barrier polishing is carried out using barrier slurry (abrasive slurry) in platen 2. The dishing and erosion value of the pattern wafer after abrasive-free Copper CMP also affects the dishing and erosion value obtained after barrier polish. Therefore, in this work, the Copper CMP was performed using the optimized polishing conditions obtained from the polishing data of Cu blanket wafers.



1. Wafer Cassette
2. Wafer delivery and collecting robot
3. Entrance of wafer in Mirra Unit
4. Mirra Mesa robotic handler
5. Mirra CMP polisher
 - 5.a Copper polishing pad
 - 5.b Buffing pad
6. Abrasive-free slurry container
7. DI water container
8. Mesa Cleaning Unit
 - 8.a Megasonic Tank
 - 8.b & 5.c. Brush Scrubbing Station
 - 8.d Spin-rinse-dry Module
 - 8.e Wafer Collection Chamber

Figure 3.6 Schematic diagram of copper CMP system

3.5 Metrology Tool

The metrology tools used for the experimental investigations are introduced in the following sections

3.5.1 Four-Point Probe

Four-point probe from ASYST (OmniMap Auto RS75/tc) was used to measure the thickness of the copper layer before and after polishing. The difference of thickness

between pre and post CMP gives the material removal rate of the respective CMP process. The thickness of the layer is measured by measuring the resistivity of the copper thin film. The four-point probe setup consists of four equally spaced tungsten metal tips with finite radius, which are made to contact the sample under test. Each of them is supported by springs on the other end to minimize sample damage during probing. The current is supplied by a high impedance source. On the other hand, the voltmeter is used to measure the voltage. Both of them are utilized to determine the resistivity of the sample. If the spacing between the probe points is constant, and the conducting film thickness is less than 40% of the spacing, while the edges of the film are more than four times the spacing distance from the measurement point, the average resistance of the film or sheet resistance is given by:

$$R_s = 4.53 (\text{Voltage/Current}) \quad (3.1)$$

The thickness of the film (cm) and its resistivity (in ohm cm) are related to R_s by,

$$R_s = \text{Resistivity/ Thickness} \quad (3.2)$$

By knowing R_s and resistivity, the thickness of the layer can be measured. In this study, the thickness of the wafer was measured at 80 point in order to get the no-uniformity of removal rate across the wafer. In addition, the average removal rate was calculated by averaging the data of all 80 points.

3.5.2 Standard Mechanical Inter-face (SMIF) Profiler

SMIF profiler is a tool for measuring the dishing and erosion of pattern wafer. These measurements are very crucial for CMP process development. A KLA Tencor P-30 SMIF profiler was used in this study which gives precision profiles using the stylus and Standard Mechanical Inter-face (SMIF) technique. A built-in vibration isolation system

ensures high-precision measurement errors. It was quite convenient to use this profiler to select the required test structures and to measure dishing and erosion of that particular structure.

3.5.3 Therma Wave Opti-Probe-5250I

The Opti-Probe was used to measure the dielectric loss (oxide) after polishing the overlying barrier layer of pattern (copper/oxide) wafers. The design of Opti-Probe provides simultaneous, continuous and independent measurements of thickness and refractive index of films. It integrates up to six different technologies for measuring films. Those are Beam Profile Reflectometry (BPR), Beam Profile Ellipsometry (BPE), Absolute Ellipsometry (AE), Visible Spectrometer (VS), Broad Band Spectrometer (BBS), and Spectroscopic Ellipsometry (SE). In this study, the subtractive mapping of film thickness measurement was used to measure the pre and post CMP dielectric thickness of pattern wafer after barrier polishing.

3.5.4 Scanning Electron Microscopy (SEM) and Energy Dispersive X-ray (EDX)

A Defect Review Scanning Electron Microscopy (DR-SEM) manufactured by Applied Materials was used in this study. This equipment was used for both surface analysis polished wafer and the elemental and structural analysis of chemically formed layers and defects. The SEM with one electron beam can be operated with a resolution of 4 nm. The maximum values of magnification and accelerating voltage which can be attained by the microscope, are 50,000X and 600V-10000V respectively. The probe current ranges from 10^{-12} to 10^{-6} A. An Energy Dispersive X-ray (EDX) machine

associated with the SEM was also used for the elemental analysis of the chemically modified layers and the defects generated from CMP.

3.5.5 Atomic Force Microscopy



Figure 3.7 Atomic Force Microscopes

The Atomic Force Microscope (AFM) (Nano Scope III) Digital Instruments was used in this study. The AFM measures the topography of the sample by detecting the atomic-level forces through an optical measurement of the movement of a very sensitive cantilever tipped usually hard, pyramid-shaped crystal moved along surfaces. In this study, tapping mode AFM technique has been used to scan the blanket wafers in order to get the 3D surface topography and surface roughness after abrasive-free polishing.

3.5.6 Mitutoyo FORMTRACER

Mitutoyo FORMTRACER (CS-5000), operated with a cone type stylus (F-421895), was used to measure the surface roughness of the pad used for polishing copper wafer. The photograph of the machine is shown in Figure 3.8. The height, radius and angle of the

stylus are 14.08 mm, 2 μm and 60° respectively. The resolutions of the machine in X and Z directions are 0.00625 μm and 0.002 μm respectively. The machine, which has diaphragmatic air spring as a vibration isolator, can also be operated with measuring force of 4 mN and measuring speed of 0.2 mm/s.



Figure 3.8 Mitutoyo FORMTRACER (CS-5000)

3.6 Experimental Plan

Abrasive-free CMP for copper blanket and pattern wafers was carried out at different polishing conditions. Copper blanket wafers were polished in order to investigate the role of the polishing conditions on material removal rate, within-wafer non-uniformity, surface quality, material removal mechanism, etc. Based on the surface analysis and the results of MRR and WIWNU of blanket wafer polishing, fundamental understanding of abrasive-free CMP was developed and some optimized polishing conditions were selected. In order to verify the understanding developed so far, those optimized polishing conditions were chosen for polishing pattern wafers. In addition, from the experimental investigation, some dominant wear mechanisms were established. Finally, based on the developed

concepts, a pad based MRR model was developed which was further verified by the experimental data of abrasive-free CMP of copper blanket wafer. For experimental investigations, wide ranges of polishing conditions were chosen, and the polishing conditions of different experimental study would be mentioned in the respective part of the following chapters.

Chapter 4

Material Removal Mechanism in Abrasive-free Copper CMP Process

4.1 Introduction

Abrasive-free CMP is one of the popular polishing techniques for copper/low-k multilevel interconnect fabrication. Since the abrasive-free slurry does not contain any hard particle, the direct interaction between the pad asperities and the wafer surface along with chemical action of slurry greatly influence the material removal mechanism during polishing. It is generally known that wear is a kind of material removal from one or both of the two sliding surfaces by mechanical or/and chemical means which is usually accelerated by the application of friction force/temperature. Therefore, the study of wear phenomena can effectively explain the material removal mechanisms in abrasive-free copper CMP process.

This chapter describes the analysis of wear mechanism in abrasive-free copper CMP process supported by extensive experimental results. A comprehensive discussion on the results is also incorporated. In this study, the method of elimination has been followed to figure out the possible wear mechanisms. The qualitative analysis has been carried out on the surface of the wafers polished at different polishing conditions. Besides, the role of the process parameters in wear mechanisms has been investigated. The qualitative analysis involves the surface morphology analysis, sectional analysis, elemental analysis, etc which are carried out by SEM, AFM, and EDX. Based on those analyses, the material removal or wear mechanisms in abrasive-free copper CMP process have been identified.

4.2 Theory of Material Removal Mechanism

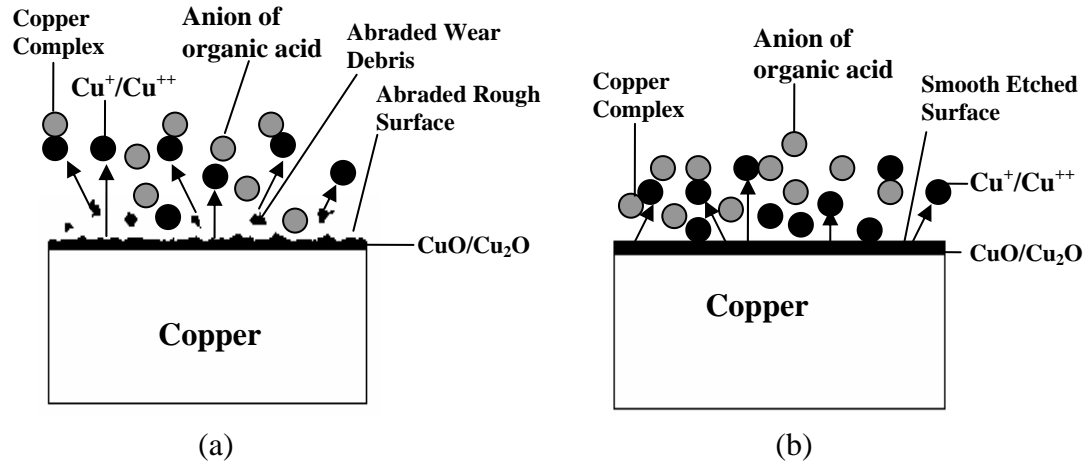


Figure 4.1 Schematic of material removal using slurry of low pH and high oxidizer concentration: a) dissolution of abraded $\text{CuO}/\text{Cu}_2\text{O}$ wear debris in abrasive CMP process, b) direct etching of $\text{CuO}/\text{Cu}_2\text{O}$ layer in abrasive-free CMP process

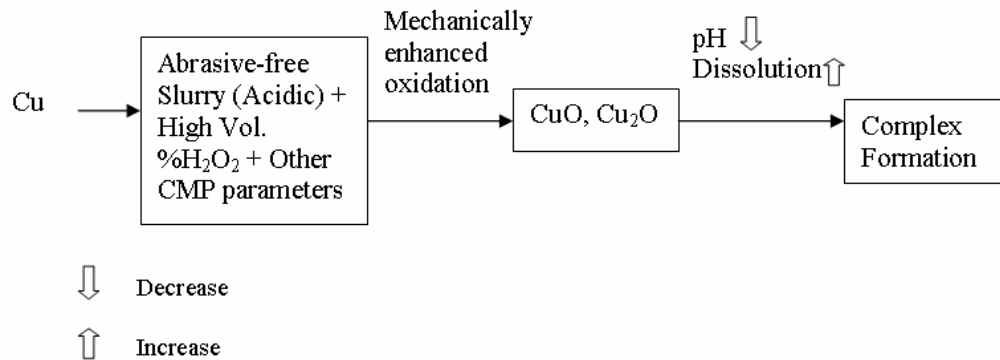


Figure 4.2 Steps of copper removal in CMP process using acidic slurry

4.2.1 Material Removal/ Wear Mechanism in CMP Process

CMP is the combination of mechanical component (mostly the abrasion of surface) and chemical component (dissolution of abraded species) [Steigerwald et al., 1995]. In

conventional abrasive CMP process, copper oxide is abraded by the hard abrasives followed by chemical dissolution of wear debris. The mechanism of MRR in conventional abrasive CMP process explained by Hernandez et al. (2001) is shown in Figure 4.1.a. This is equally true for abrasive-free CMP process but the nature of those components is fairly different. The conventional slurry usually contains hard abrasive particle, oxidizer, corrosion inhibitor and etchant. According to Kondo et al. (2000), abrasive-free slurry also contains all those ingredients except the hard abrasive particles. Oxidizer acts as electron acceptor to oxidize copper. Different kind of organic acid such as Citric Acid, Oxalic Acid, Succinic Acid, etc are used as etchant to dissolve the copper oxide layer. In abrasive CMP process, the thick CuO/Cu₂O layer formed on the top is mechanically removed (abrasion, microcutting, erosion, burnishing, etc) by the abrasive particles followed by the dissolution of the wear debris by etchant [Steigerwald et al., 1995; Hernandez et al. 2001]. Conversely, in abrasive-free CMP process, the cupric layer is expected to be directly etched out leaving smooth surface on the top of the wafer as shown in Figure 4.1.b. Since the dissolution or etching basically depends on the pH of slurry, the abrasive-free slurries are basically kept acidic in nature [Fischer et al., 1988], and the steps of material removal using acidic slurry are shown in Figure 4.2. In this study, the pH of abrasive-free slurry was found between 2.2 and 2.5.

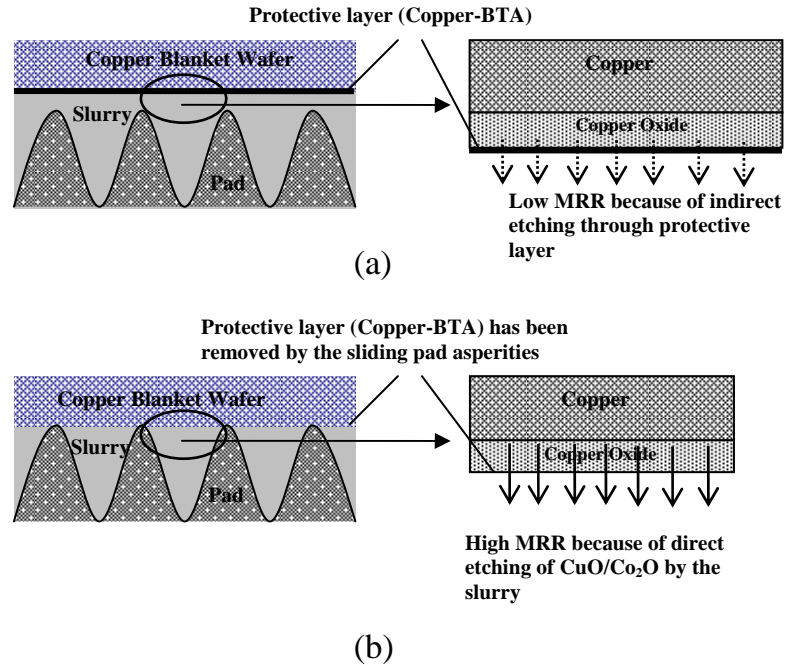


Figure 4.3 Mechanism of material removal: a) indirect etching at floating/hydroplaning contact, b) direct etching at sliding contact

The main problem in using acidic slurry is isotropic etching at both raised and recessed area of the pattern wafer [Steigerwald et al., 1995]. BTA (Benzotriazole) forms a mono-layer of copper-BTA which protects the wafer from etching/corrosion. In abrasive free CMP process, for pattern wafer polishing, the protective layer at raised area does not allow etching until it is removed by pad asperity. For blanket wafer polishing, although there is no raised and recessed topography similar to pattern wafer, total material removal rate greatly depends on the cyclic removal of the BTA layer. If the polishing condition (pressure, velocity and removal rate) is such that the polishing is similar to the floating polishing process (hydroplaning mode), sufficient number of pad asperity can not come in contact with wafer to remove the protective layer. Hence, the material is removed through the pores or fissures of the protective layer giving significantly less material removal rate

as shown in Figure 4.3.a [Rabinowicz, 1995]. Conversely, if the polishing condition provides the sliding contact of sufficient number of pad asperities with the wafer, the protective layer will be removed by soft friction giving high MRR because of direct etching as shown in Figure 4.3.b. In this work, types of material removal as shown in Figure 4.3.a and 4.3.b will be designated as Indirect Etching and Direct Etching respectively, and these will be supported by the MRR data in Chapter 5.

The most frequent wear mechanism in conventional CMP process noticed in literature are mechanical wear (abrasion, erosion, adhesion, fatigue, fretting, rolling, burnishing, etc) and chemical wear (corrosive wear) [Rabinowicz, 1995; Lai, 2001; Bhushan, 2002]. The abrasive-free slurry does not contain any hard particle. So, the abrasion, erosion and rolling wear caused by the mechanical action of hard particles are practically impossible in abrasive-free CMP process. Therefore, it can be primarily speculated that the possible mechanisms of wear in abrasive-free CMP process, which do not involve the particle-surface interaction, are corrosive wear, adhesion wear and fatigue wear. In this chapter, surface analysis has been performed to figure out all possible wear mechanisms of abrasive-free CMP process.

4.2.2 Pressure and Velocity Distribution across the Wafer

Apart from corrosive wear, all other form of wear is predominantly mechanical. According to Preston's equation [Preston, 1921], pressure and velocity play significant role in removing material by mechanical means. So, in order to understand the role of those mechanical parameters on the with-in wafer wear variation (WIWWV), it is essentially important to understand the distribution of pressure and velocity across the wafer.

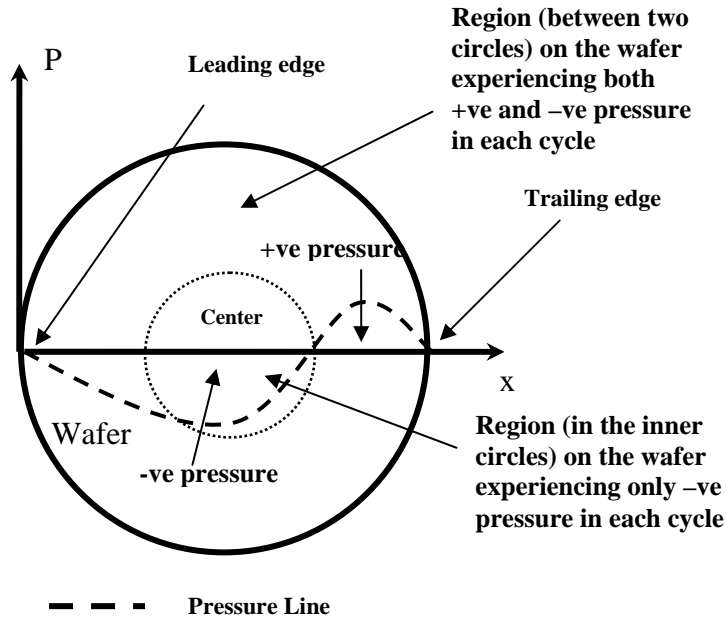


Figure 4.4 Schematic of pressure distribution across the wafer

Zhou et al. (2002) proved that the leading two thirds of the wafer experiences a “negative” fluid pressure, and the trailing one third experiences “positive” pressure during polishing (Figure 4.4). Therefore, in each cycle or rotation, the center portion of the wafer experience negative pressure. On the other hand, the edge and middle portion experience both positive and negative pressure in each half cycle respectively. Thus, the load that is exerted on the middle and edge of a wafer is a kind of repeated loading and unloading which might cause the fatigue wear in CMP process. In addition, the pressure distribution may have significant influence in holding the volume of slurry at wafer pad interface, and consequently, corrosive wear will also be influenced.

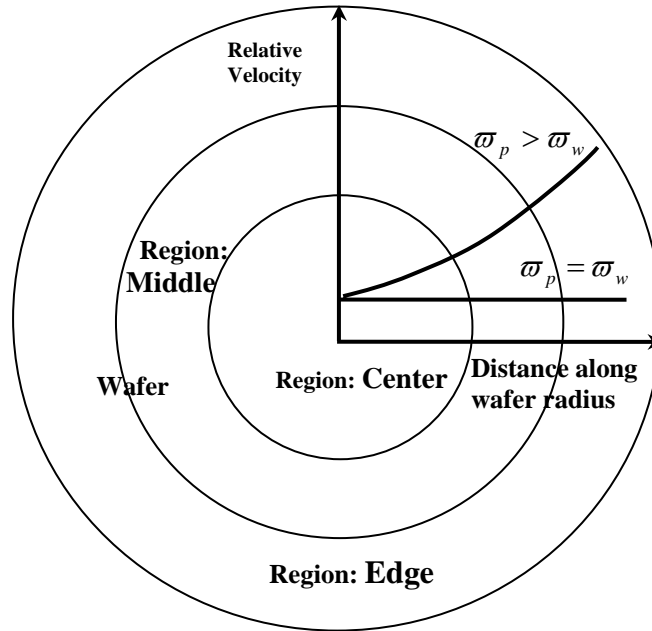


Figure 4.5 Schematic of velocity distribution across the wafer

The relative velocity at any point of wafer with respect to pad varies in a non-linear fashion across the wafer [Tseng et al., 1999]. A typical velocity distribution from center to edge has been given in Figure 4.5 where it has been shown that if the pad rotation rate is kept higher than that of wafer, the center portion of the wafer experience low relative velocity than that of edge. But if the rotation rates of pad and wafer are kept almost equal to each other, which have also been maintained in this study, the velocity distribution will be uniform across the wafer [Art. 5.2.2]. Therefore, the effect of the variation of relative velocity on WIWWV is expected to be negligible.

4.2.3 The Possible Wear Mechanisms in Abrasive-free CMP

The theory of the possible wear mechanisms has been discussed as follows:

4.2.3.1 Corrosive (Chemical) Wear

The corrosive wear of metal occurs if the metal is placed in the environment where a sliding surface interacts chemically with it and wears the surface [Rabinowicz, 1995]. The most dominant corrosive agent of the environment is oxygen of air or the oxidizing agent of liquid. The chemically modified surface of metal initially protects the surface from further corrosion but if it is under sliding condition, the chemical layer is worn off so that chemical action continues. Therefore, corrosive wear requires both the chemical reaction and rubbing. There are mainly two kinds of corrosive wear given by Rabinowicz (1995). Firstly, if the chemically modified surfaces are harder than the surface on which it is formed, the layer is worn off after getting certain thickness. In this type of wear, the total thickness flakes off in one cycle giving high material removal rate. Secondly, if the product layer is ductile and softer than the surface, then the part of the layer is removed. Fischer et al. (1988) proposed another kind of corrosive wear where he described the tribochemical dissolution of silicon nitride in water at the contacting asperities which gives extremely smooth surface.

4.2.3.2 Adhesion Wear

The adhesion wear of surface occurs because of the attractive force acting between the surface atoms of two materials. The attractive force acting between the two sliding surfaces pull off the material from one surface to the other surface resulting in the formation of fragments. The adhesion wear takes place both in solid-solid contacts and

liquid mediated contact. Strong adhesion occurs if the two sliding surfaces are very clean and smooth having little or no chemical films in between. On the other hand, the presence of contaminants, liquid films, etc at the sliding surfaces reduces adhesion wear. Generally, very weak adhesion is observed at the well lubricated surfaces [Bhushan, 2002].

4.2.3.3 Surface Fatigue Wear

Surface fatigue wear is observed when a brittle surface experiences repeated loading and unloading cycles. Fatigue wear makes surface or subsurface crack with the formation of fragments. The CuO/Cu₂O layer formed in CMP process is brittle in nature [Rajiv et al., 2002], and two third of a wafer experience repeated loading and unloading in each cycle. Therefore, fatigue wear is assumed to be a possible mechanical wear in CMP process.

4.3 Experimental Findings

During polishing, the wafers experienced two kinds of pressure, namely membrane pressure and retaining ring pressure, and the membrane pressure was kept higher than the retaining ring pressure. On the other hand, the rotation rate of pad was kept higher than the rotation of wafer. The reason of such selection of pressure and rotation rate will be discussed in Chapter 5. However, for experimental investigation of wear phenomena, a wide range of pressure (6.89/9.85 kPa, 10.34/13.1 kPa, and 13.7/16.54 kPa), rotation rate (30/27 rpm, 78/75 rpm and 120/117 rpm) and slurry flow rate (100 ml/min, 150 ml/min and 200 ml/min) was selected for both DI water and abrasive-free CMP process. Since both DI water and abrasive-free slurry do not contain abrasive particle, the wear found in

DI water CMP process may help to understand the possible mechanical wear in the chemically dominated abrasive-free CMP process. In this study, qualitative analysis was performed to comprehend the wear mechanism which involved the analysis of surface morphology using SEM and AFM, sectional analysis using AFM and the elemental analysis using EDX.

4.3.1 Effect of Polishing Conditions in Wear Mechanisms

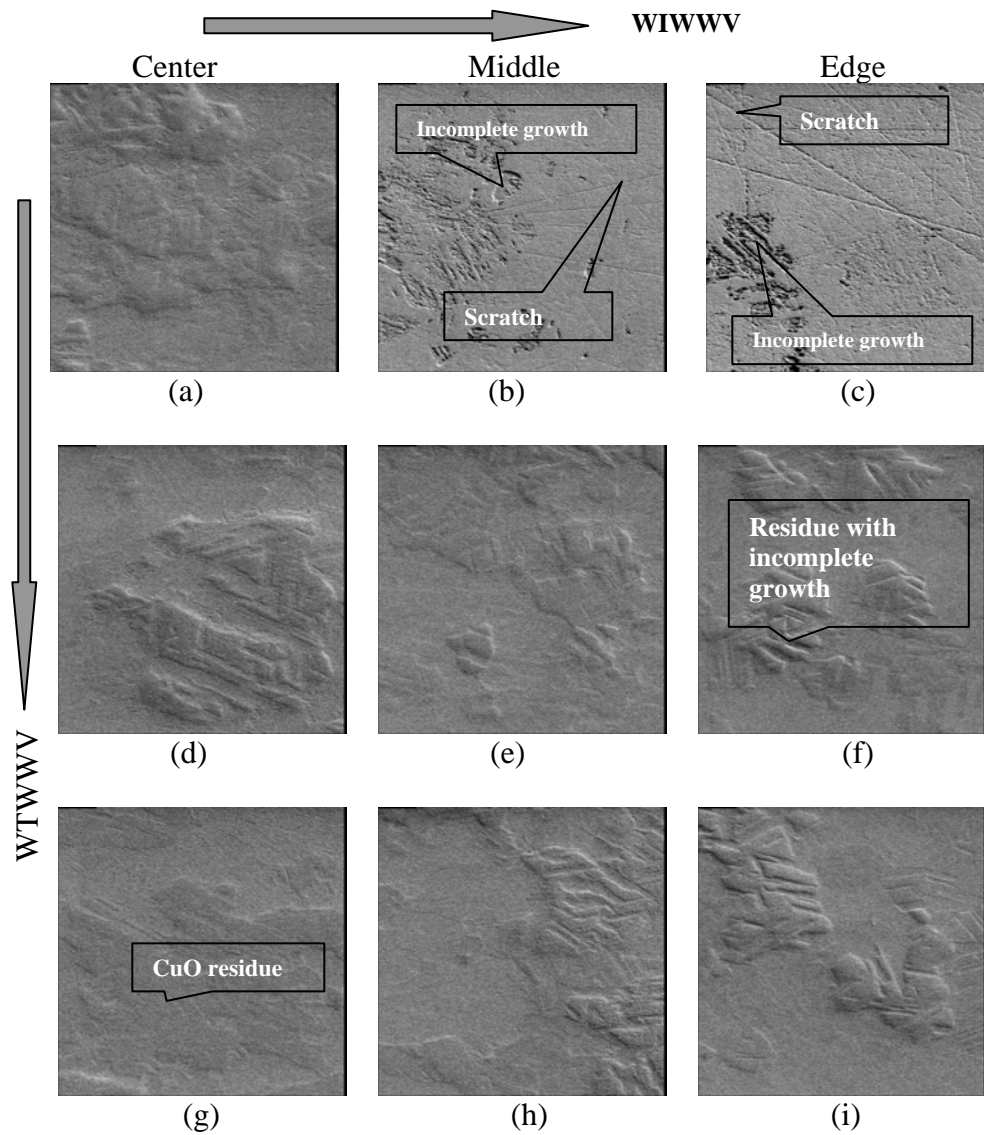


Figure 4.6 Effect of slurry flow rate on polished surface at 100 ml/min (a, b, c), 150 ml/min (d, e, f) and 200 ml/min (g, h, i) on WIWWV and WTWWV ($10\ \mu\text{m} \times 10\ \mu\text{m}$)

The surface analyses of the polished wafers were carried out at different polishing conditions. Such analyses helped to understand the role of different process parameters in the wear mechanism. It is interesting to note that, for same polishing condition, surface characteristics of polished wafers were found different at different locations of the wafer. Such variation of wear has been defined as with-in wafer wear variation (WIWWV). Therefore, the surface analyses were performed at center, middle and edge of the wafers. Furthermore, because of the change of polishing conditions, the wear mechanism of one wafer varies from other which has been defined as wafer-to-wafer wear variation (WTWWV).

Experiments were performed to study the effect of flow rate on the wear mechanism in abrasive-free copper CMP process. Low, moderate and high slurry flow rates were used at rotation rate and pressure at 78/75 rpm (pad / wafer) and 10.34/13.1 kPa (membrane / retaining ring) respectively. Some residue was found at center of the wafers irrespective of flow rate as shown in Figure 4.6. On the other hand, residues were also found all over the wafer at high flow rate (150 ml/min and 200 ml/min). Incomplete growth and scratches on the oxide layer were found only at middle and edge of wafers when the flow rate was 100 ml/min (Figure 4.6.b and 4.6.c).

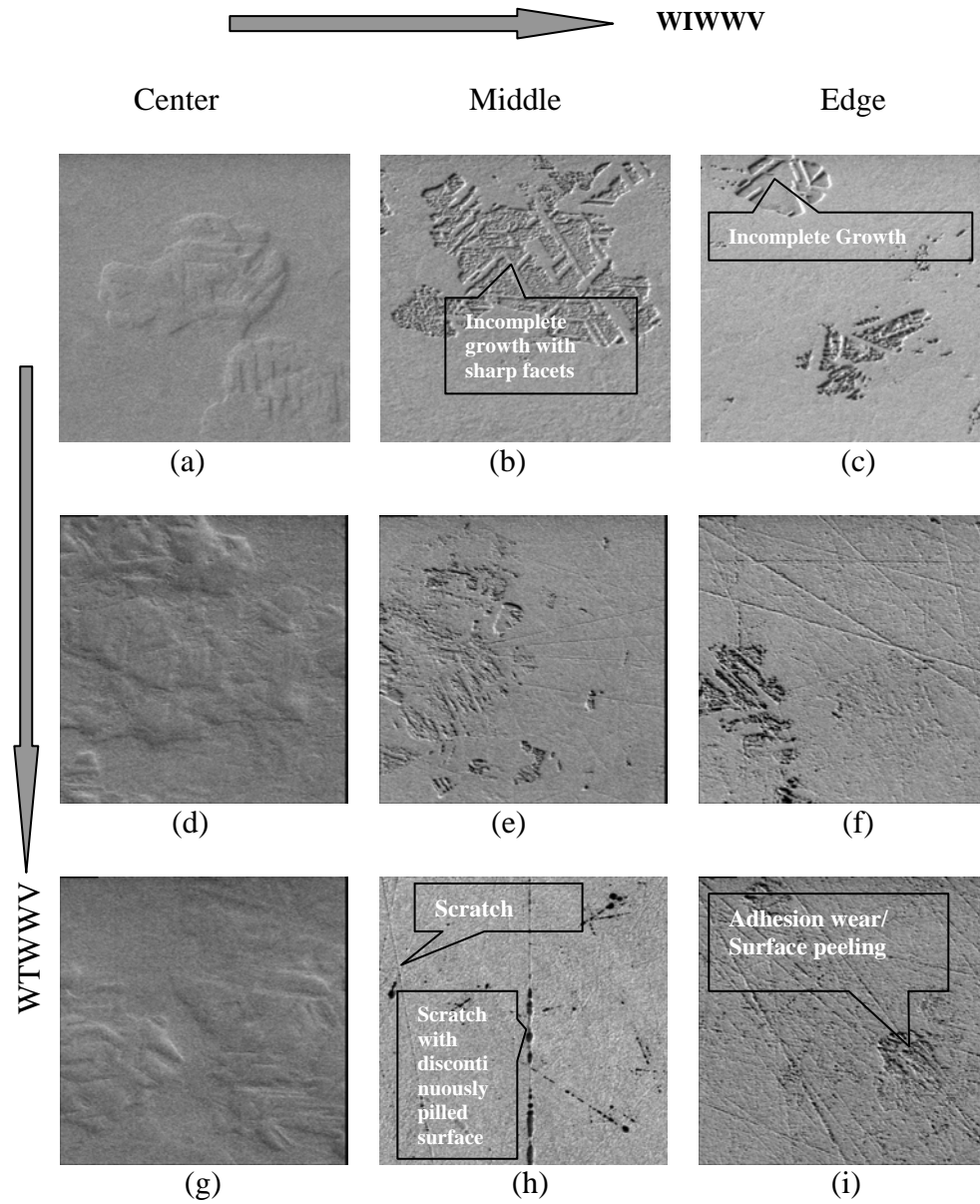


Figure 4.7 Effect of pressure on polished surface at 6.89/9.65 kPa (a, b, c), 10.34/13.1 kPa (d, e, f) and 13.7/16.54 kPa (g, h, i) on WIWWV and WTWVV ($10\ \mu\text{m} \times 10\ \mu\text{m}$)

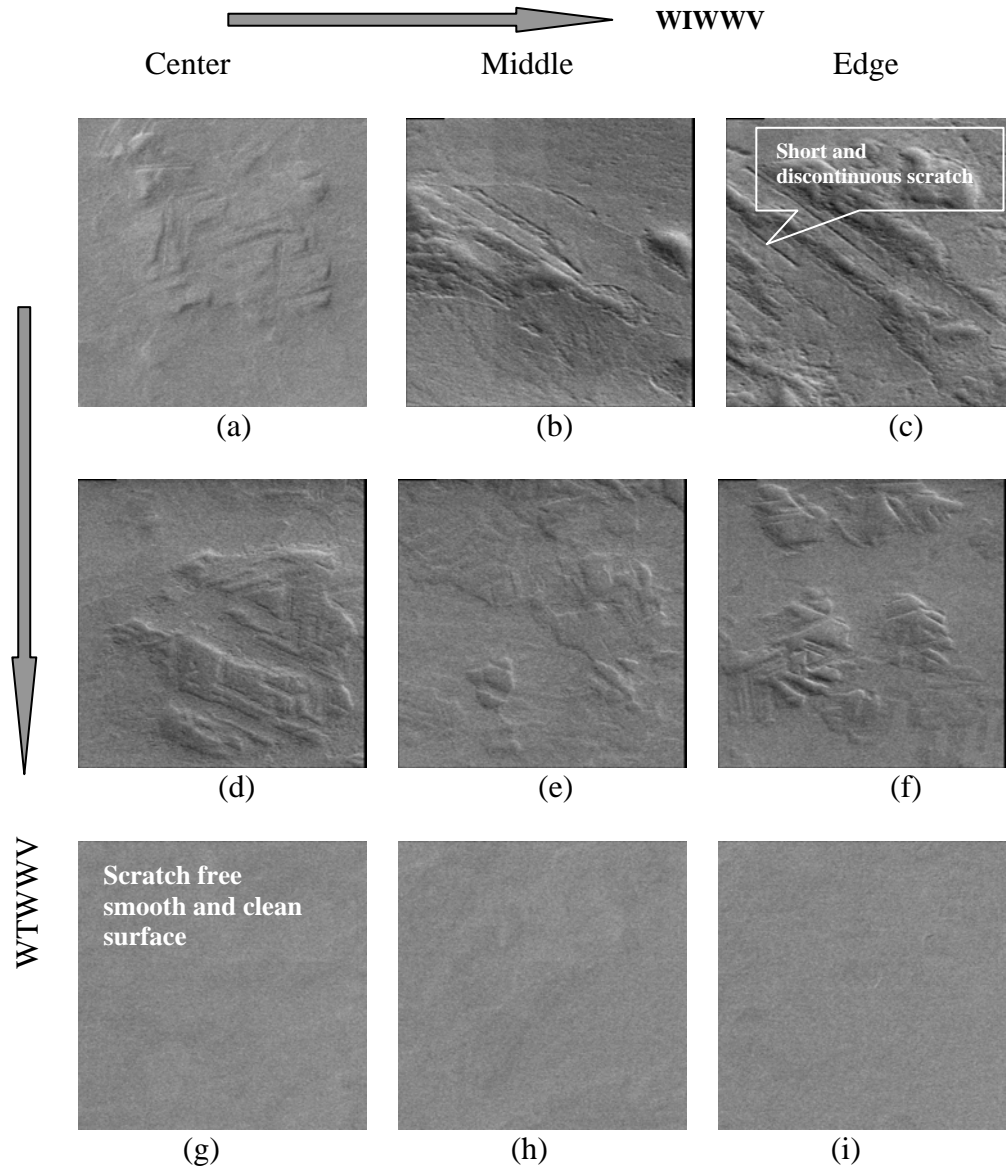


Figure 4.8 Effect of velocity at 30/27 rpm (a, b, c), 78/75 rpm (d, e, f) and 120/117 rpm (g, h, i) on WIWWV and WTWWV ($10\ \mu\text{m} \times 10\ \mu\text{m}$)

In order to understand the effect of pressure on the mechanism of wear, wafers were polished at three different pressures keeping the flow rate (100 ml/min) and rotation rate (78/75 rpm) constant. Residues were visible at center of the wafers at all three pressures as shown in Figure 4.7.a, 4.7.d and 4.7.g. Conversely, at low pressure CMP

(6.89/9.85 kPa), the incomplete growth of the layer was noticed at middle and edge of the wafer (Figure 4.7.b, 4.7.c). At moderate and high pressure CMP (10.34/13.1 kPa and 13.7/16.54 kPa), severe scratches and surface peeling were observed at middle and center of the wafer as shown in Figure 4.7.e, 4.7.f, 4.7.h and 4.7.i. Interestingly, no scratches were found at center of the wafers at any pressure and at any location of the wafer polished at 6.89/9.85 kPa. Moreover, the middle portion of the wafers experience lesser and shallower scratches than the edge.

The effect of rotation rate on the mechanism of wear was studied at three different rotation rates while the pressure (10.34/13.10 kPa) and flow rate (150 ml/min) were kept constant. Residues were found in both 30 rpm and 78 rpm pad speed (Figure 4.8a-4.8.f). The residue with incomplete growth was visible in both low rotation rate and moderate rotation rate. It is interesting to note that some sort of discontinuous scratches were found on the wafer polished at low rotation rate (30/27 rpm). On the other hand, at high rotation rate (120/117 rpm), very clean and smooth surfaces were found at any location of the wafer (Figure 4.8.g-4.8.i). Besides, the variation of wear phenomena across the wafer is insignificant at any particular relative velocity which validates the argument of Art.4.2.2.

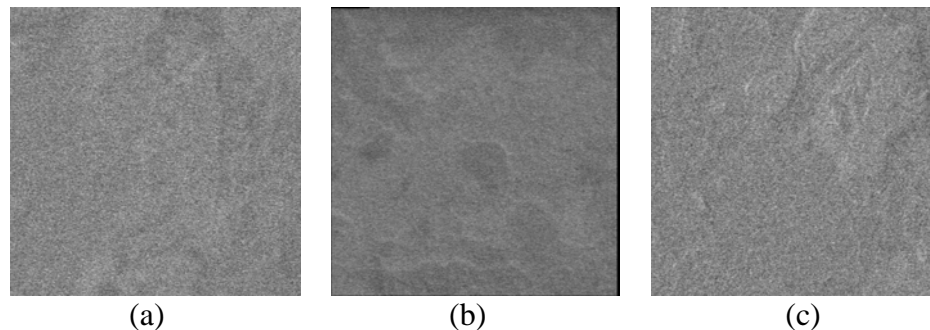


Figure 4.9 Wear characteristics of abrasive-free CMP at pressure 6.89/9.65 kPa, rotation rate 78/75 rpm and slurry flow rate 200 ml/min ($10\ \mu\text{m} \times 10\ \mu\text{m}$)

From the experimental observation, it was presumed that better surface can be achieved if low pressure, moderate rotation rate and high flow rate (e.g. 6.89/9.85 kPa, 78/75 rpm and 200 ml/min) is selected during polishing. After observing the polished surface under SEM, very clean etched surface was found all over the wafer surface (Figure 4.9). Interestingly, no residue, incomplete growth and scratches were found at any location of the wafer surface.

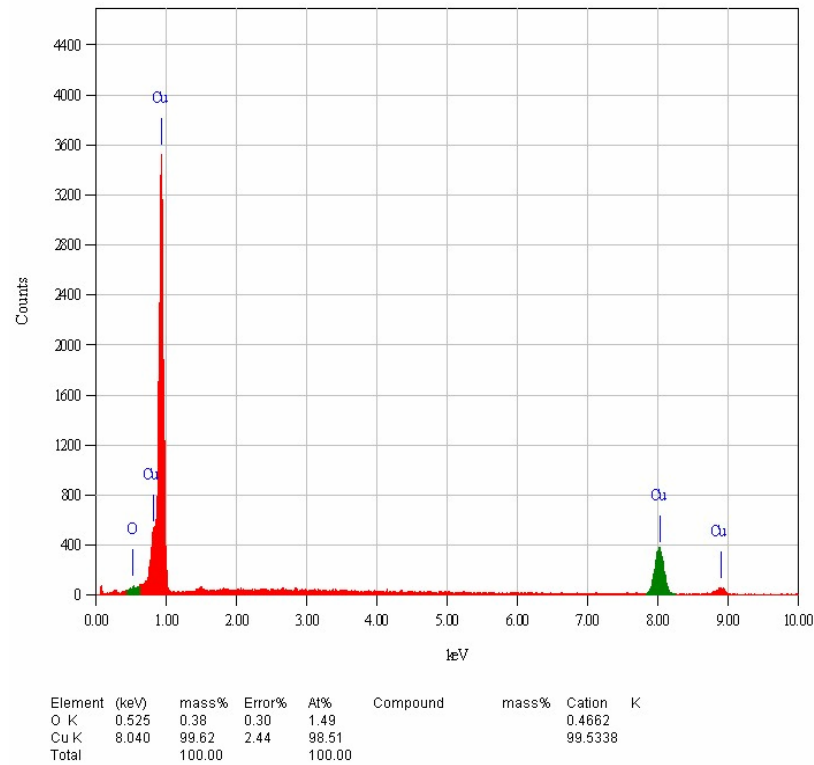


Figure 4.10 EDX (Energy Dispersive X-Ray) analysis of wafer surface polished in abrasive-free copper CMP process

4.3.2 Elemental Analysis of the Polished Surface Using EDX

For qualitative analysis of wear mechanism, it is essential to know the composition

of the layer formed on the top of polished wafers. The EDX analysis of the polished wafer as shown in Figure 4.10 shows the presence of copper and oxygen on the wafer surface. Interestingly, the trace of oxygen was found only 0.38% while the trace of copper was found 99.62% on the wafer surface. Therefore, it is quite evident that CuO/Cu₂O is formed on wafer surface during polishing. The lack of oxygen found on the polished wafer might be because the oxygen ions (coming from CuO/Cu₂O) combine with the hydrogen ions (coming from organic acid) resulting in the formation of water. The elemental analysis clearly indicates that as soon as the CuO/Cu₂O layer is formed, it is etched out by the chemically active abrasive-free slurry leaving almost pure copper surface.

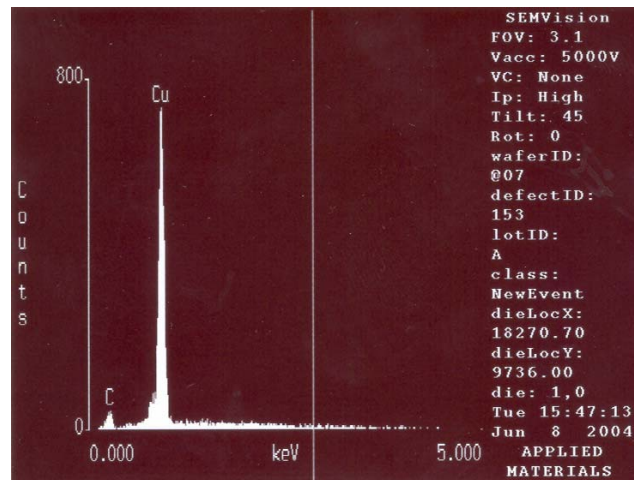


Figure 4.11 EDX analysis of wafer surface polished in DI water CMP process

4.3.3 Surface Analysis of Wafer Polished in DI Water CMP Process

DI water CMP is a kind of abrasive-free CMP process where the DI water is used as the slurry. Since the DI water is not chemically active, if the chemical wear (corrosive wear) is excluded, the possible wear mechanisms are supposed to be mechanical wear.

Besides, as the DI-water does not contain any abrasive, it can give idea about the possible mechanical wear mechanism of abrasive-free CMP process. To understand such mechanical wear, copper blanket wafers were polished with DI water. The dominance of mechanical wear in DI water CMP process was also noticed by Xu et al. (2004). In this study, the material removal rate of DI water CMP was found fairly low as given in Table 4.1. This proves that, the role of chemistry is almost absent while the scratches and grooves on the surface proves the dominance of mechanical parameters. The EDX analysis of the polished wafer shows that there is no trace of oxygen on the wafer surface (Figure 4.11). Therefore, the formation of brittle CuO/Cu₂O is almost absent in this CMP process. The trace of carbon was found which may come from the polymeric pad material.

Table 4.1 Material removal rate at different polishing conditions in DI water CMP process

Type of slurry	Flow Rate (ml/min)	Pressure (kPa) Membrane/ Retaining Ring	Rotation Rate (rpm) Pad/Wafer	Removal Rate (Å/min)
DI water	200	6.89/9.85	78/75	31.86
	ml/min	10.34/13.86		95.63
		13.7/16.54		29.38

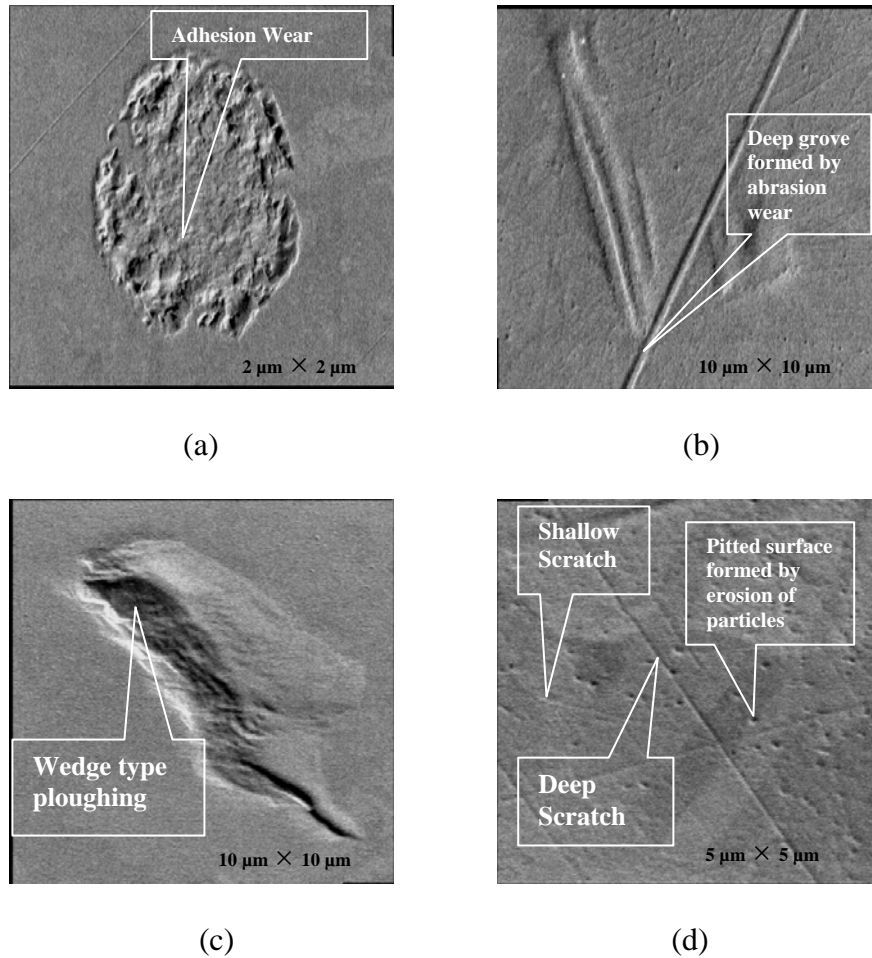


Figure 4.12 Surface analysis of wafer polished in DI water CMP: a) adhesion wear, b) formation of scratches and grooves, c) wedge type ploughing, d) formation of pitted surface

If the corrosive wear is excluded, the possible wear mechanism in DI water CMP are chiefly adhesion wear and fatigue wear. Since the formation of brittle layer is nearly absent, the fatigue wear is reasonably absent in DI water CMP process. From Figure 4.12.a, it is quite apparent that the copper fragments were pulled off from the wafer surface that clearly gives the typical example of adhesion wear. Although no hard abrasive particles were present in DI water CMP, the scratches and grooves wear found on the polished surface as shown in Figure 4.12.b, 4.12.c and 4.12.d. According to Fischer et al.

(1988), the wear particles coming from adhesion wear may be trapped and reshaped at the interface. At the wetted condition, the inter-particle adhesion causes the fine debris to be agglomerated into rolls, loose particles, etc which subsequently results in other kinds of wear. The particles roll or tumble through the gaps, therefore gives occasional indentation and pitted surface (Figure 4.12.d). The abrasive wear resulting from the abrasion or ploughing of wear debris gives both nano scratches and micro grooves on the polished surface as shown in Figure 4.12.b and Figure 4.12.c. Rabinowicz (1995) noticed similar scratches and grooves on copper wafer during DI water polishing where he defined this kind of wear as burnishing. Though abrasive-free slurry does not contain any hard particle, similar wear phenomena can also be found in abrasive-free CMP process. It is quite obvious that if the sources of the formation of wear debris, especially if the adhesion wear can be cut off and if the wear debris can be dissolved completely by the slurry, the abrasion or erosion wear can be eliminated. The dissolution of wear debris can be achieved if the slurry is chemically active and, the adhesion can be avoided if good lubrication can be maintained during polishing. Therefore, it is quite apparent that the mechanical wear resulting from the direct interaction of pad and wafer are adhesion wear, adhesion wear induced abrasion wear and erosion wear.

4.4 Results and Discussions

4.4.1 Surface Analysis of Wafers Polished in Abrasive-Free Copper CMP Process

The experimental observation of the wafer surface polished at different polishing conditions gives several interesting wear phenomena. Analysis of those phenomena helps to understand the role of pressure, velocity and slurry flow rate in material removal mechanism of abrasive-free copper CMP process.

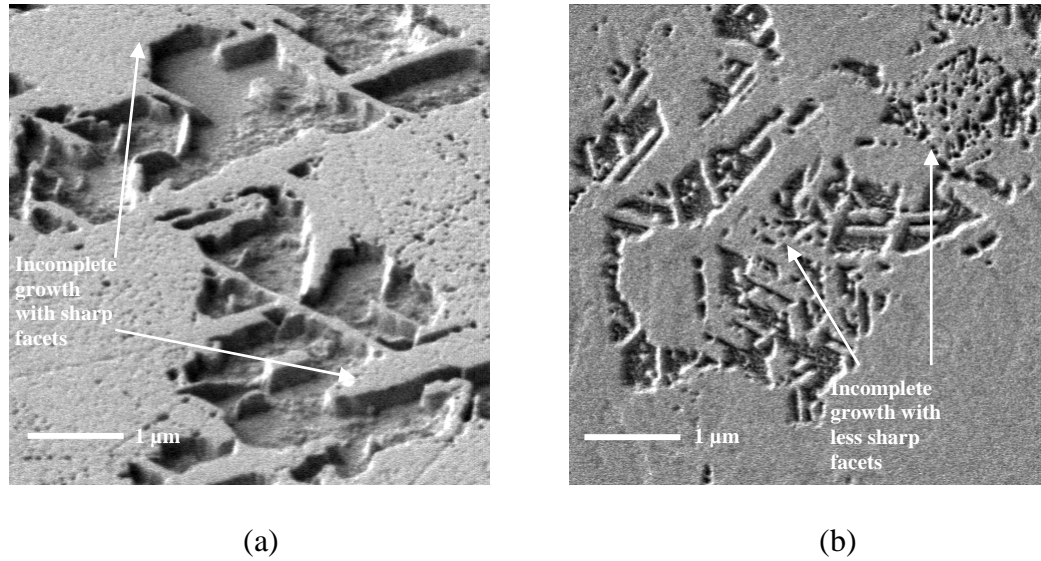
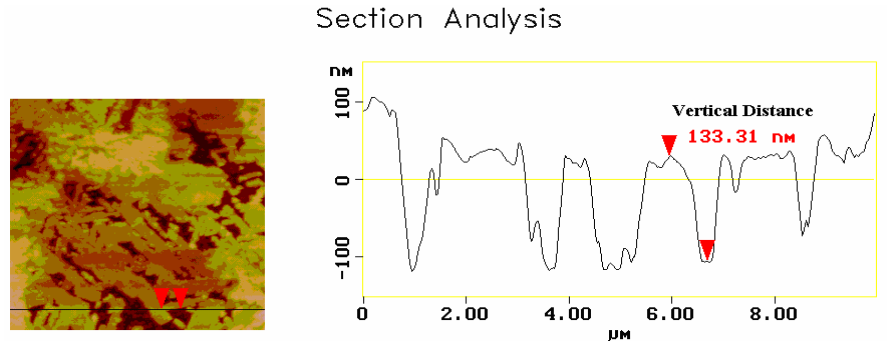


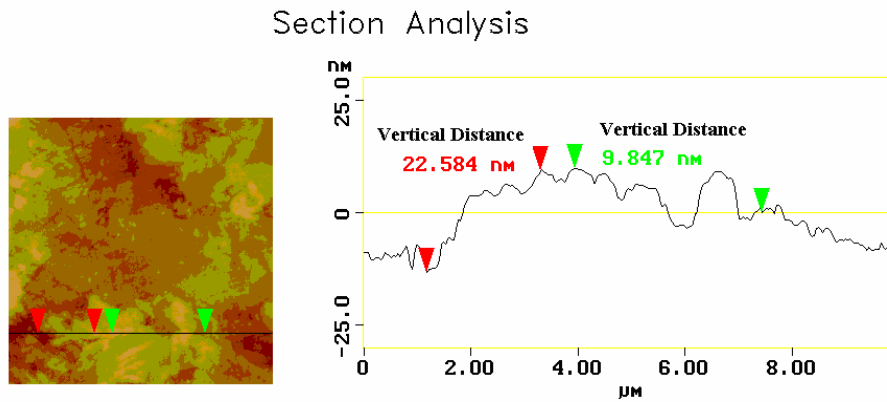
Figure 4.13 Incomplete growth of CuO/Cu₂O layer

4.4.1.1 Incomplete Growth and Faceting

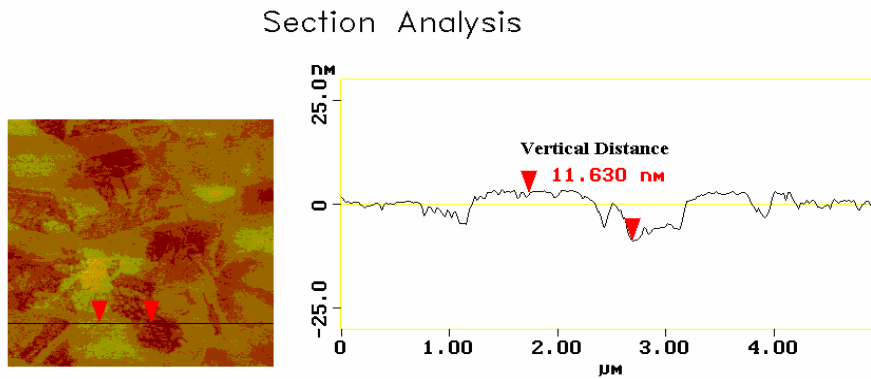
The incomplete growth of CuO/Cu₂O layer was observed on the polished blanket wafer as shown in Figure 4.13. Some of them have sharp facets (Figure 4.13.a) while other shows less sharp facets (Figure 4.13.b) which are observed on the wafers polished at 100 ml/min slurry flow rate. The sharp facets are found at low pressure CMP (6.89/9.85 kPa). On the contrary, the wafer polished at 13.7/16.54 kPa gives facets which are comparatively less sharp.



(a)



(b)



(c)

Figure 4.14 Sectional analysis of the incompletely grown oxide layers at: a) 6.89/9.85 kPa
b) 10.34/13.1 kPa c) 13.7/16.54 kPa

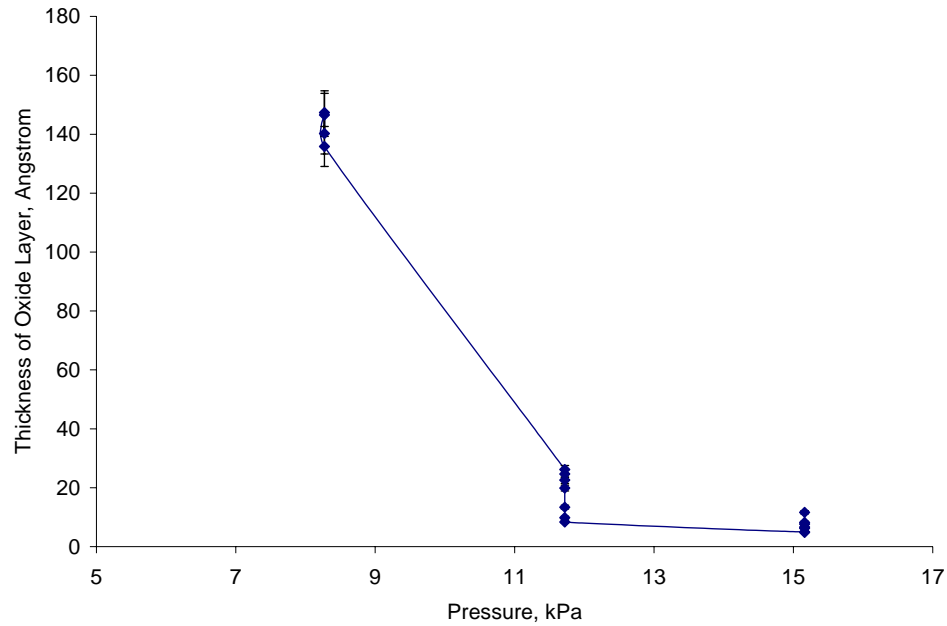


Figure 4.15 Effect of applied pressure on the oxide layer thickness

The sectional analysis at the faceted area was carried out in order to understand the effect of pressure on the layer depth. Figure 4.14.a, 4.14.b and 4.14.c give the sectional analysis of the wafers polished at 6.89/9.85 kPa, 10.34/13.1 kPa and 13.7/16.54 kPa respectively. It is observed that the depth of the layer at sharp faceted area polished at 6.89/9.85 kPa is around 1330Å. On the other hand, the depth of the faceted layers at 10.34/13.1 kPa and 13.7/16.54 kPa wear found below 220Å. These results clearly indicate that the high pressure reduces the layer thickness. The sharp drop of the layer thickness with pressure as shown in Figure 4.15 tells that the wear rate in abrasive free CMP is a strong function of pressure.

As per the mechanism of the formation of copper/cupric oxide layer discussed in Art.4.2.1, it can be claimed that the incomplete growth of CuO/Cu₂O layer can only be formed if there is insufficient amount of oxidizer (slurry) at wafer pad interface to oxidize

copper. From the experimental investigation of polished surfaces, as shown in Figure 4.7 and Figure 4.8, it is quite apparent that the lack of slurry at wafer pad interface only occurs when the slurry flow rate is quite low and the applied pressure is sufficiently high.

4.4.1.2 Mechanical Failure of CuO/Cu₂O Layers

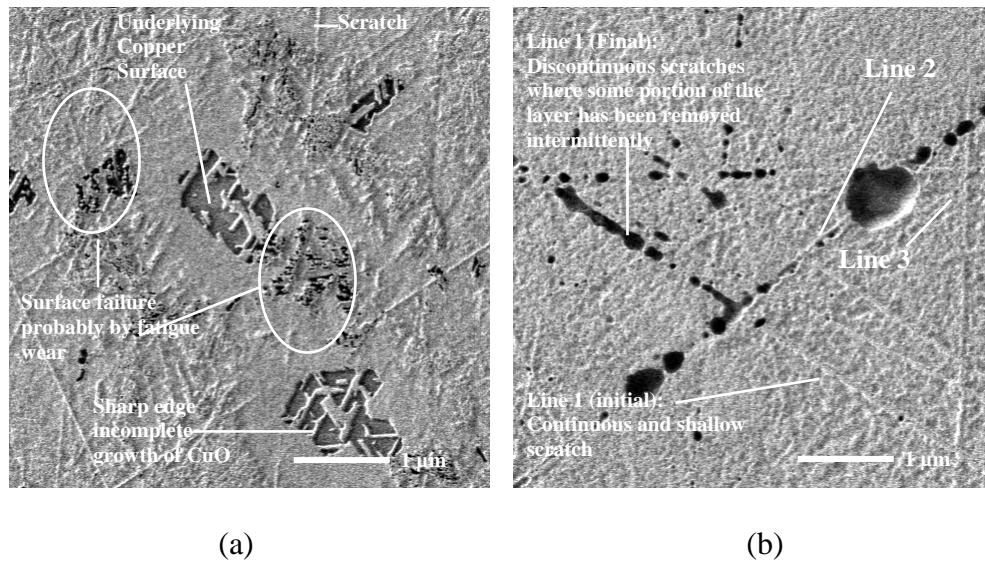


Figure 4.16 Mechanical failures of CuO/Cu₂O layers

The chemically modified surface of the copper blanket wafer shows different kind of mechanical failure during polishing. Both of the pictures of Figure 4.16 clearly indicate that the layer formed on the wafer surface is quite brittle and weak having some incomplete growth, peeled surface and shallow scratches. Figure 4.16.b shows different kind of scratches on the wafer surface. Some of the scratches are long, continuous and shallow (Line 3). The other kind of scratch is continuous and shallow at the initial stage but as it goes ahead, it becomes discontinuous making some kind of holes (Line 1 and 2). Since the slurry does not contain any hard abrasive particle, the question comes as, from

where the wear particles are coming. The corrosive wear or etching as shown in Figure 4.1.b forms the copper complex at atomic level. Therefore, the formation of wear debris by corrosive wear is fairly impossible. On the contrary, the adhesion wear, fatigue wear, etc are the other possible wear mechanisms from where the wear debris may come into the slurry. Since the CuO/Cu₂O layer is brittle in nature and, as mentioned earlier, the major portion of the wafer experience fatigue loading during polishing, fatigue wear can be one possible mechanism. The nature of wear found on the wafer surface, as shown by two circles in Figure 4.16.a, looks like fatigue wear. It is interesting to note that, similar to DI water CMP process, no copper fragments has been pulled off, i.e. the large scale adhesion wear is apparently absent in abrasive-free copper CMP process. This may be because the abrasive-free slurry provides more lubricated surface as compared to DI water CMP which provides less or no adhesion wear.

The continuous scratch (Line 3) as shown in Figure 4.16.b may be because very sharp particle slides over the surface like a single point cutting tool. But as the scratching continued, the sharp particle probably became blunted, and thereby, the surface area of the particle increases resulting in the increase of surface adhesion force. As a result, the particle pulls off the material leaving some holes along the scratch. Moreover, the holes are aligned in the same direction of scratch. If the particle is penetrated into the layer, formation of repeated holes in same direction is not possible. Therefore, such adherence of particle along the scratches can be defined as particle adhesion.

The surface analysis clearly demonstrates that the dominant mechanical wear found in abrasive-free copper CMP are fatigue wear, particle abrasion wear (by the particle coming from fatigue or other form of wear) and particle adhesion wear.

4.4.1.3 Clean and Etched Surface Having Some Residue

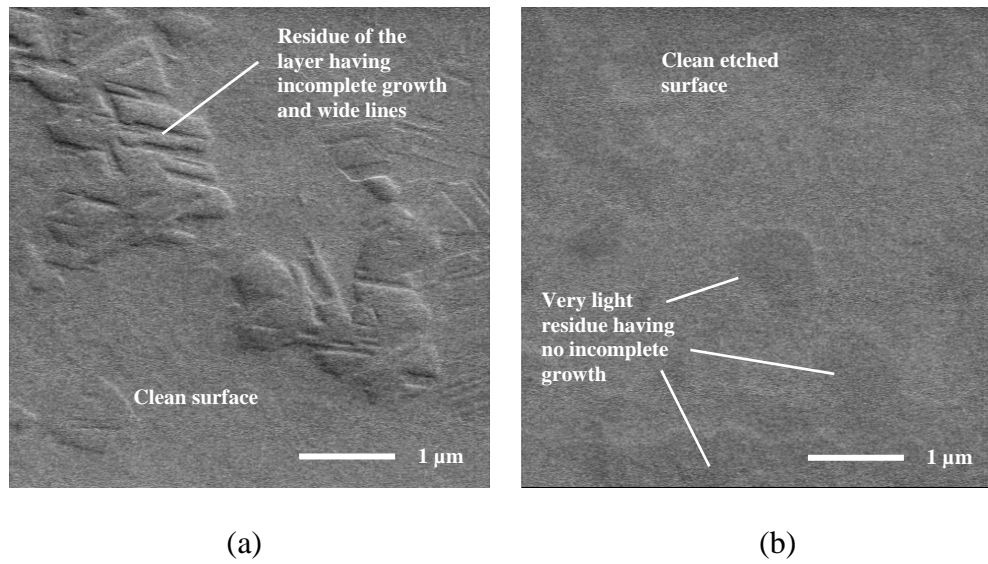


Figure 4.17 Clean and etched surface: a) with residue b) without residue

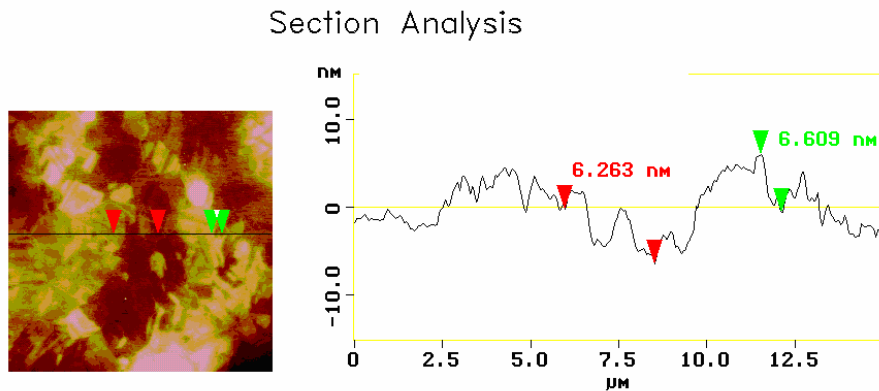


Figure 4.18 Sectional analysis of the area having residue

After polishing the wafers at different polishing conditions, some smooth surfaces having some residual layers were noticed as shown in Figure 4.17.a and 4.17.b. Some of the residues are quite thick having some incomplete growth and discontinuous wide lines

(Figure 4.17.a) while others are very shallow giving a very clean and smooth surface (Figure 4.17.b). The lines on the residue are not unidirectional, and the width of those lines (2-4 μm) is not close to the tip diameter of the pad asperity (60 μm). Hence, it can be said that those are not because of the sliding action of pad rather because of the incomplete growth and faceting of the layers by chemical means. The sectional analysis of the area having residue gives the thickness around 65 \AA as shown in Fig.4.18.

4.4.2 Effect of Polishing Conditions on Wear Mechanism

From the experimental investigation, it is quite apparent that the slurry transportation and slurry distribution at wafer pad interface during polishing plays a vital role in the wear mechanism in abrasive-free CMP. The change of slurry transportation and slurry distribution is believed to be responsible for the WTWWV and WIWWV respectively.

It is quite apparent from Figure 4.6 that with the change of slurry flow rate, the WTWWV significantly changes. The higher the slurry flow rate the better the slurry transportation at the wafer pad interface. Thereby, high slurry flow rate gives rise to the dominance of chemical wear and low slurry flow rate gives severe mechanical damage on the polished surface. On the other hand, the flow rate has little or no effect on WIWWV, especially when the slurry flow rate is very high. But significant variation of WIWWV was found at low slurry flow rate. The distribution of slurry at wafer pad interface, which mainly causes WIWWV at low flow rate, can not be correlated by slurry flow rate rather it can be logically explained by fluid pressure distribution across the wafer. The center portion of all wafers shows no mechanical wear irrespective of slurry flow rate (Figure

4.6). This is because the sub-ambient pressure mainly acts at the center which will improve the slurry flow at center [Zhou et al., 2002]. On the other hand, middle and edge of the wafer shows severe mechanical wear at low flow rate. This may be because the positive pressure at these regions tends to “squeeze out” the slurry in half cycle while it tends to “suck in” the slurry in the next half cycle. Now, if the slurry flow rate is low, such effect of pressure on slurry distribution at edge and middle not only reduce the slurry volume but also provides cyclic loading on the wafer surface which consequences in fatigue wear. But because of the lack of slurry, the wear debris (possibly coming from fatigue wear) can not be dissolved and thereby, it gives rise to other kind of mechanical wear. In this way, the pressure distribution across the wafer strongly affects the WIWWV. The similar change in WIWWV at different pressure was also noticed in Figure 4.7.

The change of applied pressure also affects WTWWV as shown in Figure 4.7. It is quite obvious that at low pressure, the wear mechanism of abrasive-free CMP is chemically dominated. Conversely, with the increase of pressure, mechanical wear and the formation of incomplete growth increases. It is also noticed from Figure 4.7 that the mechanical wear only occurs beyond a certain pressure limit. The pressure beyond that limit not only allows higher magnitude of loading on the wafer but also “squeeze out” more slurry from the interface. Both of those two are responsible from severe mechanical failure and incomplete growth formation. The WTWWV with pressure can only be explained by ‘Modes of Contact’ analysis because the slurry transportation significantly varies at different contact modes [Phillipossian et al., 2004; Moon et al., 1998; Denardis et al., 2003]. The application of low pressure operates in hydroplaning mode where there occurs sufficient transportation at wafer pad interface giving rise to the dominance of chemical wear (Figure 4.7.a-c). But the application of high pressure runs the wafers at

solid contact mode where the slurry transportation is sufficiently poor. As a result, severe mechanical wear has been found at high pressure CMP (Figure 4.7.g-i).

The experimental results clearly indicate that the change of velocity has little or no effect on WIWWV but it has significant effect on WTWWV (Figure 4.8). This is because the velocity distribution across the wafer remains almost uniform resulting in the uniform distribution of slurry when all other parameters are kept constant. But it was found that with the increase of velocity, the chemical wear increases and mechanical wear diminishes. Thus the change of velocity strongly affects the slurry transportation at the wafer pad interface. This can also be well explained by the ‘Modes of Contact’ analysis [Art 5.4]. Such analysis shows that at low velocity, the wafer and pad are operated at solid contact mode, and the volume of slurry at the interface is sufficiently low while at very high velocity, the hydroplaning mode is achieved which provides sufficient amount of slurry for complete chemical etching. Thus high velocity usually gives very smooth and clean surface.

4.5 Conclusions

From the analysis of experimental results of this chapter, the following conclusions can be drawn:

- Chemical etching (corrosive wear), fatigue wear, particle adhesion and abrasion wear have been found as the wear mechanisms in abrasive-free copper CMP process. However, corrosive wear has been found as the dominant wear mechanism while other mechanical wear mechanisms are less significant.

- With the increase of slurry flow rate and relative velocity, and with the decrease of pressure, the chemical wear increases and vice versa. For the usual abrasive-free copper CMP practice, corrosive wear has been found as the dominant material removal mechanism.
- Applied pressure is mainly responsible for different kind mechanical wear, and those are frequently found at middle and edge of the wafers. The repeated loading and unloading effect given by fluid pressure at wafer pad interface (positive and negative pressure across the wafer in each cycle) might be responsible for fatigue wear. The particles, coming from the wear debris of fatigue wear, give rise to abrasion and adhesion wear.
- Insufficient slurry supply at wafer pad interface causes the formation of faceted incomplete growth and some sort of residues on the polished surface. The sharpness of facets and the depth of the faceted layers sharply decrease with the increase of pressure. Insufficient slurry supply also provides poor dissolvability of wear debris which results in severe mechanical wear.
- The polishing conditions greatly affect the WTWWV and WIWWV. The applied pressure has significant effect on both WTWWV and WIWWV. On the contrary, both slurry flow rate and relative velocity have little effect on WIWWV while they have significant effect on WTWWV. Therefore, pressure is considered as the key parameter for abrasive-free CMP process.

In addition to the investigation of the material removal mechanism, the effect of different polishing conditions on MRR (wear rate) and WIWNU in abrasive-free copper CMP process will be discussed in the next chapter.

Chapter 5

Characterization of Abrasive-Free Copper CMP Process

5.1 Introduction

The process characterization usually deals with the investigation of the role of different process parameters on the process outputs. The main process parameters of copper CMP process are slurry flow rate, relative velocity and pressure. The role of those process parameters on MRR and WIWNU in abrasive-free copper CMP process has been investigated in this chapter. The synergistic effect of relative velocity and pressure on material removal rate (MRR) has been investigated from the interfacial contact condition (between wafer and pad) view point. In addition, the non-prestonian nature of MRR in abrasive-free CMP has been investigated. Using the polishing condition which gives the highest MRR and allowable WIWNU during blanket wafer polishing, the optimum polishing conditions have been recommended. Finally, an abrasive-free CMP process has been developed for Copper/Oxide pattern wafer that verifies the practicability of the optimized conditions.

5.2 Theory of Process Characterization

5.2.1 Study of the Synergistic Effect of Process Parameters

The conventional abrasive CMP process basically combines the abrasion of surface (mechanical) and dissolution of abraded species (chemical). The MRR and WIWNU are affected by the synergistic effect of pressure and relative velocity. So,

pressure and relative velocity are usually taken as the key parameters to modulate the MRR and WIWNU.

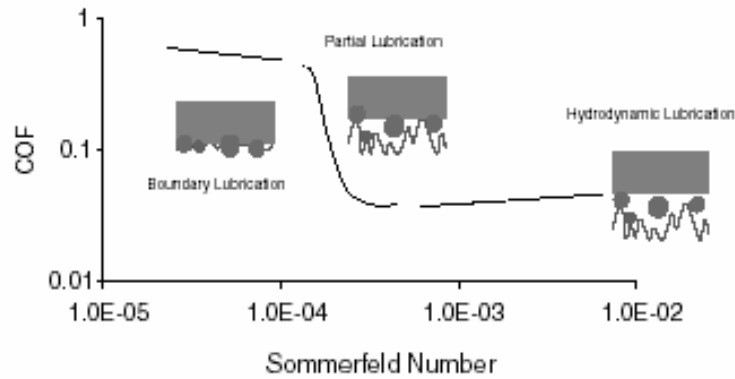


Figure 5.1 Generic Stribeck curve based on the Sommerfeld number [Ludema et al., 1996]

Conversely, the MRR greatly depends on the state of interfacial contact, and it changes with the change of process parameters. The investigation of the interfacial contact mode between wafer and pad during polishing is such an approach that helps to understand the role of pressure and relative velocity in CMP. Such analysis has been carried out for conventional abrasive CMP process by a number of researchers where they investigated the 'Modes of Contact' plotting the coefficient of friction (COF) with Sommerfeld number [Ludema et al., 1996; Liang et al., 2002; Phillipossian et al., 2004; Mullany et al., 2003; Denardis et al., 2003; Moon et al., 1998]. In their study, three modes of contact were identified namely Boundary Lubrication, Partial Lubrication and Hydrodynamic Lubrication. These contact modes are shown graphically in Figure 5.1. As discussed in the last chapter, the mechanism of material removal in abrasive-free CMP is fairly different from that of abrasive CMP process. So, the process outputs at different

interfacial conditions are presumed to be different as well. But the role of process parameters on interfacial contact mode, and different phenomena of MRR and WIWNU at different contact modes in abrasive-free copper CMP process are yet to be investigated.

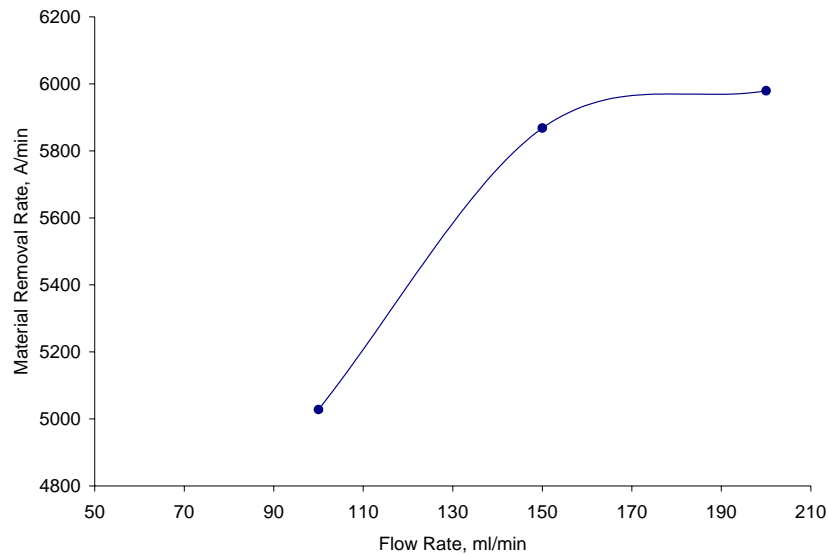


Figure 5.2 Effect of slurry flow rate on MRR at constant pressure (11.72kPa) and velocity (1.02 m/sec).

In conventional abrasive CMP process, the MRR decreases with the increase of slurry flow rate. Li et al. (2004) argued that the possible reason of such decrease of MRR is the decrease of temperature of wafer surface with the increase of slurry flow rate. On the other hand, Homma et al. (2003) claimed that the MRR is linear with frictional force, and the COF decreases with the increase of slurry flow rate resulting in low MRR. This is because the material in abrasive CMP is mainly removed by two-body or three-body abrasion, burnishing, etc which are mechanically predominant. Conversely, Figure 5.2 shows that, in abrasive-free copper CMP process, the MRR increases with the increase of slurry flow rate. It is quite obvious that COF will decrease with the increase of slurry flow

rate. Therefore, it can be said that the MRR shows inverse relation with COF in abrasive-free CMP. Because of this discrepancy, the interfacial contact analysis using the COF and Sommerfeld number is apparently misleading. Besides, chemically dominant material removal mechanism of abrasive-free CMP demands high volume of slurry transportation at wafer pad interface to ensure high MRR which is mainly controlled by pressure and relative velocity. Because of those two reasons, in this study, normalized MRR has been plotted against Sommerfeld number to study the interfacial contact conditions in abrasive-free copper CMP process.

5.2.1.1 Sommerfeld Number

In order to understand the effect of pressure and relative velocity on the interfacial modes of contact between two sliding body, a dimensionless parameter called Sommerfeld number is used. The Sommerfeld Number can be written as,

$$S_o = \frac{\mu V}{P \delta_f} \quad (5.1)$$

where, μ is the slurry viscosity, V is the relative velocity of wafer with respect to pad, P is the applied pressure, δ_f is the effective fluid film thickness.

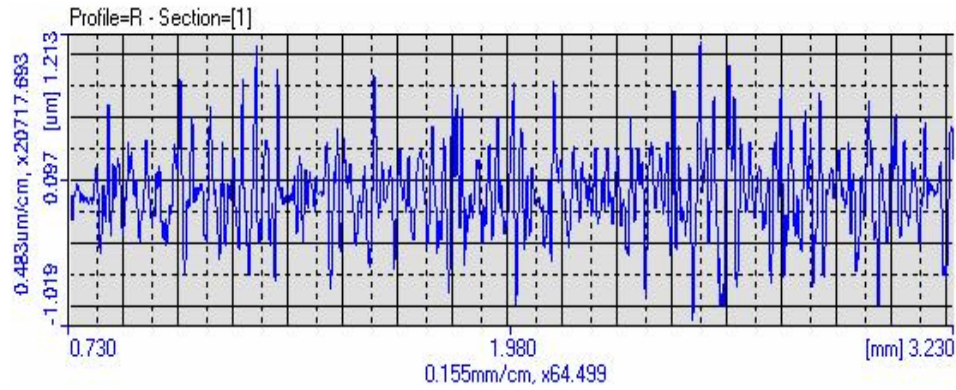


Figure 5.3 Roughness profile of copper polishing pad ($R_a = 0.23 \mu m$)

The value of δ_f can be determined by the equation [Denardis et al., 2003],

$$\delta_f = \alpha \times R_a + (1 - \alpha) \times \delta_{groove} \quad (5.2)$$

where, α is a dimensionless number which is the ratio of the area of up features to the area of the flat pad, R_a is the pad roughness and δ_{groove} is the depth of pad groove. In this study, the value of α for the 'RODEL NITTA Suba 400' XY-groove pad was 0.73. The average roughness of the pad was $0.23 \mu m$ as shown in Figure 5.3. The typical copper polishing pad as shown in Figure 3.5 has some grooves to hold slurry during polishing. The depth of the pad groove ($\delta_{groove} = 157.148 \mu m$) was measured by a Coordinate Measuring Machine (CMM).

5.2.1.2 Modes of Contact (MOC)

The interfacial contact conditions of wafer and pad asperity during polishing can be defined as: Solid Contact Mode (SCM), Hydroplaning Contact Mode (HCM) and Mixed Contact Mode (MCM) as shown in Figure 5.4. In the solid contact mode, the peaks of the pad asperities come in mechanical contact with the wafer surface. The fluid film at

this contact mode is discontinuous and no significant pressure gradient exists in the fluid film across the wafer. Therefore, the applied load is ideally supported by the pad asperities. The solid contact mode is usually found at low relative velocity and high applied pressure. On the contrary, if the velocity is too high and pressure is quite low, the wafer starts to glide over the slurry film during polishing without touching the pad asperities which is defined as hydroplaning contact mode. The applied pressure at this contact mode is supported by the pressure gradient developed in the fluid film. The mixed contact mode is found in between the solid contact mode and hydroplaning contact mode when the moderate velocity and pressure are maintained during polishing.

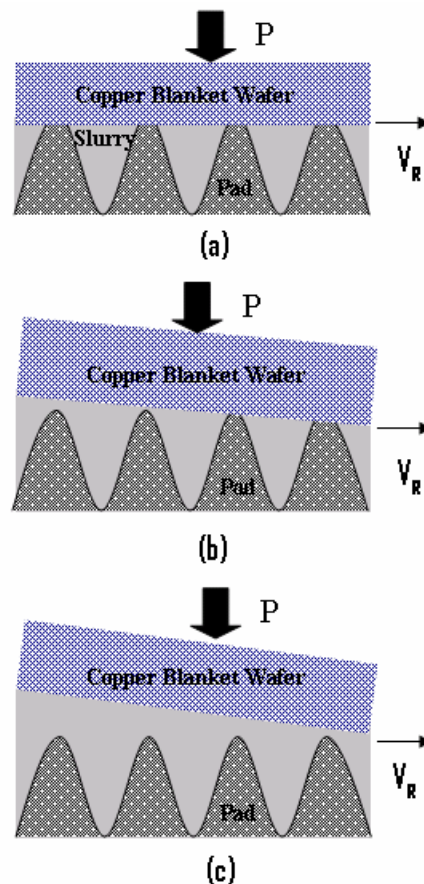


Figure 5.4 Schematic of different contact modes at wafer pad interface: a) solid contact mode, b) mixed contact mode, c) hydroplaning contact mode

5.2.2 Relative Velocity and Pressure in MOC Analysis

Pressure and relative velocity are two key parameters for material removal given by Preston's Equation [Preston, 1921]. This was found also the same for abrasive-free CMP process reported by some researchers [Kondo et al., 2000; Matshuda et al., 2003]. Therefore, selection of rotation rate and pressure is crucial for both abrasive and abrasive-free CMP processes.

5.2.2.1 Selection of Rotation Rate in Rotary CMP

The polisher used in this study is rotary type. The wafer rotates over a rotating pad where both rotate in the same direction. In order to select the rotation rate of pad and wafer, it is necessary to understand the kinematics of rotary CMP.

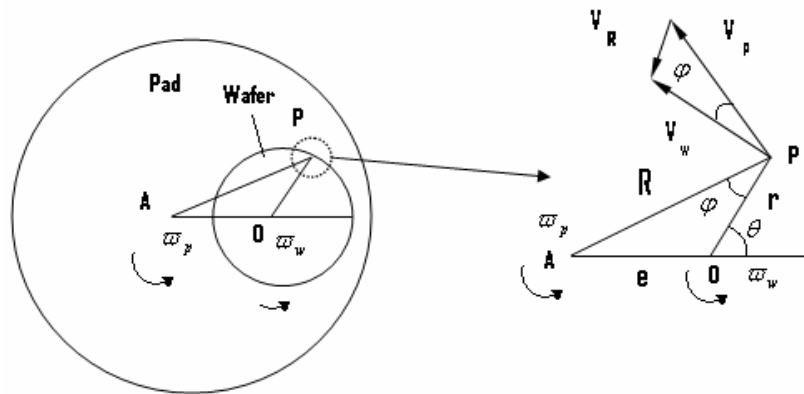


Figure 5.5 Kinematic parameters of rotary CMP

The kinematic parameters of a rotary CMP has been given in Figure 5.5. The expression of relative velocity of a point P on the wafer with respect to pad will be derived. The velocity component for pad and wafer at point P are V_p and V_w respectively. The distance

of P from the center of the wafer **O** is **R**. The eccentricity of the wafer and pad is **e** and the distance of the point P from the wafer center is **r**.

From triangle OAP,

$$e^2 = R^2 + r^2 - 2Rr \cos \varphi \quad (5.3)$$

$$R^2 = e^2 + r^2 + 2er \cos \theta \quad (5.4)$$

And the magnitude of the relative velocity,

$$V = \sqrt{(V_p^2 + V_w^2 + 2V_p V_w \cos \varphi)} \quad (5.5)$$

The liner velocity pad and wafer in Eqn. 5.5 can be written in terms of angular velocity as,

$$V = \sqrt{((\varpi_p R)^2 + (\varpi_w r)^2 - 2\varpi_p \varpi_w Rr \cos \varphi)} \quad (5.6)$$

From Eqn. 5.3, 5.4 and 5.6, the expression of relative velocity can be written as,

$$V = \sqrt{((e^2 + r^2 + 2er \cos \theta)(\varpi_p^2 - \varpi_p \varpi_r) + r^2(\varpi_p^2 - \varpi_p \varpi_r) + e^2 \varpi_p \varpi_r)} \quad (5.7)$$

Now, if the angular velocity of the wafer and the pad, $\varpi_p = \varpi_r$ and if the eccentricity, **e** does not change with time, Eqn. 5.7 can be written as,

$$V = \sqrt{e^2 \varpi_p^2} = e \varpi_p \quad (5.8)$$

The expression of relative velocity as given in Eqn. 5.8 shows that the relative velocity will remain constant across the wafer when the angular velocity of pad and wafer will be kept equal. However, to get better slurry distribution at wafer pad interface, the synchronous speed ($\varpi_p = \varpi_r$) has been recommended to avoid by Hocheng et al. (2000).

On the other hand, higher the difference between ϖ_p and ϖ_r , higher will be the velocity non-uniformity as given in Eqn. 5.6. The velocity non-uniformity across the wafer will directly affect the WIWNU of MRR given by Preston's Equation. Because of this reason,

the difference of rotation rate between wafer and pad is recommended to keep as small as possible. In this study, the rotation rate of pad was kept 3 rpm higher than wafer rotation rate which gave negligible velocity non-uniformity across the wafer.

5.2.2.1 Selection of Pressure

Two different kind of pressure were applied on the same wafer during polishing as given in Figure 5.6. It is a usual practice to keep high pressure at the edge to prevent the wafers from flying during polishing. The edge pressure is also called retaining ring pressure while the pressure at the middle and center of the wafer is called membrane pressure. In this chapter, the average of membrane pressure and retaining ring pressure has been taken for the MOC analysis.

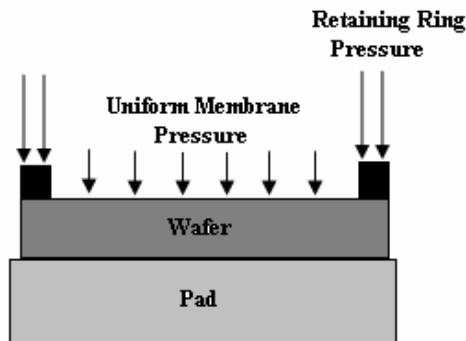


Figure 5.6 Schematic of the application of pressure on wafer

5.3 Role of Process Parameters in MRR and WIWNU

The process parameters, especially slurry flow rate, rotation rate of pad and wafer and applied pressure significantly affect MRR and WIWNU. A range of process parameters selected for the experiments are given in Table 5.1.

Table 5.1 Experimental polishing conditions for Abrasive-free Copper CMP process (blanket wafer polishing)

Abrasive-free Copper CMP	
Polishing Parameters	Range of Value
Applied Pressure (membrane)	5.51 kPa-13.78 kPa
Applied Pressure (retaining ring)	8.27 kPa-16.54 kPa
Pad Rotation Rate	30 rpm – 120 rpm
Wafer Rotation Rate	27 rpm – 117 rpm
Slurry Flow Rate	100 ml/min – 200 ml/min

5.3.1 Role of Slurry Flow Rate

The blanket wafers were polished at 100 ml/min, 150 ml/min and 200 ml/min while average applied pressure and relative velocity were kept 11.72 kPa and 1.03 m/sec respectively. The results given in Figure 5.7 shows that MRR is quite low at 100ml/min flow rate but it sharply increased at 150 ml/min. But MRR did not increase to that extent at 200 ml/min rather it shows steady behavior at high slurry flow rate. It is quite apparent from the Figure 5.7 that such transition of MRR started at around 175 ml/min for the mentioned pressure and velocity. It is interesting to note that WIWNU decreases with the increase of slurry flow rate, i.e. WIWNU was 10.1% at 100ml/min while it as 2.5 % at 200ml/min. However, from process optimization viewpoint, the allowable WIWNU is below 6%.

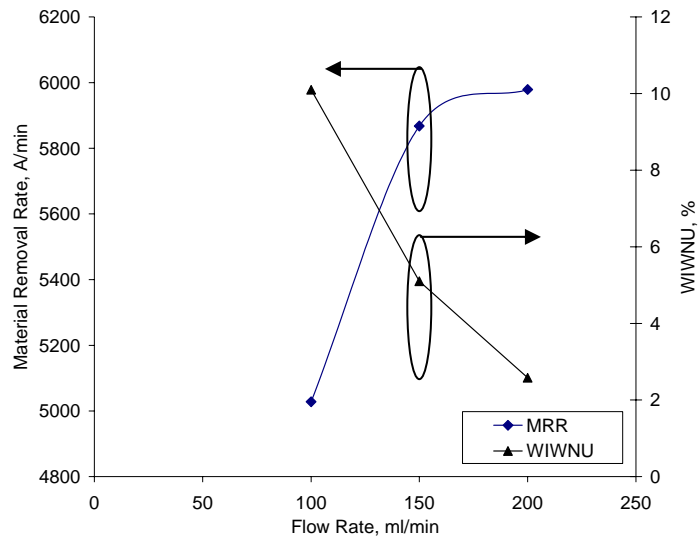


Figure 5.7 Effect of flow rate on MRR and WIWNU

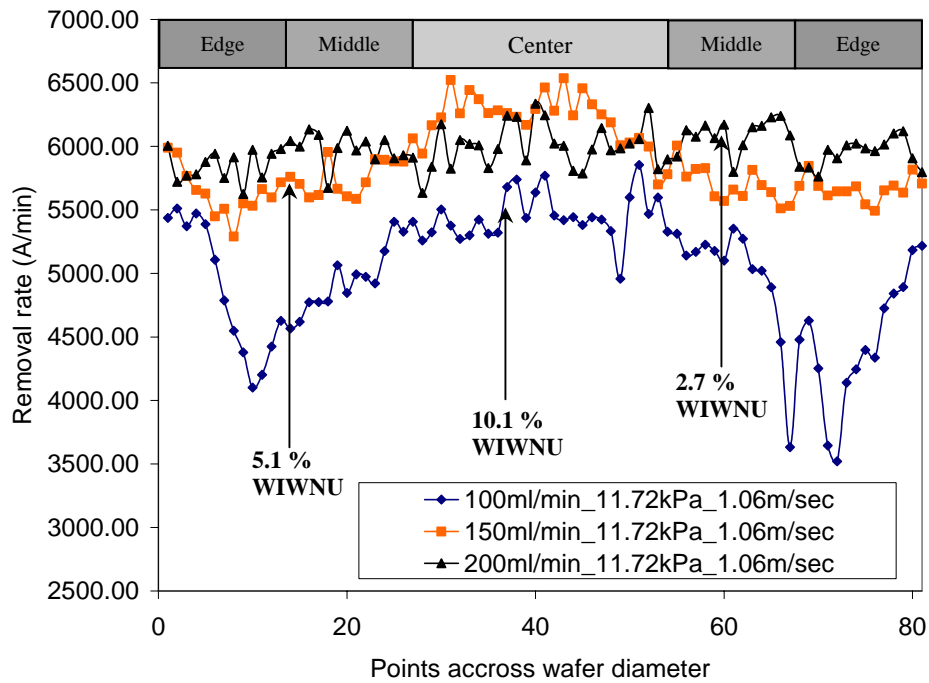


Figure 5.8 WIWNU of material removal / wear rate across the wafer in abrasive-free CMP

Study of non-uniform wear rate across the wafer is also necessary to understand the role polishing conditions in abrasive free CMP. In conventional CMP, non-uniformity increases with the increase of relative velocity, applied pressure and flow rate [Li et al., 2004]. On the contrary, in abrasive-free CMP, although the non-uniformity shows similar trend with pressure and relative velocity, it shows just opposite trend with slurry flow rate, i.e. the non-uniformity decreases with the increase of flow rate. Because of this reason, the non-uniformity of MRR across the wafer at three different flow rates (at constant pressure and rotation rate) have been studied, and results are given in Figure 5.8. It is observed in Chapter 3 that, at low flow rate, the role of pressure on the material removal rate across the wafer becomes dominant, i.e. the effect of edge pressure on removal rate comes into picture. On the other hand, selection of high flow rate gives better non-uniformity where the role of edge pressure is found quite insignificant. Although high rotation rate provided very smooth surface (Figure 4.8.g-i), the non-uniformity was found very high at high relative velocity (Figure 5.15). This may be because, at hydroplaning mode, the fluid film and the pressure gradient developed in the fluid film are very sensitive and unstable to velocity and applied normal pressure [Lai, 2001]. Therefore, the thickness of fluid film is not uniform across the wafer which will definitely increase the non-uniformity of removal rate. The experimental results of Figure 5.8 shows that MRR continued to increase and WIWNU continued to decrease with the increase of slurry flow rate. But to maintain high throughput and low manufacturing cost, CMP users prefer high MRR and low WIWNU using minimum possible amount of slurry consumption. Therefore, in this study, 150 ml/min has been found as a reasonable choice that provides sufficiently high MRR and allowable WIWNU.

5.3.2 Role of Applied Pressure

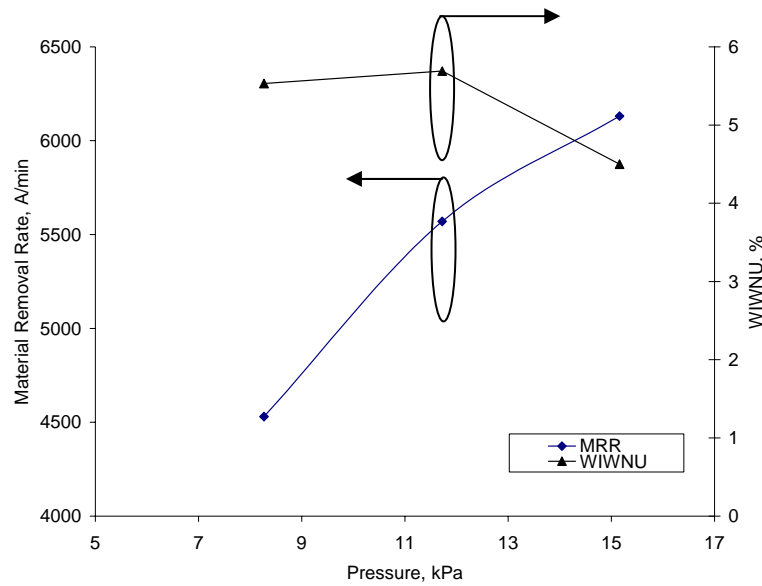


Figure 5.9 Effect of pressure on MRR and WIWNU

To observe the role of pressure on MRR and WIWNU, blanket wafers were polished at three different pressures (8.27 kPa, 11.72 kPa and 15.16 kPa) while slurry flow rate and relative velocity were kept 150 ml/min and 1.03 min/sec respectively. Figure 5.9 shows that MRR increases with applied pressure. On the other hand, WIWNU increases with pressure but it again starts to decline at high pressure. It is quite obvious that high pressure allows less slurry at the interfacial contact of wafer and pad. But high slurry flow rate is needed to ensure better non-uniformity as described earlier. However, the slurry transportation does not depend only on pressure rather it is a strong function of the synergistic effect of pressure and velocity. So, the trend of WIWNU as shown in Figure 5.9 may not be consistent at different velocity. The effect of pressure on WIWNU at different relative velocity has been discussed later in this chapter.

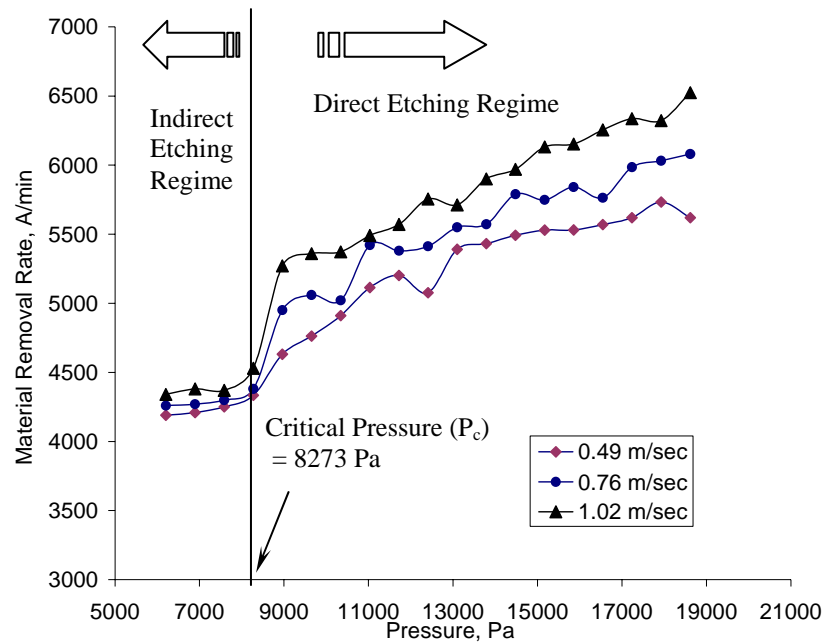


Figure 5.10 Non-prestonian effect of pressure on MRR

Abrasive free CMP shows non-prestonian nature of MRR with pressure as shown in Figure 5.10. In order to understand the non-prestonian issue, it is necessary to explain prestonian behavior of removal rate. If the MRR is linearly proportional to the energy flux i.e. if the MRR follows Preston's equation (Eqn.2.1), it is said that material removal follows prestonian behaviour. Preston's equation tells that, the MRR is zero when there is no pressure and/or no sliding velocity. Besides, this equation was developed based on the abrasion wear mechanism. Any kind of deviation in MRR from those two phenomena is usually called as non-prestonian phenomenon. The non-prestonian behaviour of MRR with pressure in abrasive-free CMP has already been reported by Boning et al. (2001) and Matshuda et al. (2003). The reason of such occurrence might be because chemical etching (corrosive wear) has been found as the chief material removal mechanism which is completely different from the mechanism considered in Preston's equation.

In order to get a better picture of the effect of pressure on MRR, a wide range of pressure was chosen to polish the blanket wafers. The experimental investigation demonstrates that, in abrasive-free CMP, MRR below a certain pressure gives almost constant value which is sufficiently low as compared to the MRR obtained at high pressure. The possible reason of such low MRR is because of indirect etching. Low pressure can not produce sufficient friction force which is necessary to remove the protective layer [Kondo et al. 2000]. Therefore, material can not dissolve directly into the slurry. If the applied pressure goes beyond a certain limit, the MRR increases with pressure because of direct etching. In this study, such pressure limit has been defined as critical pressure (P_c). Since the behaviour of MRR with pressure in abrasive-free CMP is not similar to that of conventional CMP, this special characteristic is widely known as non-prestonian nature of MRR with pressure. In this study, the critical pressure was found almost same (8.27 kPa) at two different velocities (Figure 5.10). Apart from the critical pressure issue, the MRR in both direct etching and indirect etching regimes are not linearly dependent on pressure. Figure 5.10 clearly indicates that MRR is almost constant with pressure in indirect etching regime while it increased in a non-linear fashion in direct etching regime. Such non-linear dependence of etch rate on pressure can also be defined as the non-prestonian nature of MRR.

5.3.3 Role of Relative Velocity

To investigate the role of velocity on MRR and WIWNU, a wide range of relative velocity was chosen to polish copper blanket wafers. Figure 5.11 shows the effect of relative velocity on MRR and WIWNU while the pressure and slurry flow rate were kept 11.72kPa and 150 ml/min respectively.

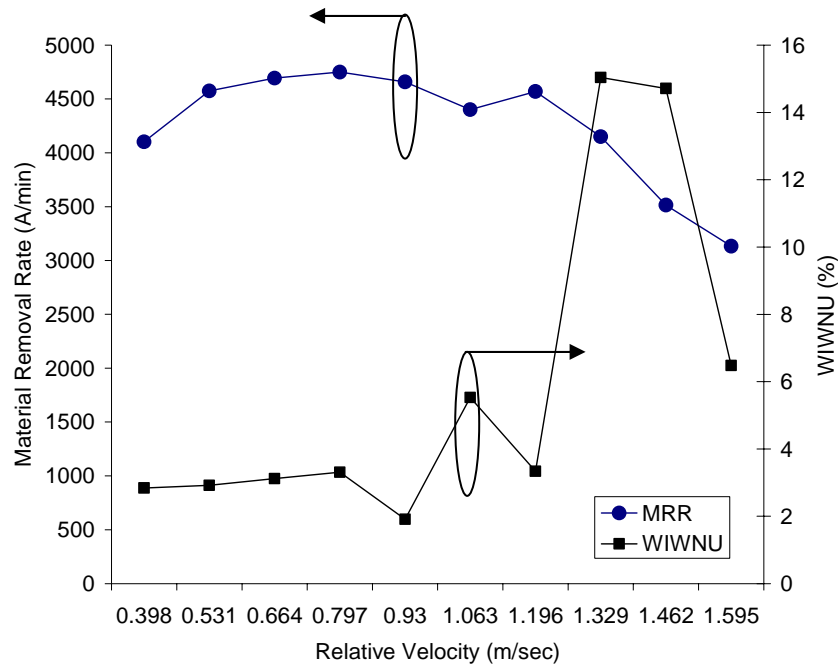


Figure 5.11 Effect of relative velocity on MRR and WIWNU

Figure 5.11 clearly presents very interesting behaviour of MRR with relative velocity. MRR was found low at low velocity (0.40 m/sec). But it increased almost in a linear fashion with velocity up to 0.67 m/sec. The MRR remained steady at moderate velocity while it again declined with further increase of velocity (>1.06 m/sec). Besides, WIWNU was quite low when the polisher was operated at low relative velocity. Conversely, it started to increase with the increase of relative velocity. However, the WIWNU became quite unstable at high velocity CMP (>1.06 m/sec). In addition, the declining of MRR and the unsteadiness of WIWNU started when the velocity went beyond 1.06 m/sec. The trend of MRR at different relative velocity clearly indicates the presence of some special contact regimes that need to be further investigated. The study of the ‘Modes of Contact’ can facilitate better understanding of the significance of those regimes.

5.4 The Synergistic Effect of Pressure and Velocity on MRR

5.4.1 Study of Modes of Contact

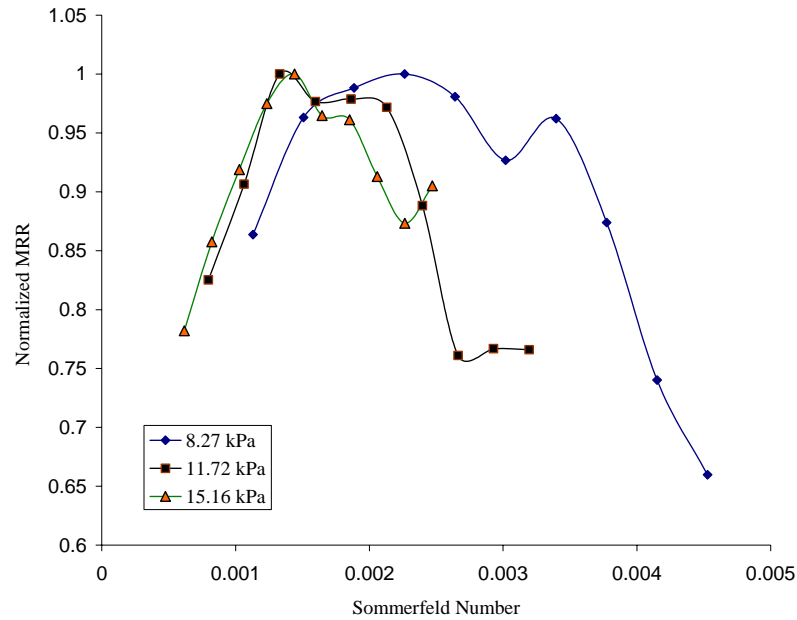


Figure 5.12 Modes of contact analysis with normalized MRR and Sommerfeld number

The synergistic effect of pressure and relative velocity on MRR at different interfacial contact mode has been investigated by plotting the normalized MRR across the Sommerfeld number. Based on the trend of MRR at different Sommerfeld number as given in Figure 5.12, the contact regimes are divided into three major parts. Those are Solid Contact Mode (SCM), Mixed Contact Mode (MCM) and Hydroplaning Contact Mode (HCM) as shown in Figure 5.13. Because of the special trend of MRR in the regime of MCM and HCM, these were subdivided as MCM-A & B and HCM-A & B respectively.

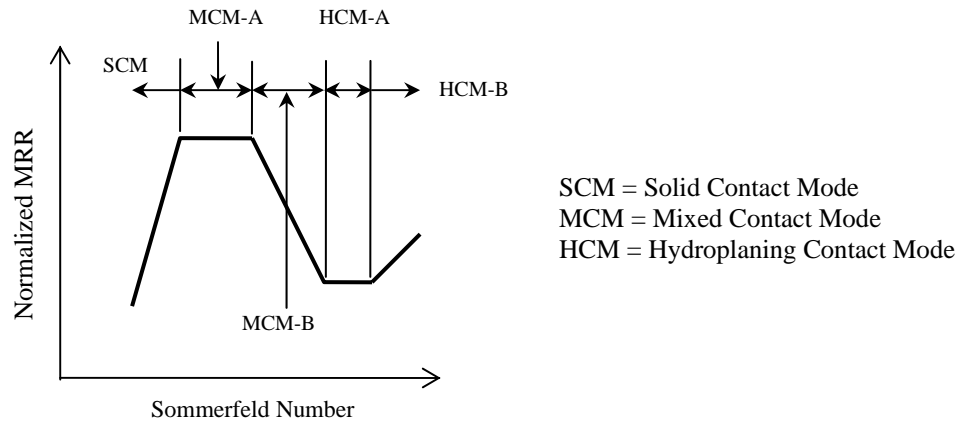


Figure 5.13 Schematic of the interfacial contact modes between pad and wafer

As per the mechanism of material removal in abrasive-free CMP, there are two reasons for getting less material removal rate. Firstly, if there is less amount of slurry at wafer pad interface. Secondly, if the major portion of the wafer is separated from the pad by the slurry film. Therefore, both wafer-asperity contact and sufficient volume of slurry transportation at wafer-pad interface are necessary to achieve high MRR. Based on this concept, the synergistic effect of pressure and relative velocity on MRR at different contact regimes has been discussed.

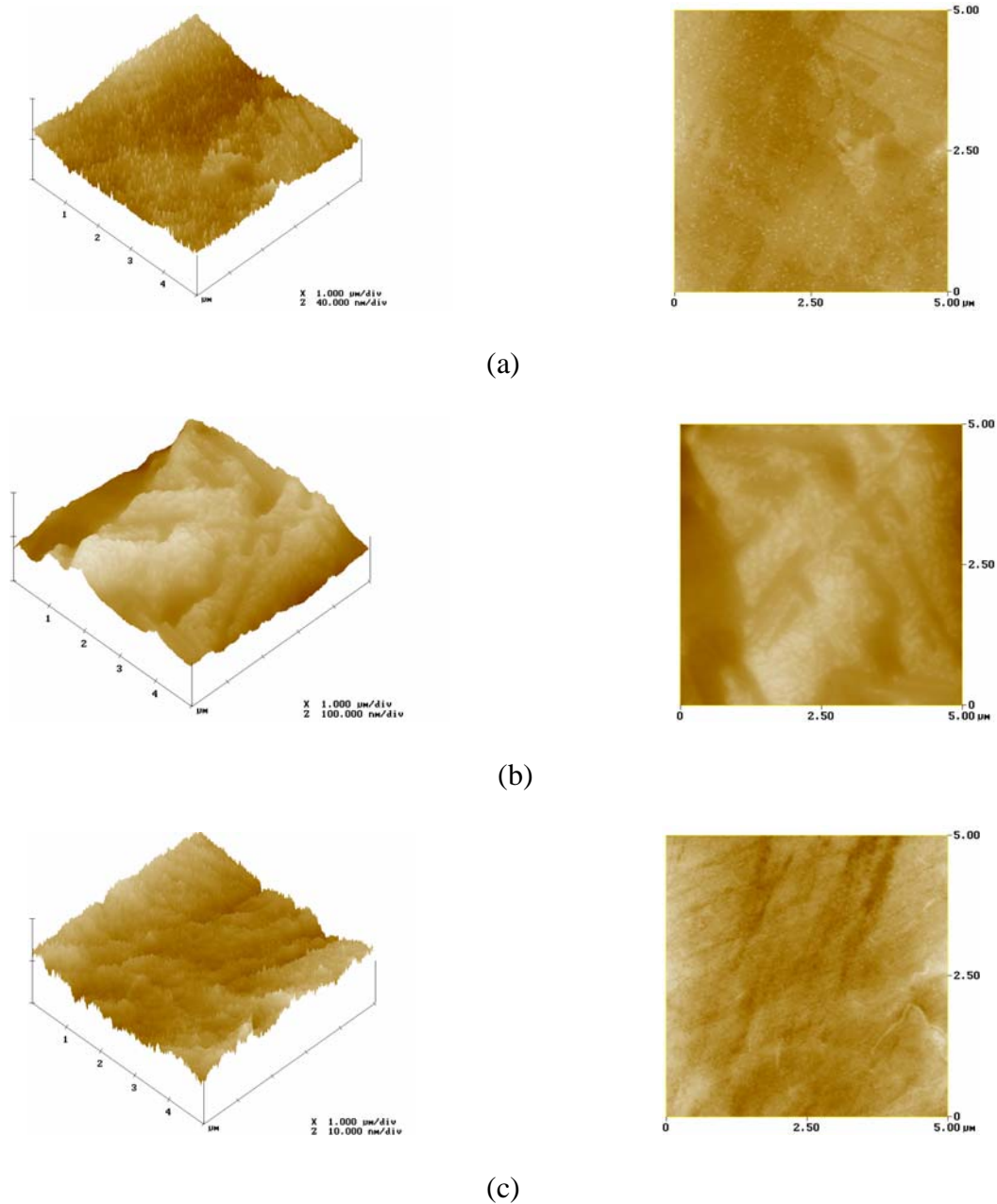


Figure 5.14 Two dimensional (right) and three dimensional (left) AFM picture of the surface of copper blanket wafer polished at: a) SCM (0.49 m/sec) b) MCM-A (1.02 m/sec) c) HCM-B (1.56 m/sec) of MRR at 11.27 kPa

5.4.1.1 Solid Contact Mode (SCM)

In conventional CMP, the COF at SCM goes down with Sommerfeld number as shown in Figure 5.1. Because of the linear dependency of MRR on COF, MRR increases with Sommerfeld number. On the contrary, for abrasive-free slurry, MRR sharply goes up with Sommerfeld number (Figure 5.12). The MRR at SCM is fairly low as compared to MCM. This is because at SCM, there is an intimate contact between wafer and pad, and thereby, sufficient amount of slurry can not be transported at wafer pad interface. Although the wafer-pad contact is high at this contact regime, the lack of slurry reduces chemical action resulting in less MRR. This statement can be substantiated by the AFM picture of Figure 5.14.a which shows less chemical layer on the top of the wafer. Besides, with the increase of Sommerfeld number, the wafer starts to float and provides more slurry to enter at wafer-pad interface. Therefore, the chemical components come into picture resulting in high MRR. However, the window of SCM at high pressure CMP is wider than that of low pressure. This may be because the high pressure prevents the wafers to float over a wide range of velocity.

5.4.1.2 Mixed Contact Mode (MCM)

The window of MCM was divided into two parts: MCM-A and MCM-B. In MCM-A, there is a partial contact between wafer and pad. Therefore, the removal of protective layer from the wafer surface and the transportation of large volume of slurry at wafer-pad interface give the dominance of direct etching, and hence, maximum amount of material is removed at this regime. Because of the direct etching, a thick chemical layer was found on the top of the wafer even though the rinsing time was selected 50 seconds (Figure 5.14.b). In MCM-B, the MRR sharply falls with the increase of Sommerfeld

number. This is because the direct contact between wafer and pad asperity starts to decrease rapidly. As a result, a major portion of the wafer and pad was separated by slurry that results in indirect etching, and consequently, MRR starts to fall at a much higher rate. Furthermore, from Figure 5.12, it is quite apparent that the window of MCM is wider at lower pressure while it is shorter at higher pressure. At high pressure, the regime of MCM-A is too short to be distinguished. Since the process is usually optimized at MCR-A, detection of this regime is quite crucial for abrasive-free CMP.

5.4.1.3 Hydroplaning Contact Mode (HCM)

In HCM, the contact between wafer and pad are assumed to be separated by the thick film of slurry and, the material is only removed by indirect etching. As a result, the lowest value of removal rate was found at this contact mode. When the polishing was performed at low pressure (8.27 kPa), no HCM was found within the pressure range used in this study. On the other hand, when the wafers were polished at 15.16 kPa and 11.27 kPa, this contact mode was recognized but the trends of MRR with Sommerfeld number were found different from each other. At 11.27 kPa, the MRR was found almost constant with Sommerfeld number while it was found to be increased when the polishing was performed at 15.16 kPa. Based on such phenomena of MRR, HCM was subdivided in to two parts namely HCM-A and HCM-B. The contact regime of HCM-A was not found at high pressure CMP while HCM-A was identified when it was operated at 15.16 kPa while this regime was clearly identified when the wafers were polished at 11.27 kPa. On the other hand, the HCM-B was found at 15.16 kPa but it was not found at 11.27 kPa. It is presumed that HCM-B at 11.27 kPa CMP and HCM-A and B at 8.27 kPa CMP might be found if the wafers were run beyond 120 rpm. Similar phenomena were also found by Ara

et al. (2004) but they did not notice the effect of process parameters on the width of those contact regimes, and they did not explain why such things happen.

It is quite reasonable that MRR at this contact regime, especially at HCM-A, decreases because wafer glides over the pad during polishing resulting in indirect etching. But the HCM-B obtained at 15.16 kPa CMP gives somewhat different picture. It shows that MRR increases with Sommerfeld number. Such increase of MRR is not certainly due to the chemical etching rather it is because, at high pressure, the slurry from the wafer pad interface squeezes out. Therefore, there must be direct mechanical contact between wafer and pad. Hence, because of mechanical rubbing, the MRR again starts to increase. The AFM picture (Figure 5.14.c) of this regime shows less or no chemical layer and some scratches are found on the top of the polished wafer. This result clearly indicates that material at this regime is mainly removed by mechanical wear.

5.4.2 Synergistic Effect of Pressure and Velocity on WIWNU

With the increase of relative velocity, at any pressure, non-uniformity starts to increase as shown in Figure 5.15. It is quite evident that WIWNU increases almost in a linear fashion at lower relative velocity. But, as the relative velocity increases, WIWNU starts to be unstable. The instability of WIWNU is severe at the relative velocity corresponding to the late mixed contact mode (MCM-B) and hydroplaning contact mode where the slurry film partially or fully separates the wafer and pad during sliding. But, in the stable zone, the inconsistency of WIWNU with pressure at different relative velocity does not give clear information about the role of pressure on it. However, it is quite apparent that the instability of WIWNU is quite high at low pressure CMP and vice versa.

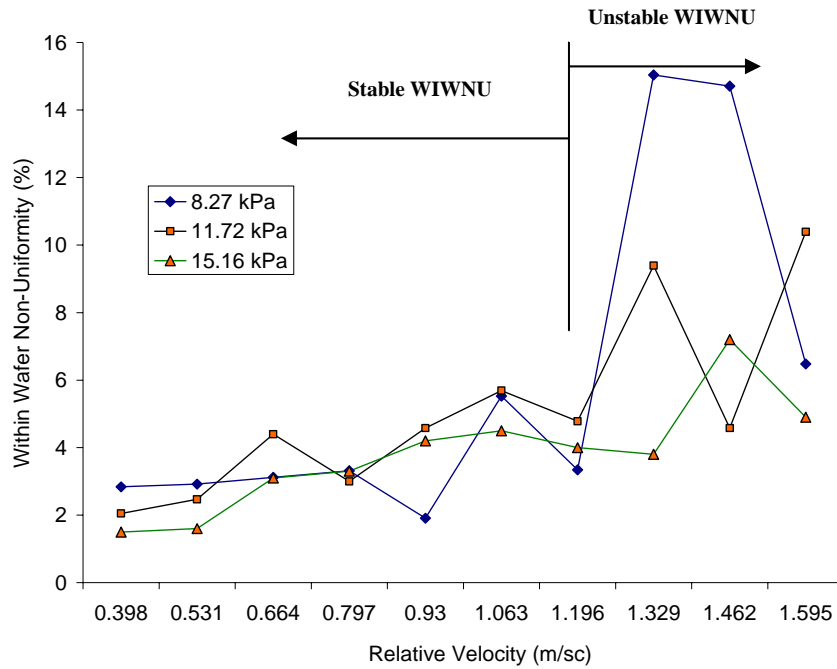


Figure 5.15 Relationship between WIWNU and relative velocity at different pressure

5.5 Development of Abrasive-free CMP Process

The process development of abrasive-free CMP involves several experimental as well as metrological steps. This is usually performed by polishing CMP test structures where the dual damascene process [A-4] has been adopted as the copper metallization technique. The process development involves some pre, in-situ and post CMP issues and better understanding of those issues are essentially important for CMP process development. The pre-CMP issue is the determination of optimum polishing condition for which the value of MRR is to be as high as possible and WIWNU is to be as low as possible. In this work, two steps polishing process has been adopted namely copper polishing and barrier polishing (Figure 5.20). The copper polishing involves determination of polishing time and an over polishing time by an optical end point detection system

while the barrier polish involves determination of over polishing time to remove residue of barrier on the oxide dielectrics. The post CMP issues comprise dishing, erosion, oxide loss, defect count, etc.

5.5.1 Pre-CMP Issue: Determination of Optimum Polishing Conditions

From the discussion on process characterization, it is quite evident that high pressure gives high MRR and low WIWNU. But high pressure results in severe mechanical failure (scratches, adhesion wear, etc) on the polished surface as shown in Figure 4.7. Conversely, peeling and delamination of low-k material is a big concern for Copper/low-k integration, and high pressure is usually avoided to prevent such mechanical failure [Balakumar et al., 2004]. In contrast, according to non-prestonian nature of MRR in abrasive-free CMP process, the low pressure CMP gives very low MRR. Besides, low pressure also results in high WIWNU. On the contrary, the polishing at moderate pressure not only gives the allowable WIWNU but also gives considerably high MRR. Therefore, moderate pressure is recommended for abrasive-free CMP provided that it must be above the lower critical pressure of the particular abrasive-free CMP process.

From the analysis of the interfacial contact mode, it was primarily selected that the MCM-A should be considered for process optimization because the MRR at this mode was found maximum. Furthermore, the window of MCM-A can be clearly identified at moderate pressure CMP while it is too short or too long to select the suitable polishing condition for high pressure and low pressure CMP respectively. Because of such pressure constraint, the MCM-A of moderate pressure CMP is recommended for abrasive-free CMP process. The average pressure and relative velocity of the respective contact mode were found 11.72 kPa and 1.02 m/sec respectively. In this work, the value of pressure of

the recommended contact mode was higher than the lower critical pressure (9.65 kPa). It was also found that WIWNU of the selected contact mode was within the allowable range (~4%). Therefore, the suggested contact mode for choosing pressure and relative velocity is fairly reasonable.

Since the chief mechanism of MRR in abrasive free CMP is chemical etching or corrosive wear, the selection of suitable slurry flow rate is also very important for abrasive-free CMP process. From experimental investigation, it was found that high slurry flow rate gives high MRR and low WIWNU. From process requirement and economic viewpoint, a moderate slurry flow rate (150 ml/min) has been chosen for this process which provides satisfactory MRR and WIWNU without giving any mechanical failure on the polished surface (Figure 4.6.d-f).

5.5.2 In-situ CMP Issues : Determination of Main Polishing and Over Polishing Time of Copper

Planarization results as material is removed faster from the protruding regions on the surface than the recessed regions. The time required to remove the bulk amount of copper up to the surface of barrier layer is called main polish time. To remove the copper residue, a copper over polishing is performed where the over polishing time is determined by an optical end-point detector. The optical end-point detector system increases the sensitivity to when copper first clears by scanning across the full wafer diameter (Figure 5.16). It enables the system to more accurately control the main polishing and over polishing time and thus, shifts from bulk copper removal step to the barrier removal step.

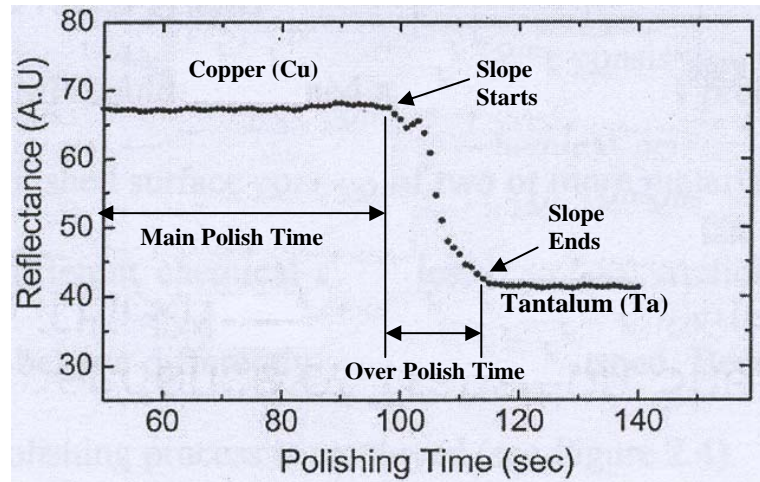


Figure 5.16 End point detection profile [Cindy, 2003]

5.5.3 Post CMP Issues : Dishing of Copper , Erosion of Dielectrics, Oxide Loss and Defect Count

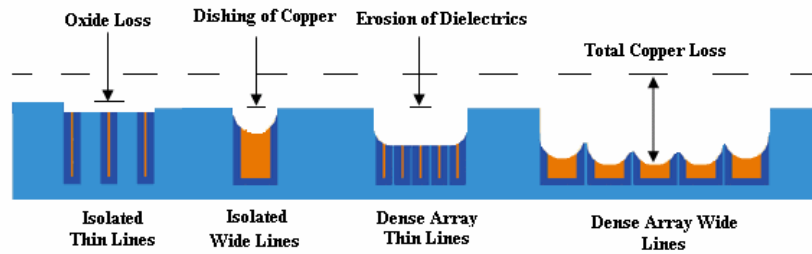


Figure 5.17 Dishing, erosion and oxide loss at different metal lines

In an ideal multilevel copper damascene technology, copper CMP would remove all the excess materials and the end result is a perfectly planar surface. In reality, on the contrary, we can not obtain such perfect flat surface primarily because of the non-uniformity of the deposited copper thickness and the difference in removal rates of different metal layers. To ensure that there is no residual copper and barrier material in the

region between the trenches requires that one clears the overburden material and everywhere on the die and wafer. This requirement implies over polishing in some regions of the die and wafer, which leads to the dishing of copper and erosion of oxide. In addition, the metal line width and density also affect the dishing and erosion value which has been shown in Figure 5.17. It has been reported that dishing and erosion start to occur when the polishing reaches the barrier [Pan et al., 1999]. In the second step of CMP process, barrier removal rate is desired to have same order of magnitude as copper, barrier layers are tough CMP materials, showing extremely low removal rate because of the requirement of being a good diffusion barrier. Therefore, considerable amount of copper and dielectric (oxide) is removed during barrier removal phase which results in dishing of copper and erosion of oxide respectively. The dishing of copper and erosion of dielectric create two major challenges for CMP, i.e. increase of RC time delay and the difficulty in fabrication of the next copper level due to excessive surface topology. Thus it is critically important to characterize and control the dishing and erosion value in CMP. The dishing and erosion value significantly changes with the pattern density of the metal interconnect [Steigerwald et al., 1997]. However, in this study, standard locations on the CMP test structures have been chosen to measure dishing and erosion. The typical location for the measurement of dishing and erosion and their respective profiles are given in Figure 5.18 and Figure 5.19 respectively. In addition, the oxide loss and defect count were also measured to check the quality of the developed abrasive-free CMP process.

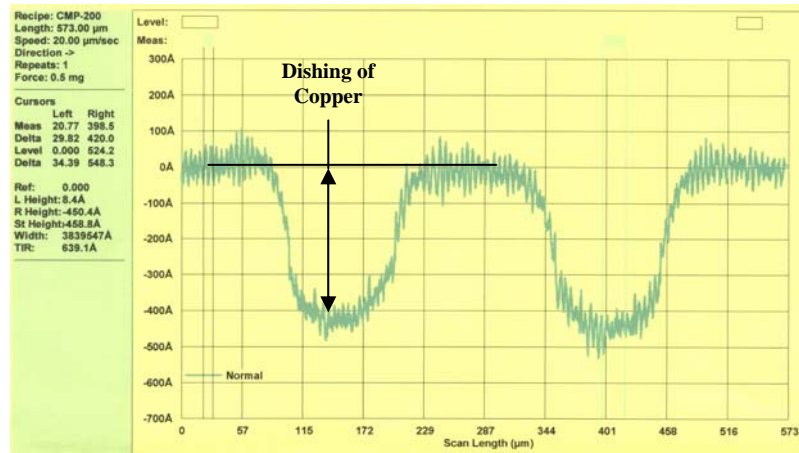


Figure 5.18 Dishing of copper interconnect at bond pad

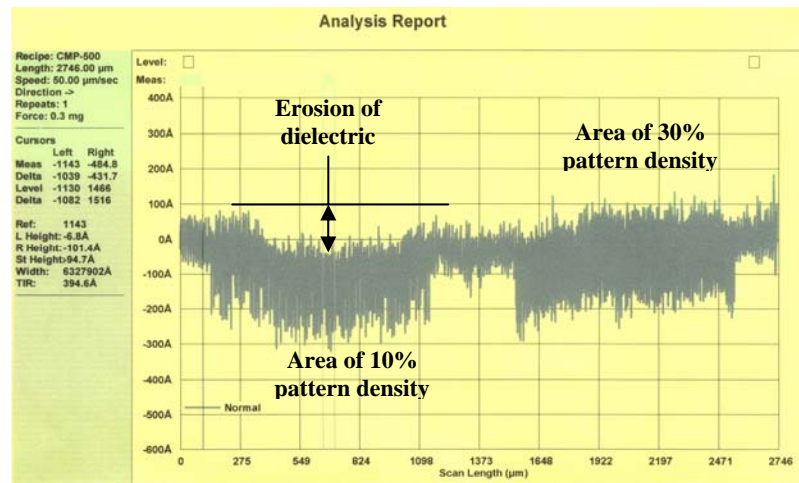


Figure 5.19 Erosion of dielectrics at pattern density 10% and 30%

5.5.4 Polishing of Copper/Oxide Pattern Wafer with Optimized Polishing Condition

Using the optimized polishing condition, the abrasive-free CMP process was characterized by polishing the patterned wafers (Cu/Oxide). Since the abrasive-free CMP process has evolved to avoid application of high pressure, the developed processes are usually identified by the value of applied pressure. In this study, two step polishing was

performed namely, Copper Polishing and Barrier Polishing as shown in Figure 5.20. The barrier polishing was performed using the base line polishing condition as given in Table 5.2.

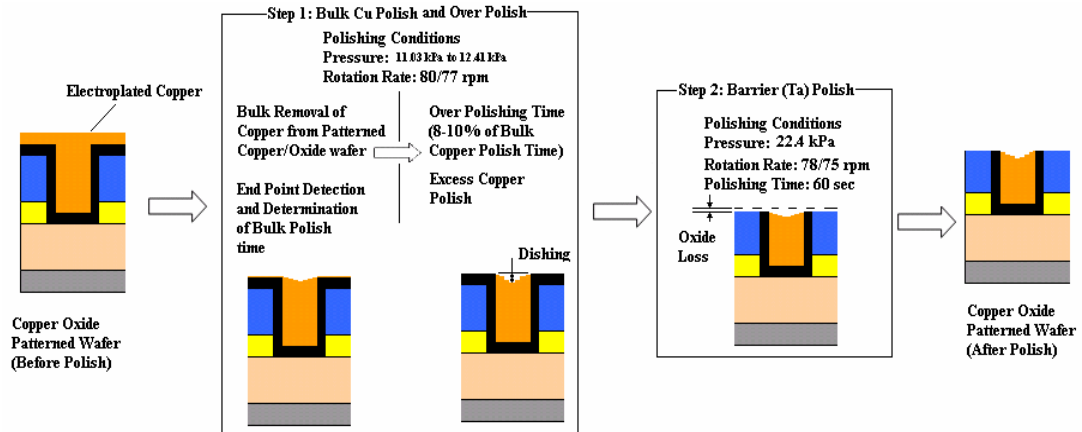


Figure 5.20 Copper/Oxide pattern wafer polishing process

Table 5.2 Barrier (Ta) polishing conditions

Barrier CMP	
Polishing Parameters	Base line value
Applied Pressure (membrane)	20.68 kPa
Applied Pressure (retaining ring)	24.13 kPa
Pad Rotation Rate	78 rpm
Wafer Rotation Rate	75 rpm
Slurry Flow Rate	200 ml/min

In the first step, bulk Cu and remaining Cu residue are removed with the process using copper slurry which stops on the underneath barrier layer (Ta). In the second step, abrasive slurry (10k2) was being used to polish barrier and to remove the dielectric for topography adjustment for better planarization.

In the present work, taking the recommended pressure (11.72 kPa) as the base line parameter, a pressure window was made to check the viability of the recommended recipe,

i.e. the bulk polishing of patterned was carried out at 11.03 kPa, 11.72 kPa and 12.41 kPa. The end point detector gives the bulk polishing time and, the over polishing of copper was carried out for 8 to 10 percent of bulk polish time which was sufficient enough to clear excess copper. In the second approach, barrier polish step was carried out using 6.89 kPa and fixed over polish time (60 sec). It was optimized by running a few experiments with different over polish time, and subsequent dishing measurements were performed on the bond pad CMP test structure (Figure 5.18). The end point detection for Cu removal confirmed the process stability for all three pressures (11.03 kPa, 11.72 kPa, 12.41 kPa) which was monitored for several wafers. It was observed that the polishing time was consistent for wafer to wafer. The polishing conditions, polishing times, oxide loss and defect count for the mentioned recipes are given in Table 5.3

Table 5.3 Polishing data of copper/oxide wafers polished with abrasive-free slurry

AF CMP process (kPa) (membrane pressure/ retaining ring pressure)	Rotation Rate (rpm) (Platen/ Wafer)	Main Polishing Time (sec)	Over Polishing Time (sec)	Oxide Loss (Å)	Defect Count
9.65/12.41	80/77	165	13(8%)	1187.80	4352
10.34/13.10 kPa		129	13(10%)	1044.6	4848
11.03/14.47 kPa		121	10(8%)	1146.86	4302

After first step polishing, the dishing at copper interconnect were measured. The variation of dishing value from center to edge also represents the non-uniformity issue. The dishing values after first step polishing greatly influence the final value of dishing and oxide loss (after second step polishing). Besides, the defect count and electrical data also helps to understand the excellence of the process.

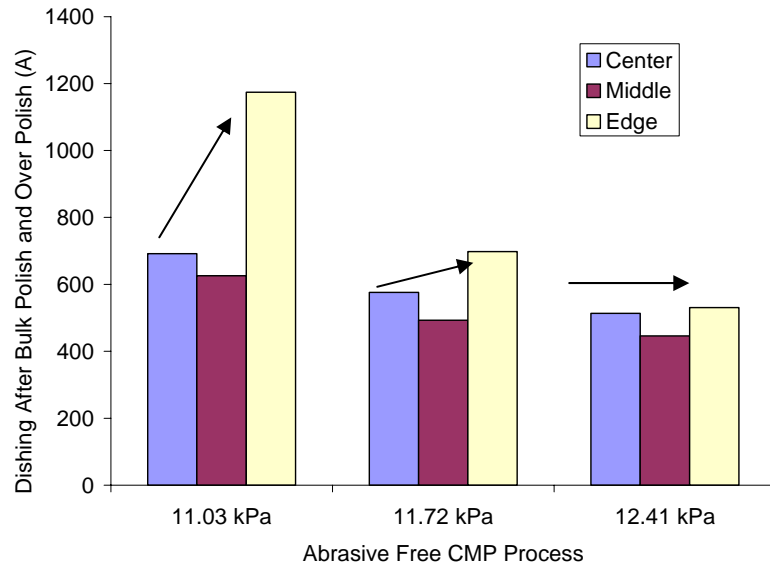


Figure 5.21 Dishing after copper bulk polish and over polish

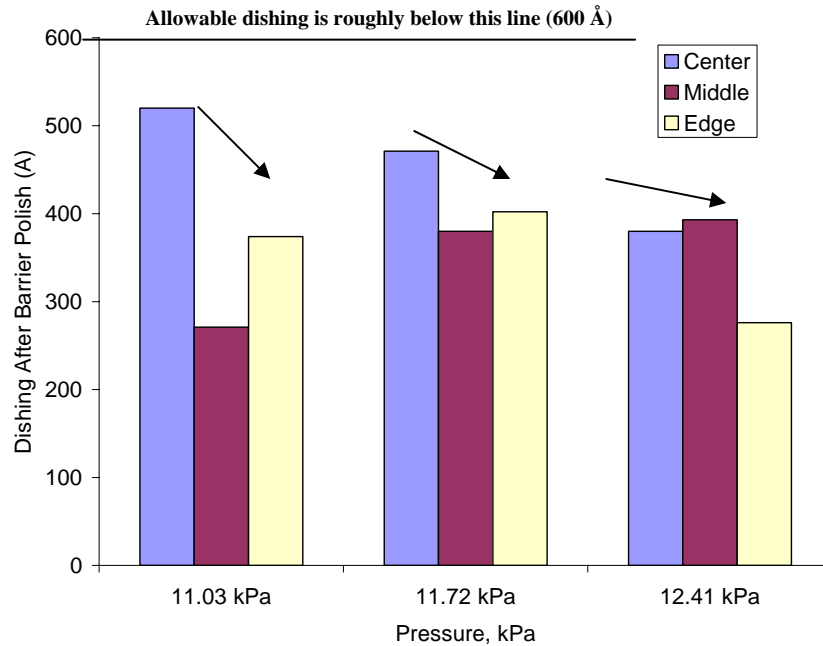


Figure 5.22 Dishing after barrier polish

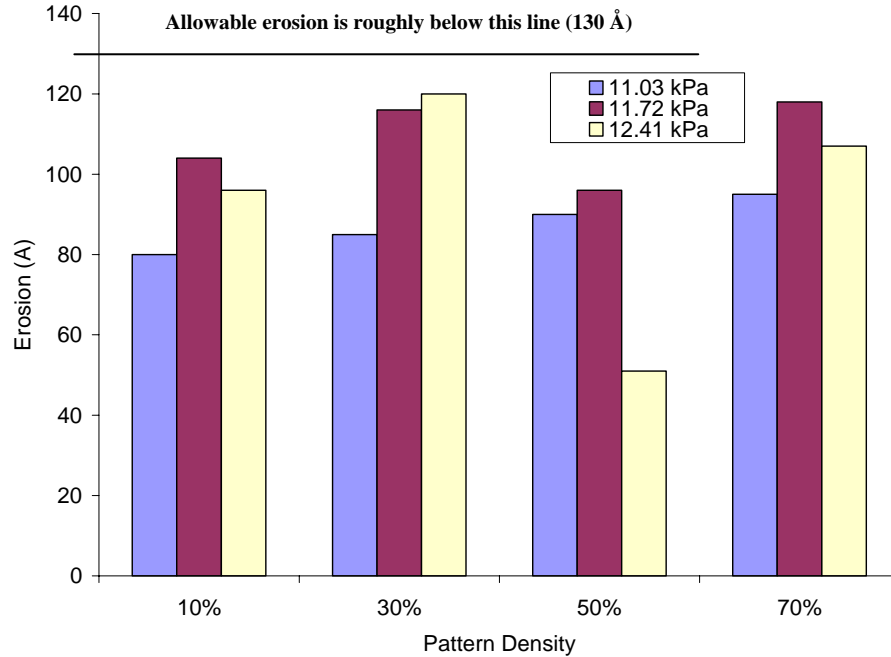


Figure 5.23 Erosion of dielectric material after barrier polish

The dishing data as shown in Figure 5.21 shows that the abrasive-free CMP process at 12.41 kPa gives the lowest dishing value and, the uniformity of dishing across the wafer is better than that of other two processes. The dishing data also provided good non-uniformity to the dishing value in barrier polishing as shown in Figure 5.22. In usual CMP practice, the allowable dishing value is below 600 \AA which has been satisfied by both polishing steps. On the other hand, the results of Figure 5.23 shows that 12.41 kPa process gives quite low value of erosion of dielectrics at the areas of four different pattern densities. Besides, the main polishing time for 12.41 kPa process was lower than other two processes which will definitely give high throughput. However, the oxide loss and defect count for all the processes are fairly low as shown in Table 5.3. The electrical data showed that there is no leakage issues in Cu/Oxide system as compared to abrasive slurry, and the value was within the allowable range (below $1\text{E-}09$) as given in Figure 5.24. Therefore,

the recommended abrasive-free CMP process which was chosen based on the modes of contact analysis is practically reasonable.

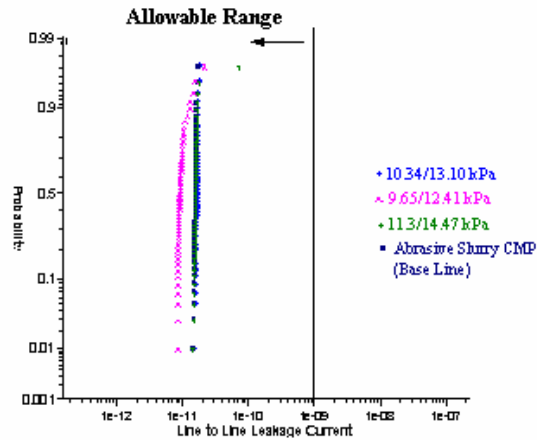


Figure 5.24 Leakage current at copper interconnects of pattern wafers

5.6 Conclusions

The conclusions concerning the process characterization are given as follows:

- The role of slurry flow rate on MRR and WIWNU in abrasive-free copper CMP has been found completely opposite to that of conventional CMP process, i.e. MRR increases and WIWNU decreases with the increase of slurry flow rate, and vice versa.
- The change of MRR with pressure gives the critical pressure issue which introduces two different kind of MRR: direct etch rate and indirect etch rate. In addition, both of those two etch rates show non-linear dependence of MRR on pressure.
- From ‘Modes of Contact’ analysis, two significant contact regimes in both MCM and HCM have been identified namely MCM-A & B and HCM-A&B.

- WIWNU steadily increases with relative velocity but it becomes unsteady at hydroplaning contact mode. Besides, WIWNU shows more stable behaviour at high pressure CMP.
- The MCM-A is recommended for abrasive-free copper CMP process because the highest MRR and allowable WIWNU are found in this regime.
- At high pressure, the window of MCM-A is too short to be distinguished. So, moderate pressure is recommended for abrasive-free copper CMP process.
- The recipe of the recommended contact mode (MCM-A) provides satisfactory outputs (over polishing time, dishing value, oxide loss, defect count and leakage current loss) in pattern wafer polishing.

This chapter introduces the non-prestonian effect of pressure on MRR. Besides, the previous chapter proves that the dominant material removal mechanism is chemical etching (corrosive wear) which is mainly influenced by pressure. In the next chapter, a MRR model will be developed taking into account those two important issues.

Chapter 6

A Material Removal Rate Model for Abrasive-free Copper CMP Process

6.1 Introduction

Modeling and simulation of CMP process is a very critical part that transfers the CMP from engineering ‘art’ to engineering ‘science’. The absence of particle in abrasive-free slurry and its chemical dominance in material removal has brought new challenges in modeling and simulation of copper CMP process. The chemically dominant abrasive-free CMP can not be explained by the existing MRR models which are mechanically predominant. However, the material removal mechanism in abrasive-free CMP investigated in Chapter 3 clearly indicates that chief mechanism of material removal is chemical etching or corrosive wear, and no MRR model has been developed based on corrosive wear mechanism. Besides, the non-prestonian nature of MRR noticed in Chapter 4 has not been included in any MRR model of CMP. In fact, no quantitative model has been developed so far that explains the special issues of the chemically dominant abrasive-free copper CMP process. Since there is no interaction of particles with pad and wafer, the particle scale models are not applicable for abrasive-free CMP process. So, the pad based MRR model can only explain the effect of the direct interaction of pad with wafer on MRR. But the only pad based model, developed by Zhao et al. (1998), considers the presence of particle in between pad asperity and wafer, i.e. higher the real contact area, higher will be the number of abrasive at pad wafer interface resulting in higher MRR. Since this pad based MRR model is developed based on the abrasion wear mechanism

and, it does not take into account the non-prestonian issue, it is no longer applicable for abrasive-free copper CMP process.

In this chapter, a MRR model has been developed for abrasive-free copper CMP process. The mechanical process parameters i.e. the pressure and relative velocity have been taken as the main input for the model. For abrasive-free CMP process, applied pressure is responsible for non-prestonian behavior of MRR. So, the role of pressure and its effect on MRR has been taken as the main concern of this work. The approach of this model is based on periodic distribution of pad asperity, elastic contact between wafer and pad interface and chemical etching (corrosive wear) theory. In this study, the influence of applied pressure on direct and indirect etching and the contribution of those two etchings to total MRR have been quantified. Finally, the MRR predicted by the developed model will be verified by experimental data. The model also includes the dependence of MRR on pad geometry, material properties and chemical reactivity.

6.2 Formulation of MRR Model

6.2.1 Assumptions

CMP mainly depends on the synergy between the chemical and mechanical effect on material removal from the wafer surface. The shear force acting at the contact surface of the sliding abrasive particle and wafer is responsible for material removal in mechanically dominated material removal mechanisms such as abrasion/micro-cutting, brittle fracture, particle rolling and erosion, burnishing, etc [Rabinowicz, 1995; Lai, 2001]. Abrasion can be a possible material removal mechanism in CMP process only when the hardness of the asperity or particle is higher than wafer material. Since there is no particle

in abrasive-free slurry and the pad modulus is much lower than that of electroplated copper, material removal by abrasion / micro-cutting, brittle fracture, erosion, particle rolling are absent. Lai (2001) proved that burnishing, that occurs at molecular scale (adhesive force), is also not a dominant mechanism in CMP. Because of those reasons, the effect mechanical shear on the removal of copper oxide layer has been neglected. Besides, Jiang et al. (2000) argued that the average shear stress exerted by slurry flow is several orders of magnitude smaller than polishing pressure. So, the material removal caused by fluid share is assumed to be negligible. However, it is assumed that the slurry transportation rate at wafer-pad interface is uniform with pressure.

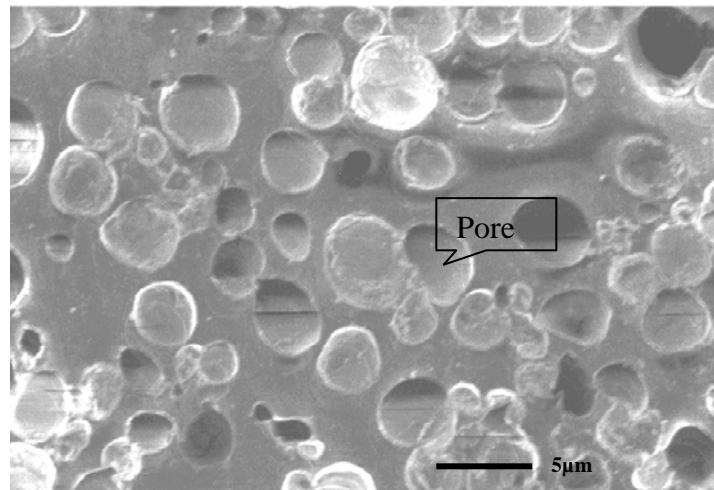


Figure 6.1 SEM picture of copper polishing polyurethane pad

The polyurethane pad used for copper polishing is a kind of foamed pad having lots of pores and voids on the surface (Figure 6.1). For simplicity, the size of the pores has been assumed equal and the distribution of the asperity summit has been considered

periodic where the pores resemble the valley and the solid surface is considered as the peak. This means that the heights of the summits are equal or close to each other such that the asperities come in contact with wafer and elastically deform under down pressure. However, this assumption can be substantiated by the fact that the typical polyurethane pad modulus (2.5×10^8 GPa) is 4.16×10^2 times smaller than that of copper wafer (1.04×10^{11} GPa). Similar assumption of pad asperity distribution was made by some other researchers in developing MRR model for conventional CMP process [Luo et al., 2001; Zhao et al., 1998]. The wafer surface is assumed as smooth and flat because the typical value of surface roughness of Cu wafer is around 1-2 nm.

As discussed in Chapter 4, chemical etching (corrosive wear) is the only convincing dominant material removal mechanism in abrasive-free copper CMP process. The protective layer is removed by the ‘soft friction’ (shear) force, and the newly exposed CuO/Cu₂O layer is etched out. It is assumed that the applied pressure is only supported by the pad asperities. In this work, based on the nature of material removal at different contact modes, the chemical etching has been categorized as direct etching and indirect etching as shown in Figure 4.3. In order to know the removal rate, determination of the respective areas of etching is the main step towards the development of MRR model for abrasive-free copper CMP process. We assume that the wafer and pad asperities are in solid contact during polishing. It is quite obvious that the higher the contact area higher will be the etch rate. Besides, the wafer-asperity contact area is a function of applied pressure which can be determined using the theory of elastic contact [Johnson, 1995]. The protective film at the contact area is removed at each cycle of sliding that exposes a fresh portion of copper oxide layer which is then rapidly dissipated into the slurry.

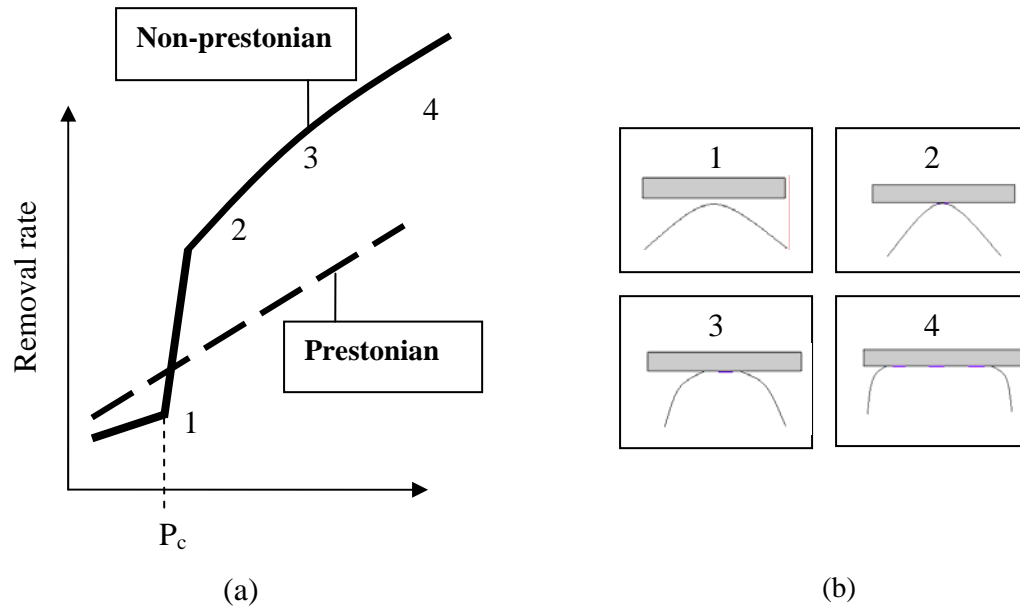


Figure 6.2 Schematic diagram of: a) the prestonian and non-prestonian behavior of MRR [Matsuda et al., 2003] b) the wafer-pad asperity contact at different locations of non-prestonian curve

The MRR in conventional CMP process shows a linear prestonian relation with pressure. In contrast, in abrasive-free CMP process, the material removal follows a non-prestonian relation with pressure as shown in Figure 6.2. Below the critical pressure, the MRR remains almost constant with pressure. As soon as pressure goes above a critical value (P_c), the pad asperity starts to come in contact with wafer. Therefore, the soft sliding friction force removes the protective layer that results in direct etching, and consequently, the MRR sharply increases above the critical pressure [Matsuda et al., 2003; Homma et al., 2003]. Since pressure rapidly increases the etch rate when polishing is performed above the critical pressure, direct etching can be defined as pressure assisted etching. Apart from the critical pressure issue, non-prestonian issue involves the non-linear

dependence of MRR on pressure. In contrast, the prestonian phenomenon always gives linear MRR with pressure.

6.2.2 Determination of the Area of Direct Etching and Indirect Etching

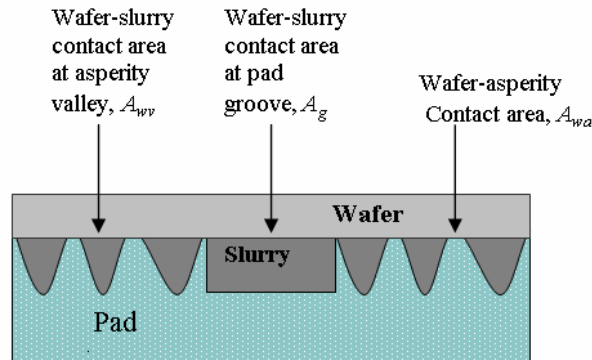


Figure 6.3 Different kinds of areas at wafer-slurry and wafer-pad contact

As mentioned earlier, at any instance, there are three different kinds of areas those experience three different kinds of etching (Figure 6.3). Firstly, the area at wafer-pad asperity contact (A_{wa}) where the soft sliding force removes the protective layer. Since this contact is assumed as solid-solid contact, no etching occurs because of the absence of slurry in between the two sliding surfaces. Secondly, the area having no protective layer experiences direct etching. This area usually goes under the wafer-asperity contact (A_{wa}) just before that instance. Thirdly, the area (A_{ie}) having the protective layer on the surface experiences indirect etching. The area experiencing indirect etching is the summation of the wafer-slurry contact area at asperity valley (A_{wv}) and wafer-slurry contact area at pad grooves (A_g), i.e.

$$A_{ie} = A_{wv} + A_g \quad (6.1)$$

So, based on the areas experiencing different kind of etching, total contact area of wafer with pad and slurry can be written as,

$$A = 2A_{wa} + A_{ie} \quad (6.2)$$

From contact mechanics [Johnson, 1995], based on the hertz theory of elastic deformation, the contact between solid surfaces is discontinuous where the real area of contact is a small fraction of apparent contact area. Furthermore, we assumed that the applied pressure is only supported by pad asperities at wafer-asperity contact. So, it is quite evident that wafer and pad asperity contact will be increased with applied pressure. As a result, the wafer and slurry contact area at pad valley and pad groove will also decrease. Now, if the density of asperity is η and the asperity summits are presumed as spherical in shape having radius R , then real area of contact between wafer and pad asperity can be given by,

$$A_{wa} = \pi \left(\frac{3RP}{4\eta E^*} \right)^{2/3} \quad \eta A_p = \xi A_p P^{2/3} \quad (6.3)$$

$$\text{Where, } \xi = \pi \left(\frac{3R}{4\eta E^*} \right)^{2/3} \eta \text{ and } E^* = \left[\frac{1-\gamma_w^2}{E_w} + \frac{1-\gamma_p^2}{E_p} \right]^{-1}$$

here, ξ involves both material property of pad and wafer and the physical property of pad asperities.

6.2.3 Material Removal by Chemical Etching (Corrosive Wear)

According to the theory of corrosive wear, the volume of material etched is directly proportional to the sliding contact area and sliding relative velocity [Rabinowicz, 1995]. So, the volume of material removed by chemical etching can be given by,

$$MRR_{cw} = kA_cV \quad (6.4)$$

where, k is the corrosive wear coefficient and A_c is the contact area between wafer and slurry that goes under corrosive wear.

6.2.3.1 Material Removal by Direct Etching

The wafer-asperity contact area is nothing but the real contact area where the direct etching takes place, i.e.

$$A_c = A_{wa} = A_{de} \quad (6.5)$$

Now, from Eqn. 6.4 and 6.5, the MRR by direct etching can be written as,

$$MRR_{de} = k_{de}A_{de}V = k_{de}\xi A_p P^{2/3}V \quad (6.6)$$

where, k_{de} is the function of wear coefficient for direct etching that also takes into account other CMP parameters.

6.2.3.2 Material Removal by Indirect Etching

Copper oxide is dissolved by etchant through the pores or fissures of the protective layer at weak locations during indirect etching as shown in Figure 4.3. In addition, Figure 5.10 shows that the MRR below critical pressure remains almost constant with pressure. So, this proves that the type of contact area at pad-wafer interface below critical pressure is identical, i.e. the entire wafer is separated from the pad by slurry film which results in indirect etching. As soon as the applied pressure goes above the critical value, the wafer and pad asperity contact area increases in a nonlinear fashion given by Eqn. 6.3. Therefore, the area for indirect etching also decreases in a nonlinear fashion (Eqn. 6.2) which causes the nonlinear decrease of MRR.

Now, the volume of corrosive wear at the area of indirect etching can be given by,

$$MRR_{ie} = k_{ie} A_{ie} V \quad (6.7)$$

As described above, below critical pressure, the entire surface of wafer A is equal to A_{ie} , and the thickness of material removed is δ_c . Hence, the volume of material etched at or below the critical pressure is,

$$MRR_{ie_c} = \delta_c A = k_{ie} AV \quad (6.8)$$

Using Eqn. 6.7 and Eqn. 6.8, we get,

$$MRR_{ie} = \delta_c A_{ie} \quad (6.9)$$

When the wafer comes in contact with pad asperity, from Eqn. 6.2 and 6.9, the indirect etch rate can be written as,

$$MRR_{ie} = \delta_c (A - 2A_{wa}) \quad (6.10)$$

6.2.3.3 Total Material Removal Rate

Combining the direct etch rate and indirect etch rate, the total volume removal rate can be written as,

$$MRR_T = k_{de} A_{wa} V + \delta_c (A - 2A_{wa}) \quad (6.11)$$

Now, putting the expression of A_{wa} in Eqn. 6.11,

$$MRR_T = k_{de} \xi A_p P^{2/3} V + \delta_c (A - 2\xi A_p P^{2/3}) \quad (6.12)$$

In abrasive-free CMP process, it is the usual practice to choose the polishing pressure above the critical pressure. Now, according to non-prestonian nature of MRR in abrasive-free CMP process, the material at critical pressure is removed from the entire wafer surface in the form of indirect etching,

i.e. at $P = P_c$,

$$MRR_T = MRR_{ie_c} = \delta_c A \quad (6.13)$$

So, putting the critical pressure issue in Eqn. 6.12,

$$\delta_{lc} A = k_{de} \xi A_p P_c^{2/3} V + \delta_c (A - 2 \xi A_p P_c^{2/3}) \quad (6.14)$$

Subtracting Eqn. 6.14 from Eqn. 6.12, the expression of total MRR becomes,

$$MRR_T = k_{de} \xi (P^{2/3} - P_c^{2/3}) A_p V + \delta_{lc} (A - 2 A_p \xi (P^{2/3} - P_c^{2/3})) \quad (6.15)$$

where, $P > P_c$

And,

$$MRR_T = MRR_c \quad (6.16)$$

where, $P \leq P_c$

At any pressure $P \geq P_c$, total MRR can be written as,

$$MRR_T = \delta_T A \quad (6.17)$$

Equating Eqn. 6.15 and Eqn. 6.17, the MRR can be written in terms of thickness removal rate as,

$$\delta_T = k_{de} \xi \left(P^{2/3} - P_c^{2/3} \right) \left(\frac{A_p}{A} \right) V + \delta_c \left(1 - \frac{2A_p \xi \left(P^{2/3} - P_c^{2/3} \right)}{A} \right) \quad (6.18)$$

where, $P_c < P$

and

$$\delta_T = \delta_c \quad (6.19)$$

where, $P \leq P_c$

6.3 Discussions

6.3.1 Model Evaluation

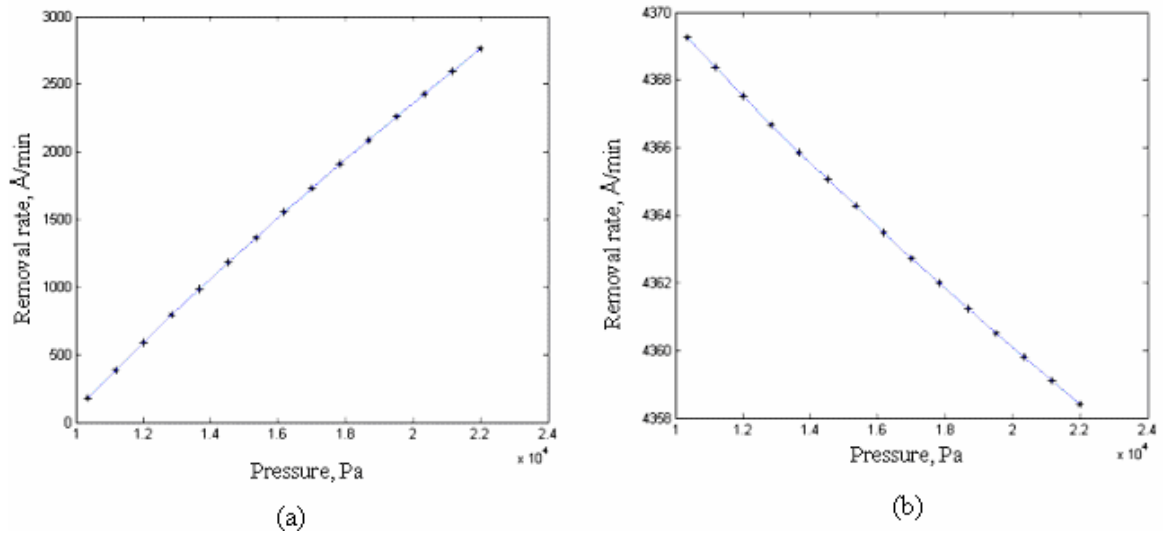


Figure 6.4 Change of MRR with pressure: a) direct etching and b) indirect etching (At relative velocity 0.49 m/sec)

The model developed in this study reveals some insights into the fundamental mechanism of abrasive-free CMP process. Eqn. 6.2 and Eqn. 6.3 show that, with the increase of pressure, the area of direct etching increases while the area of indirect etching decreases. Since the removal rate is proportional to contact area and sliding velocity and, since the contact area is proportional to applied pressure, the volume of material removed by direct etching increases with pressure (Figure 6.4.a). Conversely, the material removed by indirect etching decreases with pressure as shown in Figure 6.4.b.

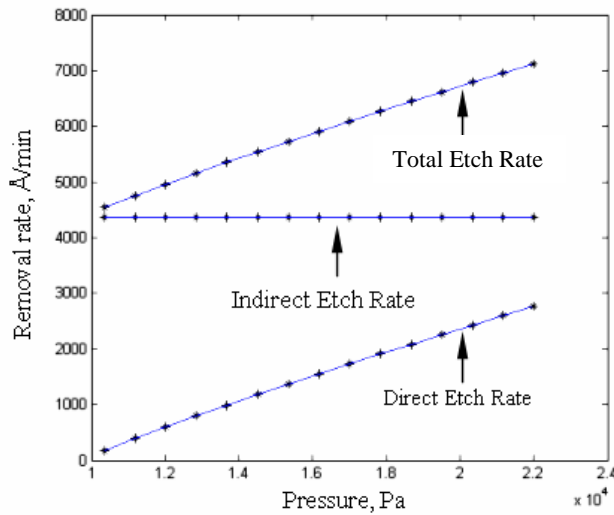


Figure 6.5 Comparison between the change of direct etch rate and indirect etch rate with pressure (At relative velocity 0.49 m/sec)

Combining the direct and indirect etch rate, it is apparent from Figure 6.5 that the rate of change of direct etching with pressure is several times higher than that of indirect etching. Thus the MRR model shows that pressure has very little or no effect on indirect etch rate while it has significant effect on direct etch rate. This fundamental information is

essentially important to control the abrasive-free CMP process because pressure has been found as the main modulating parameter in abrasive-free copper CMP process. Since the indirect etch rate remained almost constant with pressure within the given pressure window, the MRR model for abrasive free CMP can be written as,

$$\delta_T = k_{de} \xi \left(P^{2/3} - P_c^{2/3} \right) \left(\frac{A_p}{A} \right) V + \delta_c \quad (6.20)$$

where, $P > P_c$

And,

$$\delta_T = \delta_c \quad (6.21)$$

where, $P \leq P_c$

Therefore, the model shows that indirect etching is mainly determined by the value of δ_c . The value of δ_c depends on the chemical activity and relative velocity of wafer with respect to pad given by Eqn. 6.8. So, determination of the value of δ_c is also very important for the developed MRR model.

Figure 6.5 also demonstrates that indirect etch rate contributes the major amount to the total removal rate, especially at low pressure. Since indirect etching occurs at low pressure CMP, as mentioned in Chapter 4, it ensures dominance of chemical wear which normally provides very clean and smooth surface. Therefore, the contribution of indirect etching, which mainly depends on the chemical reactivity of slurry, is very much expected in abrasive-free copper CMP process. On the other hand, direct etching requires high

pressure which causes the dominance of mechanical wear giving rise to poor surface quality of the polished wafer. But from process control view point, pressure is a very important tool which is necessary to modulate the CMP process. Since the pressure has very little or no effect on indirect etching, in order to establish the control over the process, it is required to operate the polishing above the critical pressure to ensure the presence of direct etching. Therefore, a judicial balance between the direct etching and indirect etching must be made to get good surface finish as well as high MRR.

The model takes in account the effect of area on MRR, i.e. higher the wafer-asperity contact area, higher the dominance of pressure assisted direct etching. Conversely, higher the pad groove area and pad pore area, higher the dominance of indirect etching. It has already been mentioned that indirect etching provides major portion to total MRR at low pressure, and pressure has little or no effect on indirect etch rate. In addition, the abrasive-free copper CMP has been introduced to avoid application of high pressure CMP. Therefore, it is advisable to increase the indirect etch rate as high as possible in order to ensure high throughput. This can only be made if the pad groove area and pore area is increased and/or the chemical reactivity of slurry is increased. Thus the requirement of high pressure, which is usually needed to ensure high MRR but advised to avoid in abrasive-free CMP, can be reduced to a greater extent.

The MRR model successfully includes the non-prestonian issue, i.e. the critical pressure limit (P_c) has been included in the model. In addition, the model also explicitly incorporates the role of material property on MRR which is very important to select the pad and wafer material for abrasive free copper CMP process.

6.3.2 Experimental Verification of the Model

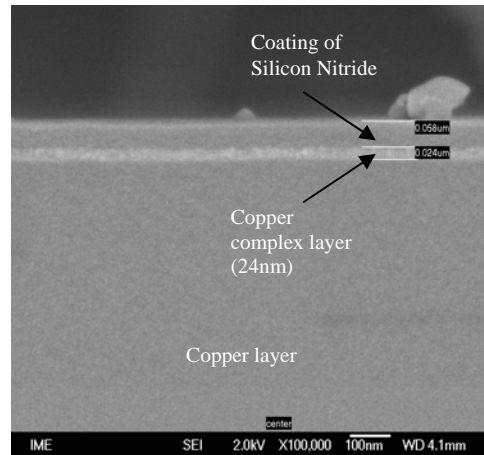
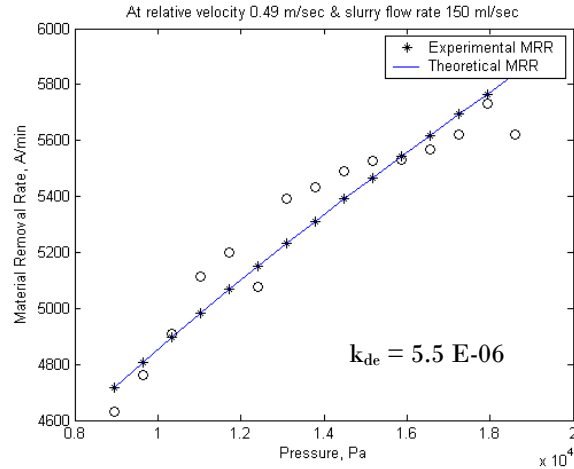


Figure 6.6 X-SEM of copper oxide layer formed after dipping 24 hours in the abrasive free slurry

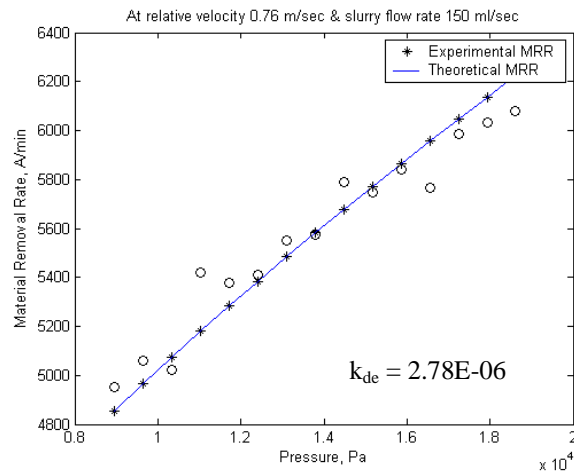
A typical abrasive-free copper CMP process has been selected in this study. The material properties and process parameters have been given in Table 6.1. Experiments were carried out with a polyurethane pad of diameter 500 mm, copper wafer of 200 mm and commercial abrasive-free slurry. The blanket copper wafers were polished in AMAT Mirra-Mesa polisher. The thickness and uniformity of the copper films were obtained using a four point probe to measure the sheet resistance at eighty one fixed points on the wafer. After dipping the wafer into slurry for 24 hours, the layer formed on the top was found to be 24 nm as shown in Figure 6.6. The thickness of the complex layer was measured by X-SEM analysis. In order to protect the copper complex layer during X-SEM analysis, a Silicon Nitride layer of 58 nm was formed on the top of the copper complex layer. The Plasma Enhanced Chemical Vapor Deposition (PECVD) technique (Novellus) was used to deposit the silicon nitride layer.

Table 6.1 Operating conditions and other parameters used for MRR modeling

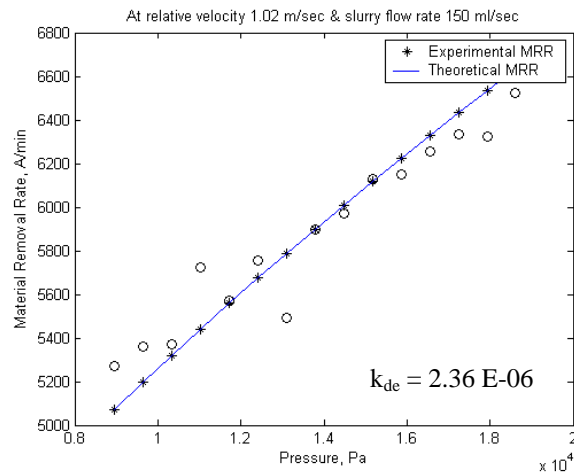
Pad wafer sliding velocity, V (m/sec)	0.49, 0.76 and 1.02
Applied pressure, P (kPa)	6 – 20
Asperity density, η (m^{-2})	1.2×10^9
Average asperity radius, R (m)	3×10^{-5}
Pad modulus, E_p (Pa)	2.5×10^8
Wafer modulus, E_w (Pa)	1.04×10^{11}
Pad Poisson ratio, γ_p	0.05
Wafer Poisson ratio, γ_w	0.352
Eccentricity between wafer and pad, e (m)	0.127
Slurry flow rate (ml/min)	150
The volume ratio of slurry to Hydrogen Per Oxide	2.23:1



(a)



(b)



(c)

Figure 6.7 Experimental MRR versus theoretical (predicted by abrasive-free MRR model) MRR at relative velocity: a) 0.49 m/sec b) 0.76 m/sec and c) 1.02 m/sec

The composition and mechanical properties of the complex layer formed on the top of the wafer during abrasive-free polishing has not been characterized but estimated according to the data from literature [Zhao et al., 2000]. Furthermore, from high-frequency spectral analysis, Denardis et al. (2003) recommended that the periodicity of the formation and removal of copper complex layer is 10 ms. So, the thickness of such film formed during polishing at each cycle will be much lower, and the property of that film is hardly possible to measure. Because of this reason, the property of the pure copper thin film has been considered to evaluate the model. The parameters of surface topology of a typical polishing pad have been used which is similar to the data used by Zhao et al. (2002) given in Table 6.1. Substituting the values, Eqn. 6.20 yields removal rate at various pressures and three relative velocities as shown in Figure 6.7. Since the abrasive-free CMP process is usually operated above the critical pressure, the experimental MRR above the critical pressure has been plotted with the predicted MRR. The predicted MRR of the model clearly conforms to the experimental MRR by showing the non-linear dependence of MRR on pressure. In order to avoid the delamination and the damage of low-k material, low pressure is usually preferred in abrasive-free CMP process provided that pressure must not go below the critical pressure as shown in Figure 6.7. In this study, the polishing was carried out between average pressure 6 kPa and 20.6 kPa. The agreement of the removal rates predicted by the model with experimental data proves that the model is fundamentally sound.

During the formulation of model, the constant k_{de} was assumed to be strongly associated with corrosive wear and weakly with other CMP parameters. It is experimentally found that the value of corrosive wear coefficient was of the order of 10^{-6} .

Robinowicz (1995) argued that the corrosive wear co-efficient for partially lubricated surface is close to 10^{-5} . This also proves that the fundamental concept of material removal mechanism based on which the MRR model has been developed is fairly reasonable.

6.4 Conclusions

From the evaluation and experimental verification of the MRR model, following conclusions can be drawn:

- The MRR model presents that pressure has very little or no effect on indirect etch rate while it has significant effect on direct etch rate.
- The model demonstrates that the indirect etch rate contributes the major portion to the total MRR, especially when the polishing is performed at low pressure.
- The model also indicates that higher value of chemical reactivity, pad groove size and the pad pore size provides higher indirect etch rate, and vice versa.
- The effect of pad modulus, wafer modulus and asperity density on MRR can be understood from this model.
- The predicted MRR of the model closely fits with the experimental MRR by showing the non-linear dependence of MRR on pressure and giving a wear coefficient that lies in the given range of corrosive wear.

Thus the MRR model gives some fundamental information regarding the key issues of process parameters and consumable sets of abrasive-free copper CMP process.

Chapter 7

Thesis Contributions and Recommendations for Future Work

7.1 Introduction

The fundamental aspects of abrasive-free copper CMP process are investigated in this study. This chapter summarizes the significant conclusions drawn in Chapter 4, 5 and 6 in the form of thesis contributions. In addition, considering the limitations and prospects of this work, some recommendations have also been made in this chapter for its future work.

7.2 Thesis Contributions

The following important contributions of this thesis are quite noteworthy:

- In this study, the material removal mechanism in abrasive-free copper CMP process has been investigated. Experimental investigation clearly indicates that chemical etching (corrosive wear) is the dominant material removal mechanism in abrasive-free CMP process while some other form of mechanical wear has also been noticed on the polished surface.
- The role of process parameters in wear mechanisms has been studied in this work. The decrease of pressure and the increase of relative velocity and slurry flow rate give the dominance of chemical wear, and vice versa. However, the effect of pressure on both chemical and mechanical wear has been found much higher than that of slurry flow rate and relative velocity.

- An abrasive-free copper CMP process has been characterized and developed in this study. The experimental results demonstrate the non-prestonian behaviour of MRR by introducing the critical pressure issue and by explaining the non-linear dependence of MRR on pressure in both direct and indirect etching. Moreover, the interfacial contact analysis shows that pressure significantly affects the window of different contact modes.
- Taking into consideration the non-prestonian behaviour of MRR and corrosive wear as the material removal mechanism, in this study, a MRR model has been developed. Besides, the MRR model can explain the effect of pressure, velocity, chemical reactivity of slurry, pad surface geometry (groove size, asperity radius and asperity density), material property of pad and wafer on direct and indirect etch rate. The good agreement of the predicted MRR of the model with experimental MRR gives the validity of the model.

7.2 Recommendations for Future Work

The following recommendations are made for the further investigation of material removal mechanism, process characterization and the improvement of MRR model:

- Mechanism of material removal in abrasive-free CMP was found to be dominated by chemical etching or corrosive wear. In order to get real picture how the material of wafer is chemically modified and how the material is etched out from the wafer surface, it is necessary to know the exact chemical composition of the abrasive-free slurry. Thus the fundamental understanding of chemical etching can be

achieved which will undoubtedly reduce the ambiguity of some special phenomena of abrasive-free CMP process.

- The Coefficient of Friction (COF) usually decreases with the increase of slurry flow rate, and MRR in conventional abrasive free CMP increases with the increase of COF. But MRR in abrasive-free CMP increases with slurry flow rate which means that the MRR increases with decrease of COF. The in situ measurement of COF at various flow rates, pressure and relative velocity can be checked out and compared with the conventional CMP characteristics. This will not only help to optimize the abrasive-free CMP process but also help to design the abrasive-free CMP consumables.
- The investigation of wear mechanism of abrasive-free CMP showed that slurry transportation at wafer pad interface significantly affects the MRR. In addition, the slurry transportation remarkably changes with slurry flow rate, applied pressure and relative velocity. The present model successfully incorporated pressure and velocity as an input parameter. Here, the inclusion of slurry flow rate as an input parameter in the model is strongly recommended which will certainly make the model more robust.

Bibliography

Ahmadi, G. and Xia, X., A Model for Mechanical Wear and Abrasive Particle Adhesion During the Chemical Mechanical Polishing Process, *Journal of the Electrochemical Society*, 148, No. 3, pp. G99-G109, 2001.

Archard, J. F., Contact and Rubbing of Flat Surfaces, *Journal of Applied Physics*, 24, pp. 981-985, 1953.

Balakumar, S., Chen, X. T., Chen, Y. W., Selvaraj, T., Lin, B. F., Kumar, R., Hara, T., Fujimoto, M. and Shimura, Y., Peeling and delamination in Cu/SiLK™ process during Cu-CMP, *Thin Solid Films*, 462-463, pp. 161-167, 2004.

Beilby, S. G., *Aggregation and Flow of Solids*, Macmillan & Co., London, 1921.

Bhushan, B., *Introduction to Tribology*, John Wiley and Sons, Inc., 2002.

Blake, L.H. and Mandel, E., Chemical-Mechanical Polishing of Silicon, *Solid State Technology*, 13, pp. 42-46, 1970.

Boning, D, Tugbawa, T, Park, T, Brian Lee, Lefevre, P. and Nguyen, J., Modeling of Pattern Dependencies in Abrasive-Free Copper Chemical Mechanical Polishing Processes, *Proc. of VMIC*, pp.22-32, 2001.

Bowden, F.P. and Hughes, T.P., Physical Properties of Surfaces IV - Polishing, Surface Flow and the Formation of the Beilby Layer, *Proc. Roy. Soc.*, 160A, pp. 575-587, 1937.

Cindy, K., Copper CMP Studies for Copper/Black Diamond with Three Different Barriers, Final Year Project Report, Dept. of Electrical Engineering, National University of Singapore, pp. 10-11, 2003.

Cook, L.M., Chemical Processes in Glass Polishing, *J. Non-Crystalline Solids*, 120, pp. 152-171, 1990.

Danyluk, S., What is Chemical Mechanical Polishing?, Available from: <http://www.me.gatech.edu/eml/cmp.htm> (accessed on November 2, 2004).

Denardis, D., Sorooshian, J., Habiro, M., Rogers, C. and Philipossian, A., Tribology and Removal Rate Characteristics of Abrasive-free Slurries for Copper CMP Applications, *Jpn. J. Appl. Phys.*, 42, pp. 6809-6814, 2003.

Fischer, T.E., Anderson, M.P., Jahanmir, S. and Salher, R., Friction and Wear of Tough and Brittle Zirconia in Nitrogen, Air, Water, Hexadecane and Hexadecane Containing Stearic Acid, *Wear*, 124 (2), pp.133-148, 1988.

Hernandez, J., Wrschka, P. and Oehrlein, G.S., Surface Chemistry Studies of Copper

Chemical Mechanical Planarization, Journal of the Electrochemical Society, 148 (7), pp. G389-G397, 2001.

Hipple, E., The Source of Innovation, Oxford University Press, Oxford, UK, 1988.

Hocheng H., Tsai, H.Y. and Tsai, M.S., Effects of Kinematic Variables on Nonuniformity in Chemical Mechanical Planarization, International Journal of Machine Tools & Manufacture, 40, pp. 1651–1669, 2000.

Holm, R., Electric Contacts, Almqvist and Wiksells, Stockholm, 1946.

Homma Y., Fukushima, K., Kondo and S., Sakuma, N., Effect of Mechanical Parameters on CMP Characteristics Analyzed by Two-Dimensional Frictional-Force Measurement, Journal of The Electrochemical Society, 150 (12), pp. G751-G757, 2003.

Jiang J. and Arnell R.D. The Dependence of The Fraction of Material Removed on The Degree of Penetration in Single Particle Abrasion of Ductile Materials, J. Physics: D, 31, pp. 1163-1167, 1998.

Johnson, K. L., Contact Mechanics, Cambridge University Press, Cambridge, 1985.

Kondo, S., Sakuma, N., Homma, Y., Goto. Y., Ohashi, N., Yamaguchi, H. and Owada, N., Abrasive-Free Polishing for Copper Damascene Interconnection. Journal of The Electrochemical Society, 147(10), pp. 3907-3913, 2000.

Lai J.Y, Mechanics, Mechanisms, and Modeling of the Chemical Mechanical Polishing Process, PhD thesis, MIT, 2001.

Larsen, B. J. and Liang H., Probable Role of Abrasion in Chemo-Mechanical Polishing of Tungsten, Wear, 233-235, pp. 647-654, 1999.

Li, Z., Borucki, L., Koshiyama, I. and Philipossian, A., Effect of Slurry Flow Rate on tribological, Thermal, and Removal Rate Attributes of Copper CMP, Journal of The Electrochemical Society, 151 (7), pp. G482-G487, 2004.

Liang, H., Kaufman, F., Sevilla, R. and Anjur, S., Wear Phenomenon in Chemical Mechanical Polishing, Wear, 211, pp. 271-279, 1997.

Liang, H. and Xu, G. H., Lubricating Behaviour in Chemical-Mechanical Polishing of Copper, Scripta Materialia, 46, pp. 343-347, 2002.

Liu, C. W., Dai, B. T., Tseng, W. T. and Yeh, C. F. , Modeling of The Wear Mechanism During Chemical-Mechanical Polishing, Journal of the Electrochemical Society, Vol. 143 (2), pp. 716-721, 1996.

Ludema, K. and Friction, Wear, Lubrication: A Textbook in Tribology, CRC Press, Boca Raton, p. 117, 1996.

Luo, J., and Dornfeld, D. A., IEEE Transaction: Semiconductor Manufacturing, 14 (2), pp. 112-133, 2001.

Matshuda, T., Takahashi, H., Tsurugaya, M., Miyazaki, K., Doy, T.K. and Kinoshita, M., Characteristics of Abrasive-free Micelle Slurry for Copper CMP, Journal of The Electrochemical Society, Vol. 150 (9), pp. G532-G536, 2003.

Maury, D. Ouma, D. Boning and J. Chung, A Modification to Preston's Equation And Impact on Pattern Density Effect Modeling, Proc. of Advanced Metalization and Interconnect Systems for ULSI Applications, Sept. 30- Oct. 2, 1997.

Mazaheri, R. and Ahmadi, G., Modeling of The Effect of Bumpy Abrasive Particles on Chemical Mechanical Polishing, Journal of the Electrochemical Society, 149 (7), pp. G370-G375, 2002.

Mazaheri, R. and Ahmadi, G., A Model for Effect of Colloidal Forces on Chemical Mechanical Polishing, Journal of the Electrochemical Society, 150 (4), pp. G233-G239, 2003.

Moon, Y. and Dornfeld, D. A., The Effect of Slurry Film Thickness Variation in Chemical Mechanical Polishing (CMP), Proceedings of the American Society for Precision Engineering (ASPE), ASPE Annual Conference, St. Louis, Missouri, 18, p. 591-601, 1998.

Moon, Y, Mechanical aspects of the material removal mechanism in chemical mechanical polishing (CMP), Ph.D. Thesis, Department of Mechanical Engineering, University of California at Berkeley, Berkeley, CA, U. S. A., 1999.

Moore, G.E., Cramming More Components onto Integrated Circuits, Electronics, pp. 114-117, 1965.

Mullany, B. and Byrne, G., The Effect of Slurry Viscosity on Chemical-Mechanical Polishing of Silicon Wafers, Journal of Materials Processing Technology, 132. pp. 28-34, 2003.

Newton, Sir Isaac, 1695, Opticks, Dover Publication, Inc., New York, 1952, 4th ed., London, 1730.

Philipossian, A. and Olsen, S., Effect of Slurry Flow Rate on Pad Life during Interlayer Dielectric CMP, Journal of The Electrochemical Society, 151 (6), pp. G436-G439, 2004.

Philipossian, A. and Mitchell, E., Mean Residence Time and Removal Rate Studies in ILD CMP, Journal of The Electrochemical Society, 151(6), pp. G402-G407, 2004.

Pan J. T., Li P., Wijekoon K., Tsai S., Redeker F., Perk T., Tugabawa T., Boning D., Copper CMP and Process Control, CMP-MIC, pp. 121-126, 1999.

Preston, F., The Theory and Design of Plate Glass Polishing Machines, Journal Of The Society Of Glass Technology, 11, pp. 214-256, 1927.

Rabinowicz, E., Polishing, Scientific American, 218, pp. 91-99, 1968.

Rabinowicz, E., Friction and Wear of Materials, 2nd Edition, John Wiley and Sons, Inc., 1995.

Rayleigh, L., Polish, Nature, 64, pp. 385-388, 1901.

Rajiv, K. S., Rajeev, B.j., Guest, E., Advances in Chemical Mechanical Planarization. MRS Bulletin, pp. 743-748, 2002.

Runnels, S. R., Feature-Scale Fluid-Based Erosion Modeling for Chemical Mechanical Polishing, Journal of the Electrochemical Society, 141(7), pp. 1900-1904, 1994.

Samuels, L.E., Metallographic Polishing by Mechanical Methods, 2nd ed., Elsevier, New York, 1971.

Silvey, G.A., Regh, J. and Gardiner, 1966, U.S. Patent No. 3,436,259, assigned to IBM 1966.

Steigerwald, J.M., Murarka, S.P., Gutmann, R.J. and Duquette, D.J., Chemical Processes in the Chemical Mechanical Polishing of Copper, Materials Chemistry and Physics, 41, pp.217-228, 1995.

Stiegwald J. M., Murarka, S. P. and Guttman, R.J., Chemical Mechanical Planarization of Microelectronic Materials, John Wiley and Sons, Inc., 1997.

Su, Y. T., Investigation of Removal Rate of a Floating Polishing Process, J. Electrochem. Soc., 147 (6), pp. 2290-2296, 2000.

Tseng, W. T. , Chin J.H. and Kang L.C., A Comparative Study on the Roles of Velocity in the Material Removal Rate during Chemical Mechanical Polishing, Journal of the Electrochemical Society, 146(5), pp.1952-1959, 1999.

Tseng, W. T. and Wang, Y. L., Re-Examination of Pressure and Speed Dependence of Removal Rate During Chemical Mechanical Polishing Processes, Journal of the Electrochemical Society, 144, pp. L15-L17, 1997.

Walsh, R.J. and Herzog, A., 1965, U.S. Patent No. 3,170,273, issued 23 February 1965.

Wang, S.Y. and Su. Y. T., An Investigation on Machinability of Different Materials By Hydrodynamic Polishing Process, Wear, 211, pp.185-191, 1997.

Williams, J.A. and Hyncica, A. M., Mechanism of Abrasive Wear in Lubricated Contacts, Wear, 152, pp. 57-74, 1992.

Wrschka, P., Hernandez, J., Hsu, Y., Kuan, T. S., Oehrlein, G. S., Sun, H. J., Hansen, D. A., King J. and Fury, M. A., Polishing Parameter Dependencies and Surface Oxidation of Chemical Mechanical Polishing of Al Thin Films, *Journal of the Electrochemical Society*, 146, No. 7, pp. 2689-2696, 1999.

Xu, G., Liang, H., Zhao, J. and Li, Y., Investigation of Copper Removal Mechanisms during CMP, *Journal of The Electrochemical Society*, 151 (10), pp. G688-G692, 2004.

Zhao, B. and Shi, F. G., Modeling of Chemical-Mechanical Polishing with Soft Pads, *Applied Physics A*, 67, pp. 249-252, 1998.

Zhao, J., Du, Y., Morgen, M. and P. S. Ho, Simultaneous Measurement of Young's Modulus, Poisson Ratio, and Coefficient of Thermal Expansion of Thin Films on Substrates, *Journal of Applied Physics*, 87(3), pp. 1575-1577, 2000.

Zhao, Y. and Chang, L., A Micro-Contact and Wear Model for Chemical–Mechanical Polishing Of Silicon Wafers, *Wear*, 252, pp. 220-226, 2002.

Zhang F. and Busnaina, A., The Role of Particle Adhesion and Surface Deformation in Chemical Mechanical Polishing Processes, *Electrochemical and Solid-State Letters*, 1 (4), pp. 184-187, 1998.

Zhang, L., and Subramanian, R.S., A Model of Abrasive-Free Removal of Copper Films Using an Aqueous Hydrogen Peroxide–Glycine Solution, *Thin Solid Films*, Vol. 397, pp. 14-1513, 2001.

Zhou, C., Shan, L., Robert H. J., Ng S.H., Danyluk S., Fluid pressure and its effects on chemical mechanical polishing, *Wear*, 253 (3), pp. 430-437, 2002.

Appendix A

A-1 Multilayer Metal Interconnects and the Role of CMP

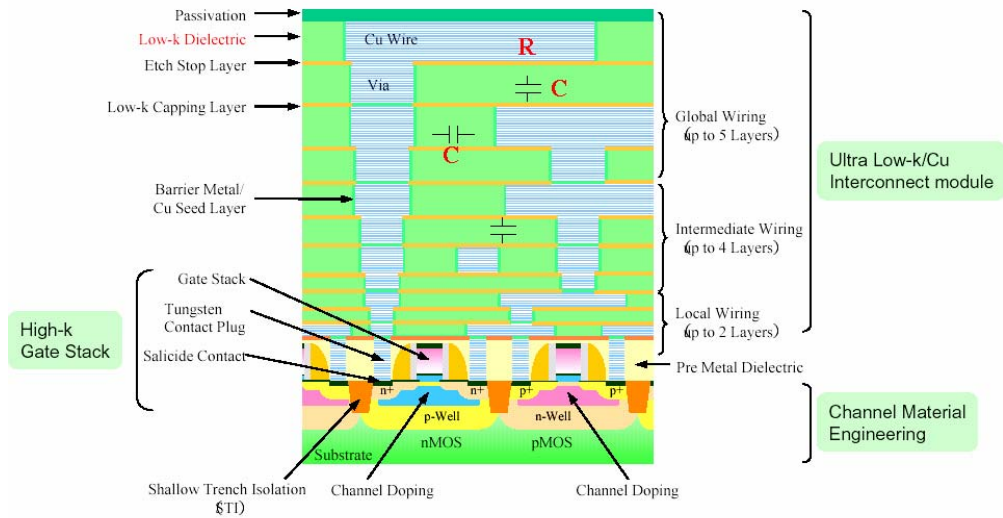


Figure A.1 Cross sectional view of a microelectronic chip

The high performances ICs require increased number of metal layers to increase the device density. The technology node below 90 nm requires more than 10 metal layers. The schematic of the cross sectional view of a typical high performance IC shows multilevel interconnects and other components as given in Figure A.1.

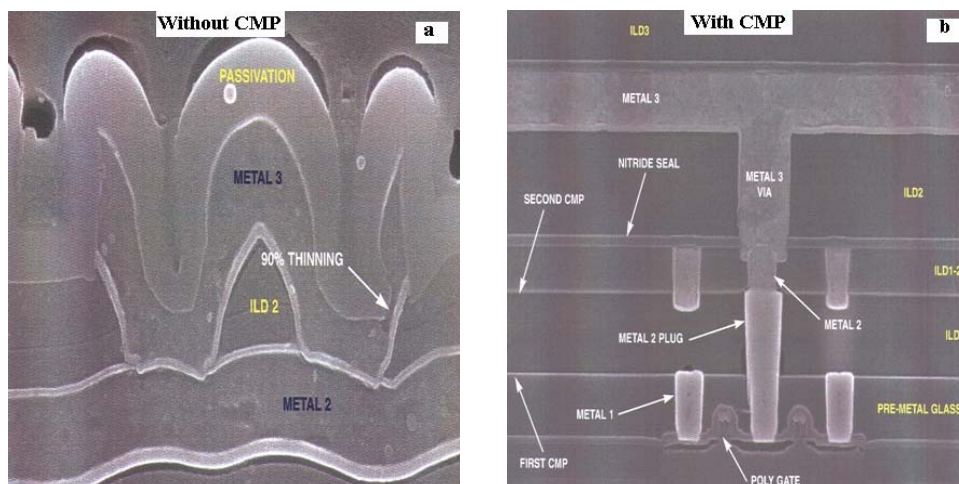


Figure A.2 Multilevel interconnects: a) without CMP, b) with CMP

In order to achieve global planarity of the surface at each metal layer, the surface is polished using both front end CMP (Shallow Trench Isolation, polysilicon CMP for deep capacitance isolation, etc) and back end CMP (Copper CMP for Cu/low-k integration, etc). The multilevel interconnects obtained with and without CMP as shown Figure A.2.a and A.2.b respectively clearly indicates the essence of CMP process.

A-2 International Technology Roadmap for Semiconductors (ITRS)

National Technology Roadmap for Semiconductors (NTRS) was inaugurated in 1992 as an initiative of SIA (Semiconductor Industry Association). It became an international effort in 1997 by introducing as The International Technology Roadmap for Semiconductors (ITRS). It provides bi-annual updates on 15 year road-map. ITRS is the joint effort of industry, government, consortia, and universities. The objective of the ITRS is to ensure advancements in the performance of integrated circuits. It identifies the technological challenges and needs facing the semiconductor industry up to 2011.

Table A.1 SIA International technology roadmap for semiconductors (ITRS) for interconnect technology (1998 updated)

Year of First Product Shipment Technology	1997	1999	2002	2005	2008	2011
Number of Metal Levels - DRAM	2-3	3	3	3-4		
Number of Metal Levels - Logic	6	6-7	7	7-8		
Maximum Interconnect Length- Logic (m/chip)	800	1700	3300	5000	9200	17000
Planarity Requirements within Litho Field for Minimum Interconnect Critical Dimension (CD) (nm)	300	250	200	175	175	175
Minimum Contacted / Noncontacted Pitch - DRAM (nm)	550/500	400/360	280/260	220/200	160/140	110/100
Minimum Contacted / Noncontacted Pitch - Logic (nm)	640/590	460/420	340/300	260/240	190/170	140/130
Minimum Metal CD for Isolated Lines (nm)	250	180	130	100	70	50
Minimum Contact / Via CD (nm)	280/360	200/260	140/180	110/140	80/100	60/70
Metal Height / Width Aspect Ratio - Logic (Microprocessor)	1.8	1.8	2.1	2.4	2.7	3
Via Aspect Ratio – Logic	2.2	2.2	2.5	2.7	2.9	3.2
Minimum Metal Effective Resistivity ($\mu\Omega/\text{cm}$)	3.3	2.2	2.2	2.2	<1.8	<1.8
Barrier / Cladding Thickness (nm)	100	23	16	11	3	1
Minimum Interlevel Metal Insulator - Effective Dielectric Constant (k)	3.0-4.1	2.5-4.1	1.5-2.0	1.5-2.0	≤ 1.5	≤ 1.5

A-3 Ideal Oxide ILD CMP

The oxide CMP is basically used for conventional Al (aluminum) metallization (Figure A.3). Al is deposited on ILD oxide, patterned by lithographic technique followed by etching. Then another ILD oxide is deposited on the etched Al and smoothed by CMP so that the oxide is flat enough for next stage lithography.

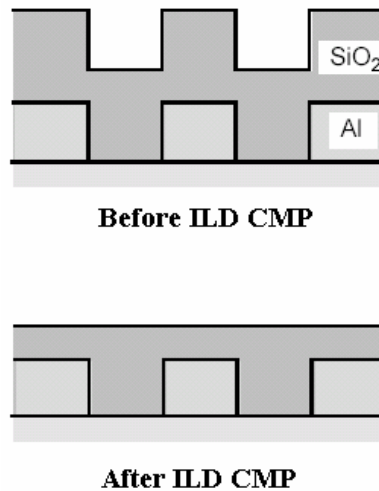


Figure A.3 Ideal oxide ILD CMP

A-4 Dual Damascene Interconnects Fabrication Process

Dual Damascene process is basically used for fabricating copper interconnects. Since copper does not form any volatile by-product, it is difficult to etch and, therefore copper metallization can not be done by subtractive etching method which is mainly used for Aluminum interconnect fabrication. The Dual Damascene is such a interconnect fabrication technique where a columnar hole is made first followed by a trench etching into the inter layer dielectrics (ILD). Then the hole and trench is filled by copper which is subsequently polished by CMP up to the surface of ILD. Thus a vertical via connection and an inlaid copper metal line is formed. There are basically two approaches for Dual

Damascene process namely Trench-First approach and Via-First approach. Since Via-First approach is popular in semiconductor industries, the description of this process is given as follows:

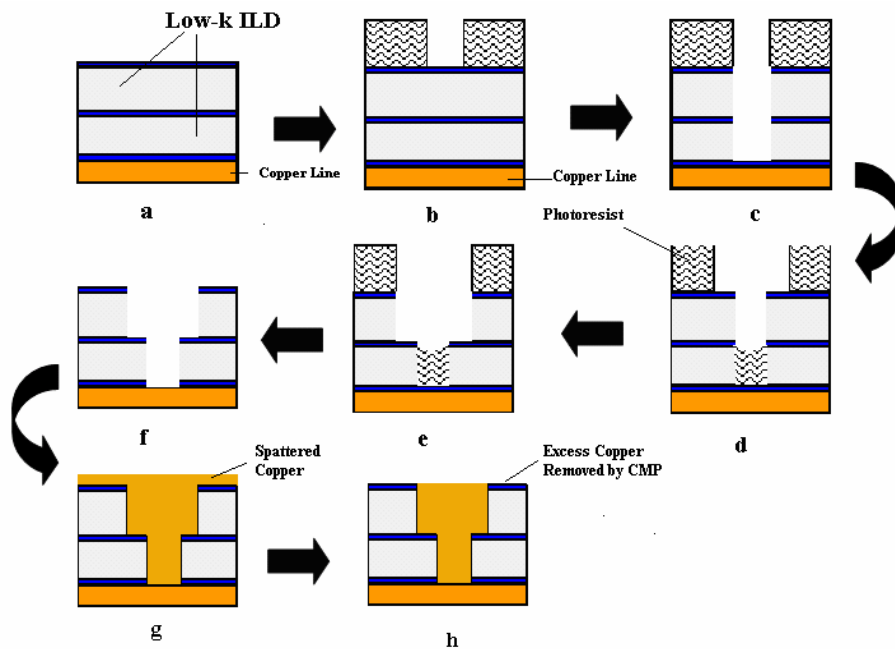


Figure A.4 Via-first approach of Dual Damascene interconnect fabrication process

To make trace and via, photoresist is patterned lithographically on the ILD surface (Figure A.4.b). Before applying the photoresist on the top of the ILD, a surface hard mask (plasma SiN) is usually applied that protects the ILD from the chemicals that is used to remove the photoresist. An anisotropic etch cuts through the surface hard mask and etches down through the ILD and the embedded etch stop, and stops on the bottom silicon Nitride barrier (Figure A.4.c). Then the photoresist at via is stripped and the trench photoresist is applied by lithographic technique. Some of the photoresist is kept in the bottom of via to protect from over etching (Figure A.4.d). An anisotropic etch cuts through the surface hard mask and down through the ILD and stops at the embedded

mask. Thus a trench is formed. After stripping the photoresist, copper is sputtered into via and trench (Figure A.4.g) followed by CMP to removing excess copper (Figure A.4.h).

A-5 Prestonian and Non-Prestonian Behaviour of MRR

Pressure and relative velocity are used as the key modulating parameters in CMP process because these two parameters considerably affect the MRR and WIWNU during polishing. If the material removal rate is linearly proportional to the energy flux i.e. the product of applied pressure (P) and the relative velocity of pad with respect to wafer (V), it is called that material removal follows prestonian nature. This can be expressed by Preston's equation as:

$$MRR = k_p PV$$

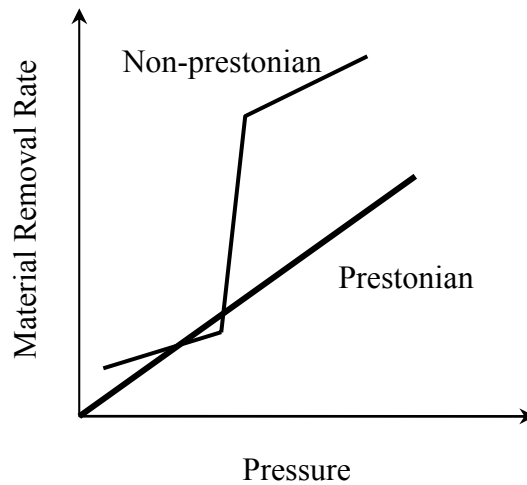


Figure A.5 Prestonian and non-prestonian behaviour of MRR

So, prestonian nature of MRR tells:

- The MRR is zero when there is no pressure and/or no sliding velocity
- Preston's equation was developed based on the abrasion wear mechanism.

The deviation from such phenomenon is usually defined as non-prestonian nature of MRR as shown in Figure A.5.